



الجمهورية الجزائرية الديمقراطية الشعبية

People's Democratic Republic of Algeria

وزارة التعليم العالي والبحث العلمي

Ministry of Higher Education and Scientific Research

جامعة الشهيد حمة لخضر - الوادي

University of Echahid Hamma Lakhdar - El Oued

كلية العلوم الطبيعية الحياة

Faculty of Natural and Life Sciences

قسم البيولوجيا الخلوية والجزيئية

Department of Cellular and Molecular Biology



THESIS

TO OBTAIN 3rd CYCLE LMD DOCTORATE DEGREE

Speciality: Applied Biochemistry

THEME

Biosynthesis and biological activities of zinc oxide nanoparticles using *Hammada scoparia* (Pomel) Iljin plant extract.

Presented by: Ms. BENINE Chaima

Discussed on: October 31th, 2024

Jury Members:

Mrs. MEDILA Ifriqya	Professor	University of El-Oued	President
Mr. DJAHRA Ali Boutlelis	Professor	University of El-Oued	Supervisor
Mr. LAICHE Ammar Touhami	AAP	University of El-Oued	Co-Supervisor
Mr. LAOUINI Salah Eddine	Professor	University of El-Oued	Examiner
Mr. BENKHERARA Salah	AAP	University of Ghardaïa	Examiner
Mr. BELGHIT Said	AAP	University of Ghardaïa	Examiner

2023/2024



الجمهورية الجزائرية الديمقراطية الشعبية

People's Democratic Republic of Algeria

وزارة التعليم العالي والبحث العلمي

Ministry of Higher Education and Scientific Research

جامعة الشهيد حمدة لخضر - الوادي

University of Echahid Hamma Lakhdar - El Oued

كلية العلوم الطبيعية الحياة

Faculty of Natural and Life Sciences

قسم البيولوجيا الخلوية والجزيئية

Department of Cellular and Molecular Biology



THESIS

TO OBTAIN 3rd CYCLE LMD DOCTORATE DEGREE

Speciality: Applied Biochemistry

THEME

Biosynthesis and biological activities of zinc oxide nanoparticles using *Hammada scoparia* (Pomel) Iljin plant extract.

Presented by: Ms. BENINE Chaima

Discussed on: October 31th, 2024

Jury Members:

Mrs. MEDILA Ifriqya	Professor	University of El-Oued	President
Mr. DJAHRA Ali Boutlelis	Professor	University of El-Oued	Supervisor
Mr. LAICHE Ammar Touhami	AAP	University of El-Oued	Co-Supervisor
Mr. LAOUINI Salah Eddine	Professor	University of El-Oued	Examiner
Mr. BENKHERARA Salah	AAP	University of Ghardaïa	Examiner
Mr. BELGHIT Said	AAP	University of Ghardaïa	Examiner

2023/2024

بِسْمِ اللَّهِ الرَّحْمَنِ الرَّحِيمِ

Acknowledgment

First of all, we would like to thank GOD and the Almighty for the will, health and patience which has given us during all the years of study, and prayers and peace be upon His Prophet Muhammad, his family and companions.

At the end of drafting this research, I am convinced that the thesis is far from being a solitary task. Indeed, I would never have been able to carry out this doctoral work without the support of many people whose generosity, good humor, and interest were shown in my research. This thesis, the fruit of several years of research, would not have seen the light of day without the valuable contribution of several people who should be mentioned here.

*I would first like to thank my research supervisor, **Pr. DJAHRA Ali Boutlelis** and Co-supervisor **Dr. LAICHE Ammar Touhami**, for their rigorous supervision, guidance, comments, corrections, and suggestions, allowed me to complete this thesis successfully. I thank you for all the contributions and support on an administrative, academic, organizational, and relational level and for all the motivations you gave me before the thesis. Throughout this adventure, Pr. DJAHRA and Dr. LAICHE rigorously and meticulously introduced me to scientific research with exceptional generosity in sharing their knowledge accumulated throughout their beautiful and rich scientific career.*

*I would also like to thank the jury members, **Pr. MEDILA Ifriqya**, a professor at El Oued University who did me the honor of agreeing to be jury president.*

*I also thank **Pr. LAOUINI Salah Eddine**, professor at El Oued University and **Dr. BENKHERARA Salah**, professor at Ghardaïa University, and **Dr. BELGHIT Said**, professor at Ghardaïa University, for the importance they gave to my work by agreeing to be members of this jury and for the time they devoted to examining this thesis.*

*I am pleased to conduct this research work in the Biology, Environment and Health Laboratory, Faculty of Natural and Life Sciences at the University of El Oued - Algeria, directed by **Pr. CHOUIKH Atef**. I want to sincerely thank him for welcoming me into the pharmacognosy laboratory, for trusting me and allowing me to carry out this work in better conditions while giving me great freedom, and for his support and generosity.*

*I sincerely thank all the technicians of Pedagogical Laboratories at the El Oued University, especially **Ms. GOBI Sana**, and **KHANOUSA Omar** for their kindness and valuable collaboration.*

*I would like to express my deep gratitude to **Dr. LANEZ Elhafnaoui** for welcoming me into VTRS research laboratory at the El Oued University and valuable collaboration in carrying out this work necessary for the successful completion of some of my experiments.*

My sincere thanks also go to the director of the Laboratory of Pastoral Ecosystems and Valorization of Spontaneous Plants and Microorganisms, Institute of Arid Regions (IRA),

Tunisia. Also all the Laboratory members, specially **Dr. NAJJAA Hanen** and **Hajer Tili** for welcoming me to their laboratory and for allowing me to better understand the use of many tools and methods necessary for the smooth running of some experiments in this thesis.

I would like to express my deep gratitude to **Dr. Maha Mezghani Khemakhem** and **Chahnez Naccache** for welcoming me Laboratory of Biochemistry and Biotechnology at the University of Tunis El Manarr, Tunisia and valuable collaboration in carrying out this work necessary for the successful completion of some of my experiments.

Warm thanks to **Mr. MEDELLEL Abdelkader**, the Prepharmacy MEDELLEL director in El Oued for their kindness and valuable help. I hope he will find here a certificate of gratitude and deep respect.

Warm thanks to **Mr. BELKHALFA Hakim**, the CRAPC Physico-Chemical Analysis Research Center director in Ouargla and all their members for their kindness and valuable help, particularly **Mr. BOUSSEBAA Walid**.

I would like to express my deep gratitude to **Mr. ABID Laala** his valuable help in carrying out this work necessary for the successful completion of this thesis.

My sincere thanks also go to the technicians of the Biochemical Analysis Laboratory at the BEN AMOR DJILANI -El Oued Hospital, particularly **Mr. HAMMOUDI Ammar Said**, for their valuable collaboration in carrying out this work.

I also extend my gratitude to **FARES Mohamed Amine** from the Laboratory of Sciences and Techniques of the Living, Institute of Agriculture and Veterinary Sciences, University of Souk Ahras, for his generous assistance. He has my deepest thanks.

I would like to express my warmest thanks to my dear friend **Azzi Manel**, for her friendship, encouragement, delightful company, and the unforgettable moments we have shared.

I would also like to express my thanks to my laboratory colleagues who participate in the smooth running of the laboratory, with whom it is possible to exchange advice and information, and who ensure a pleasant working atmosphere.

Thanks to all the other people I knew but didn't mention. I hope I haven't forgotten anyone, otherwise... thank you.

BENINE Chaima

Dedications

I begin my dedication in the name of God and salutation to Mohamed, the messenger of God.

I dedicate this modest work to

To the dearest people in the world

*To my sweet ones' parents, **EL-KADRI** and **RABIA***

The reason I have become who I am today is to thank you for your great and continued support and for always being by my side. May this work be the fruit of your prayers and sacrifices, which were of great help to me in reaching this stage of my life.

May God Almighty grant you health, happiness, and long life.

*My dear brothers **NABIL, ABDRAHMANE, BAGHDAD, OUSSAMA, MOHAMMED YAZID,** and **SALAH EDDINE** and my beautiful sisters **AMEL, OUFAFA,** and **IBTISSAM,** words are not enough to express the attachment, love and affection I have for you. Thank you for everything, for the trust and energy you gave me. I dedicate this work to you with all my wishes for happiness, health, and success.*

*To my dear sister's soul **NAZIHA.***

*To **all the teachers** who contributed to my training.*

*I dedicate this modest work **to anyone who contributed** directly or indirectly to the production of this thesis.*

Chaima

ABSTRACT

In this study, the main goal was to synthesize zinc oxide nanoparticles (ZnO-NPs) using the aqueous extract of *Hammada scoparia* (Pomel) Iljin (*H. scoparia*) and to evaluate the biological activities of the plant extract, calcined and uncalcined ZnO-NPs *in vitro* and *in vivo*. Overall, the study aims to provide a comprehensive evaluation of the potential therapeutic benefits of *H. scoparia* extract and ZnO-NPs in promoting induced wound healing in albino rats, potentially leading to new phytotherapeutic and nanotherapeutic approaches in medical applications. For this purpose, standard procedures for quantitative and qualitative analysis and extraction of bioactive compounds were used. Identification and quantification of individual phenolic compounds were conducted via HPLC and LC/MS analysis. The green synthesis and characterization of calcined and uncalcined ZnO-NPs were performed using various methods, including UV-Vis spectrophotometry, FTIR, XRD, and SEM/EDS. *In vitro* activities such as antioxidant, photoprotective, anti-inflammatory, anti-diabetic, and probiotic activities were evaluated. Anti-cancer activity was evaluated by spectrophotometric and voltametric studies assessed the interaction of *H. scoparia* and two ZnO-NPs with DNA and BSA, then the cytotoxic effects of the *H. scoparia* and ZnO-NPs samples on MCF7 cells were assessed using the MTT assay. For the *in vivo* study, 35 male Wistar rats were divided into seven groups (each group comprises five rats): No wounds + no cream, wounds + no cream, wounds + Base cream, wounds + *H. scoparia* cream, wounds + calcined ZnO-NPs cream, wounds + uncalcined ZnO-NPs, and wounds + commercial healing cream (DOUCE PLUS®). After 13 days of treatment various biochemical, hematological, and histopathology were studied.

Phytochemical analysis revealed the presence of numerous phenolic compounds. *H. scoparia* contained high levels of total phenolics (141.61 ± 0.53 mg GAE/g Extract), flavonoids (67.88 ± 0.71 mg QE/mg Extract), and condensed tannins (54.47 ± 0.86 mg CE/g Extract). HPLC analysis identified 21 phenolic compounds in high concentration, notably Rutin emerged as the most abundant, constituting a major peak at 28.288 %, succeeded by Naringenin (13.662%), Gallic Acid (11.037%), Valinin (9.436%), and Hydroxy-Comarin (6.006%). The synthesized ZnO-NPs exhibited an absorption peak at 362 nm for uncalcined and 376 nm for calcined ZnO-NPs, crystalline nature confirmed by XRD patterns, and SEM analysis showed that most nanoparticles were spherical particles with a mean diameter of 36.12 ± 4.52 nm and 40.17 ± 6.43 nm respectively for uncalcined and calcined ZnO-NPs. FT-IR analysis confirmed the presence of various functional groups involved in the reduction and capping of ZnO-NPs. *H. scoparia* and the ZnO-NPs displayed strong antioxidant, anti-inflammatory and photoprotective activities and provided good probiotic activity for *Bacillus pumilus*. Uncalcined ZnO-NPs exhibited the highest antidiabetic activity with $IC_{50} = 167.08$ μ g/mL for hemoglobin glycosylation and 38.67 μ g/mL for α -glucosidase inhibition. Calcined ZnO-NPs followed with IC_{50} values of 176.51 μ g/mL and 42.90 μ g/mL, respectively. *H. scoparia* extract showed significant effectiveness with IC_{50} values of 245.32 μ g/mL and 61.08 μ g/mL. Additionally, results indicated spontaneous interactions between ZnO-NPs and DNA as well as BSA via electrostatic interactions, reflected in parameters K and ΔG . *H. scoparia* extract showed highest cytotoxicity; uncalcined and calcined ZnO-NPs also effectively reduced MCF7 cell viability. *In vivo* results showed that the *H. scoparia* cream exhibited the highest wound healing rates, followed by ZnO-NP-UC and ZnO-NP-C creams. Hematological and inflammation parameters were more favorable in treated groups. Histological studies confirmed improved skin healing, with *H. scoparia* and ZnO-NP treatments showing significant efficacy.

In conclusion, this study comprehensively evaluated the therapeutic potential of *H. scoparia* extract, calcined and uncalcined ZnO-NPs in wound healing, cancer, and various biological activities. Results suggesting new possibilities for phytotherapy and nanotherapy in medical applications.

Keywords: *Hammada scoparia*, zinc oxide nanoparticles, green synthesis, biological activities, wound healing, albino rats.

الملخص

في هذه الدراسة، كان الهدف الرئيسي هو تخليق جسيمات أكسيد الزنك باستخدام مستخلص مائي لنبات الرمث وتقييم الأنشطة البيولوجية لمستخلص النبات، وجسيمات أكسيد الزنك المحروقة وغير المحروقة في المختبر وفي الكائن الحي. بصفة عامة، تهدف الدراسة إلى تقديم تقييم شامل للفوائد العلاجية المحتملة لمستخلص الرمث وجسيمات أكسيد الزنك في تعزيز شفاء الجروح المحفزة في الفئران، مما قد يؤدي إلى نهج علاجي نباتي وناوِي جديد في التطبيقات الطبية. لهذا الغرض، تم استخدام الإجراءات القياسية للتحليل الكمي والنوعي واستخراج المركبات الحيوية. كما تم إجراء تحليل وتقدير المركبات الفينولية الفردية عن طريق تقنية الكروماتوغرافيا السائلة عالية الأداء والكروماتوغرافيا السائلة مع طيف الكتلة. تم إجراء تخليق أخضر وتوصيف جسيمات أكسيد الزنك المحروقة وغير المحروقة باستخدام طرق مختلفة، بما في ذلك مطيافية الأشعة فوق البنفسجية المرئية، والطيف الأشعة تحت الحمراء بتحويل فورييه، وتشنت الأشعة السينية، والمجهر الإلكتروني الماسح مع التحليل الكمي بالطاقة الانتشارية. تم تقييم الأنشطة في المختبر مثل الأنشطة المضادة للأكسدة، والواقية من الأشعة فوق البنفسجية، والمضادة للالتهابات، ومضادة للسكري، ونشاط البروبيوتك. تم تقييم نشاط مضاد للسرطان من خلال دراسات مطيافية وفولطامترية لتقييم تفاعل مستخلص الرمث وجسيمات أكسيد الزنك مع الحمض النووي وبروتين الاليومين البقري، ثم تم تقييم نشاط السمية الخلوية لعينات مستخلص الرمث وجسيمات أكسيد الزنك على الخلايا السرطانية MCF7 باستخدام اختبار MTT. أما بخصوص الدراسة في الكائن الحي، تم تقسيم 35 من ذكور الفئران إلى سبع مجموعات (تتكون كل مجموعة من خمسة فئران) كالتالي: بدون جروح + بدون كريم، جروح + بدون كريم، جروح + قاعدة الكريم، جروح + كريم بمستخلص الرمث، جروح + كريم جسيمات أكسيد الزنك المحروق، جروح + كريم جسيمات أكسيد الزنك غير المحروق، وجروح + الكريم التجاري (دوس بلوس ®). بعد 13 يوماً من العلاج، تم دراسة مختلف التحاليل البيوكيميائية، الدموية، والنسجية.

توضح التحاليل الفيتوكيميائية وجود عدد كبير من المركبات الفينولية. يحتوي مستخلص الرمث على مستويات عالية من الفينولات الكلية (141.61 ± 0.53 مغ مكافئ من حمض الغاليك/غ من المادة الجافة)، والفلافونويدات (67.88 ± 0.71 مغ مكافئ من الكرسيتين/غ من المادة الجافة)، والتانينات المكثفة (54.47 ± 0.86 مغ مكافئ من الكاتيشين /غ من المادة الجافة). كشف تحليل الكروماتوغرافيا السائلة عالية الأداء عن 21 مركب فينولي بتركيز عالٍ، حيث برز الروتين كالأكثر وفرة، يليه النارينجين (13.662%)، حمض الغاليك (11.037%)، الفالينين (9.436%)، والهيدروكسي كيومارين (6.006%). أظهرت جسيمات أكسيد الزنك المصنعة ذروة امتصاصية عند 362 نانومتر للمحروق و376 نانومتر لغير المحروق، وتأكدت طبيعتها البلورية من خلال أنماط تشنت الأشعة السينية، وأظهرت تحليل المجهر الإلكتروني الماسح أن معظم الجسيمات كانت جسيمات كروية بقطر متوسط بلغ 36.12 ± 4.52 نانومتر و40.17 ± 6.43 على التوالي لجسيمات أكسيد الزنك غير المحروق والمحروق. أكد تحليل الطيف الأشعة تحت الحمراء بتحويل فورييه وجود مجموعات وظيفية مختلفة مشاركة في تخفيض وتغليف جسيمات أكسيد الزنك. أظهر مستخلص الرمث وجسيمات أكسيد الزنك نشاطاً قوياً مضاداً للأكسدة ومضاداً للالتهابات ووقائياً من الشمس، وقدمت نتائج جيدة في نشاط البروبيوتيك لـ *Bacillus pumilus*. أظهرت جسيمات أكسيد الزنك غير المحروق أعلى نشاط مضاد للسكري بقيمة $IC_{50}=167.08$ ميكروغرام/مل لارتباط الغلوكوز بالهيموجلوبين و38.67 ميكروغرام/مل لتثبيط انزيم ألفا جلوكوزيداز. واتبعت جسيمات أكسيد الزنك المحروق بقيم IC_{50} بلغت 176.51 ميكروغرام/مل و42.90 ميكروغرام/مل على التوالي. كما أظهر مستخلص الرمث فعالية كبيرة بقيم IC_{50} بلغت 245.32 ميكروغرام/مل و61.08 ميكروغرام/مل في كلا الاختبارين على التوالي. بالإضافة إلى ذلك، أشارت النتائج إلى تفاعلات تلقائية بين جسيمات أكسيد الزنك والحمض النووي والاليومين البقري من خلال التفاعلات الكهروستاتيكية، مما انعكس في الثوابت K و ΔG . أظهر مستخلص الرمث أعلى سمية خلوية. أظهرت جسيمات أكسيد الزنك غير المحروق والمحروق أيضاً تقليلاً فعالاً لنسبة البقاء على قيد الحياة لخلايا السرطانية MCF7. أظهرت النتائج في الكائن الحي أن كريم مستخلص الرمث أعلى معدلات شفاء للجروح، تلتها كريمات جسيمات أكسيد الزنك غير المحروق والمحروق. كانت معدلات التحاليل الدموية والالتهاب أكثر ملائمة في المجموعات المعالجة. كما أكدت الدراسات النسجية تحسناً في شفاء الجلد، حيث أظهرت معالجات مستخلص الرمث وجسيمات أكسيد الزنك فعالية ملحوظة.

ختمت هذه الدراسة بتقديم تقييم شامل للفوائد العلاجية لمستخلص الرمث، جسيمات أكسيد الزنك غير المحروق والمحروق في شفاء الجروح، والسرطان، والأنشطة البيولوجية المختلفة. تشير النتائج إلى إمكانية جديدة للعلاج النباتي والناوِي في التطبيقات الطبية.

الكلمات المفتاحية: نبات الرمث، جسيمات أكسيد الزنك، التصنيع الأخضر، الأنشطة البيولوجية، شفاء الجروح، الفئران.

Résumé

Dans cette étude, l'objectif principal était de synthétiser des nanoparticules d'oxyde de zinc (ZnO-NPs) en utilisant l'extrait aqueux de *Hammada scoparia* (Pomel) Iljin (*H. scoparia*) et d'évaluer les activités biologiques de l'extrait de plante, des ZnO-NPs calcinées et non calcinées *in vitro* et *in vivo*. Globalement, l'étude vise à fournir une évaluation complète des avantages thérapeutiques potentiels de l'extrait de *H. scoparia* et des ZnO-NPs dans la promotion de la cicatrisation des plaies induites chez les rats albinos, ce qui pourrait mener à de nouvelles approches phytothérapeutiques et nanothérapeutiques dans les applications médicales. À cette fin, des procédures standard pour l'analyse quantitative et qualitative et l'extraction de composés bioactifs ont été utilisées. L'identification et la quantification des composés phénoliques individuels ont été réalisées via des analyses HPLC et LC/MS. La synthèse verte et la caractérisation des ZnO-NPs calcinées et non calcinées ont été effectuées en utilisant diverses méthodes, notamment la spectrophotométrie UV-Vis, FTIR, XRD et SEM/EDS. Les activités *in vitro* telles que les activités antioxydants, photoprotectrices, anti-inflammatoires, anti-diabétiques et probiotiques ont été évaluées. L'activité anticancéreuse a été évaluée par des études spectrophotométriques et voltamétriques qui ont examiné l'interaction de *H. scoparia* et des deux ZnO-NPs avec l'ADN et la BSA, puis les effets cytotoxiques des échantillons de *H. scoparia* et des ZnO-NPs sur les cellules MCF7 ont été évalués à l'aide du test MTT. Pour l'étude *in vivo*, 35 rats Wistar mâles ont été divisés en sept groupes (chaque groupe comprend cinq rats) : Pas de plaies+pas de crème, plaies+pas de crème, plaies+crème de base, plaies+crème de *H. scoparia*, plaies+crème de ZnO-NPs calcinées, plaies+crème de ZnO-NPs non calcinées et plaies+crème cicatrisante commerciale (DOUCE PLUS®). Après 13 jours de traitement, diverses études biochimiques, hématologiques et histopathologiques ont été réalisées.

L'analyse phytochimique a révélé la présence de nombreux composés phénoliques. *H. scoparia* contenait des niveaux élevés de phénoliques totaux ($141,61 \pm 0,53$ mg EGA/g Extrait), de flavonoïdes ($67,88 \pm 0,71$ mg EQ/mg Extrait) et de tannins condensés ($54,47 \pm 0,86$ mg EC/g Extrait). L'analyse HPLC a identifié 21 composés phénoliques en haute concentration, avec notamment la Rutine émergeant comme le plus abondant, constituant un pic majeur à 28,288 %, suivi par la Naringénine (13,662 %), l'Acide gallique (11,037 %), la Valinine (9,436 %) et l'Hydroxy-coumarine (6,006 %). Les ZnO-NPs synthétisées ont présenté un pic d'absorption à 362 nm pour les ZnO-NPs non calcinées et à 376 nm pour les ZnO-NPs calcinées, une nature cristalline confirmée par les motifs XRD, et l'analyse SEM a montré que la plupart des nanoparticules étaient des particules sphériques avec un diamètre moyen de $36,12 \pm 4,52$ nm et $40,17 \pm 6,43$ respectivement pour les ZnO-NPs non calcinées et calcinées. L'analyse FT-IR a confirmé la présence de divers groupes fonctionnels impliqués dans la réduction et le capsulage des ZnO-NPs. *H. scoparia* et les ZnO-NPs ont affiché de fortes activités antioxydantes, anti-inflammatoires et photoprotectrice et ont fourni une bonne activité probiotique pour *Bacillus pumilus*. Les ZnO-NPs non calcinées ont présenté la plus haute activité antidiabétique avec un $IC_{50} = 167,08$ μ g/mL pour la glycosylation de l'hémoglobine et $38,67$ μ g/mL pour l'inhibition de l' α -glucosidase. Les ZnO-NPs calcinées ont suivi avec des valeurs IC_{50} de $176,51$ μ g/mL et $42,90$ μ g/mL, respectivement. L'extrait de *H. scoparia* a montré une efficacité significative avec des valeurs IC_{50} de $245,32$ μ g/mL et $61,08$ μ g/mL. De plus, les résultats ont indiqué des interactions spontanées entre les ZnO-NPs et l'ADN ainsi que la BSA via des interactions électrostatiques, reflétées dans les paramètres K et ΔG . L'extrait de *H. scoparia* a montré la plus haute cytotoxicité; les ZnO-NPs non calcinées et calcinées ont également réduit efficacement la viabilité des cellules MCF7. Les résultats *in vivo* ont montré que la crème de *H. scoparia* a présenté les taux de cicatrisation les plus élevés, suivie des crèmes de ZnO-NP-UC et ZnO-NP-C. Les paramètres hématologiques et inflammatoires étaient plus favorables dans les groupes traités. Les études histologiques ont confirmé une amélioration de la cicatrisation de la peau, les traitements par *H. scoparia* et ZnO-NP montrant une efficacité significative.

En conclusion, cette étude a évalué de manière exhaustive le potentiel thérapeutique de l'extrait de *H. scoparia*, des ZnO-NPs calcinées et non calcinées dans la cicatrisation des plaies, le cancer et diverses activités biologiques. Les résultats suggèrent de nouvelles possibilités pour la phytothérapie et la nanothérapie dans les applications médicales.

Mots-clés : *Hammada scoparia*, nanoparticules d'oxyde de zinc, synthèse verte, activités biologiques, cicatrisation des plaies, rats albinos.

List of Figures

Number	Title	Page
Figure 1	<i>Hammada scoparia</i> species	9
Figure 2	Zinc Oxide Nanoparticles and powder	13
Figure 3	green synthesis mechanism of ZnONPs using plant extract	14
Figure 4	Schematic illustration shown Zinc oxide nanoparticles' antibacterial mechanism	15
Figure 5	ZnO Nanoparticles activities and applications	16
Figure 6	Functional effects of oxidative stress in regulatory systems and organs	18
Figure 7	Characteristics of Cancer Cells	24
Figure 8	the stages of skin healing, showcasing the cells and molecules pivotal in restoring a robust barrier	27
Figure 9	Map of the Wilaya of Biskra and position of study station	31
Figure 10	Sequential fractionation of aqueous extract using organic solvents	35
Figure 11	The green synthesis method of zinc oxide nanoparticles using <i>H.scoparia</i> extract.	38
Figure 12	Steps Involved in DNA Extraction	47
Figure 13	UV-Vis spectrum of the isolated DNA	48
Figure 14	Cream preparation process	52
Figure 15	Calibration curve of Gallic acid for determination of total phenolic content.	58
Figure 16	Calibration curve of Quercetin for determination of total flavonoids content.	59
Figure 17	Calibration curve of Catechin for determination of condensed tannins content.	59
Figure 18	HPLC/UV chromatogram profile of the aqueous extract of <i>Hammada scoparia</i> .	60
Figure 19	Formation of ZnO-NPs using <i>H.scoparia</i> extract after different time incubation during 24h.	62
Figure 20	Characterization of calcinated ZnO-NPs by XRD (A); UV-vis spectroscopy (B); SEM micrographs (C); and EDX detection of ZnO-NPs (D); FTIR spectrum (E).	64
Figure 21	Characterization of uncalcinated ZnO-NPs by XRD (A); UV-vis spectroscopy (B); SEM micrographs (C); and EDX detection of ZnO-NPs (D); FTIR spectrum (E).	65
Figure 22	α - glucosidase inhibition of <i>Hammada scoparia</i> extract, uncalcined and calcined ZnO-NPs and positive control (Acarbose).	69

Figure 23	Microscopic observation of Morphological characteristics of isolated LAB strain from row Goat's milk.	71
Figure 24	Carbohydrate fermentation strip of LAB strain isolated from row goat's milk were tested using the API 10 S strip.	71
Figure 25	PCR amplification of 16S rRNA region of isolated LAB strain; a: Negative Control, b: Amplified 16S rRNA of the isolated strain, c: Molecular marker + 100 bp DNA ladder.	73
Figure 26	A neighbor-joining phylogenetic tree based on 16 S rRNA gene sequences of the <i>Bacillus</i> isolated strain with the closest hits obtained from the NCBI GeneBank.	74
Figure 27	Effect of <i>Hammada scoparia</i> extract, uncalcined ZnO-NPs, and calcined ZnO-NPs on <i>Bacillus pumilus</i> strain, A: test of Acid tolerance, test of Bile tolerance, test of cell surface hydrophobicity.	75
Figure 28	Cyclic voltammograms of 2 mM S1 and S2 recorded at 0.1V s ⁻¹ potential sweep rate on GC disk electrode at 298K in the absence and presence of increasing concentration of DNA and BSA in DMSO with supporting electrolyte 0.1 M Bu ₄ NBF ₄	77
Figure 29	Plots of $\log \left(\frac{1}{1 - (i_p/i_{p_0})} \right)$ versus $\log 1/[BM]$ used to calculate the binding constants of the studied compounds with DNA and BSA	88
Figure 30	UV-visible absorption spectra of 2 mM of S1 and S2 in presence of increasing concentrations of DNA and BSA in DMSO	80
Figure 31	Plots of $A_0/(A - A_0)$ versus $1/[BM]$ used to calculate the binding constants of S1 and S2 with DNA and BSA	81
Figure 32	Cytotoxic effects of the <i>Hammada scoparia</i> extract, uncalcined ZnO-NPs, and calcined ZnO-NPs samples on MCF7 cells using the MTT assay	82
Figure 33	Time schedule of the experiment <i>in vivo</i> wound healing activity of different cream treatment formulations; n = 5.	85
Figure 34	Wound healing rate at day 4, day 7,10, and day 13 <i>in vivo</i> treatment of different cream treatment formulations; n = 5.	86
Figure 35	Mean of Red Blood Cell Levels on Day 13 of Treatment Groups: <i>H. scoparia</i> , ZnO-NPs-UC, ZnO-NPs-C, DOUCE PLUS, Base, and No cream; n = 5	87
Figure 36	Mean of White Blood Cell Levels on Day 13 of Treatment Groups: <i>H. scoparia</i> , ZnO-NPs-UC, ZnO-NPs-C, DOUCE PLUS, Base, and No cream; n = 5.	87
Figure 37	Mean of Blood Platelets Levels on Day 13 of Treatment Groups: <i>H. scoparia</i> , ZnO-NPs-UC, ZnO-NPs-C, DOUCE PLUS, Base, and No cream; n = 5.	87
Figure 38	Mean of C-Reactive Protein Levels on Day 13 of Treatment Groups: <i>H. scoparia</i> , ZnO-NPs-UC, ZnO-NPs-C, DOUCE PLUS, Base, and No cream treatments; n = 5.	88

Figure 39	Mean of Sedimentation Rate on Day 13 of Treatment Groups: <i>H. scoparia</i> , ZnO-NPs-UC, ZnO-NPs-C, DOUCE PLUS, Base, and No cream treatments; n = 5.	89
Figure 40	Microscopic observation of a histological section of skin wound in different experimental groups, No Wound + No cream treatment group (A), Wound + <i>H.scoparia</i> cream treatment group (B), Wound + ZnO-NPs-UC cream treatment group (C) Wound + ZnO-NPs-C cream treatment group (D), Wound + DOUCE PLUS [®] cream treatment group (E), Wound + Base cream treatment group (F) and Wound + No cream treatment group (G), magnification x40.	90
Figure 41	Microscopic observation of a histological section of skin wound in different experimental groups, No Wound + No cream treatment group (A), Wound + <i>H.scoparia</i> cream treatment group (B), Wound + ZnO-NPs-UC cream treatment group (C) Wound + ZnO-NPs-C cream treatment group (D), Wound + DOUCE PLUS [®] cream treatment group (E), Wound + Base cream treatment group (F) and Wound + No cream treatment group (G), magnification x100.	91

LIST OF TABLES

Number	Title	Page
Table 1	Phytochemical compounds identified from <i>Hammada scoparia</i> .	10
Table 2	Biological activities of <i>Hammada scoparia</i> .	11
Table 3	Categories of sunscreens based on the value of the SPF.	42
Table 4	Absorbance Ratio of Isolated DNA	49
Table 5	Different Phytochemical of the aerial part of <i>Hammada scoparia</i> (Pomel) Iljin.	57
Table 6	Yields of Aqueous extracts of <i>Hammada scoparia</i> (Pomel) Iljin.	57
Table 7	Phenolic compound contents in aqueous extract of the species <i>Hammada scoparia</i> .	58
Table 8	HPLC results of the aqueous extract of <i>Hammada scoparia</i> .	61
Table 9	Antioxidant activity of <i>Hammada scoparia</i> extract, uncalcined ZnO-NPs, and calcined ZnO-NPs using ABTS assay	66
Table 10	Antioxidant activity of <i>Hammada scoparia</i> extract, uncalcined ZnO-NPs, and calcined ZnO-NPs using DPPH assay	67
Table 11	Antioxidant activity of <i>Hammada scoparia</i> extract, uncalcined ZnO-NPs, and calcined ZnO-NPs using FRAP assay	67
Table 12	Photoprotective activity of <i>Hammada scoparia</i> extract, uncalcined ZnO-NPs, and calcined ZnO-NPs using SPF assay.	68
Table 13	Anti-inflammatory activity of <i>Hammada scoparia</i> extract, uncalcined ZnO-NPs, and calcined ZnO-NPs using albumin denaturation assay.	68
Table 14	Anti-diabetic activity of <i>Hammada scoparia</i> extract, uncalcined ZnO-NPs, and calcined ZnO-NPs using hemoglobin glycosylation assay.	69
Table 15	Anti-diabetic activity of <i>Hammada scoparia</i> extract, uncalcined ZnO-NPs, and calcined ZnO-NPs using α -glucosidase inhibition assay.	70
Table 16	Morphological, physiological, and biochemical characteristics of bacterial strains isolated from Algerian Goat's milk.	71
Table 17	Biochemical identification of lactic acid strain bacteria using API 10 S kits.	72
Table 18	Binding constants and binding free energies values for the studied compounds with DNA and BSA from CV data	79
Table 19	Binding constant and binding free energy values for S1 and S2 with DNA and BSA from UV data	81
Table 20	Cytotoxic effects of the <i>Hammada scoparia</i> extract, uncalcined ZnO-NPs, and calcined ZnO-NPs samples on MCF7 cells using the MTT assay	83
Table 21	Physical analyzes of formulated cream	83

LIST OF ABBREVIATION

A: Absorbance
ABTS: 2,2'-azino-bis(3-ethylbenzothiazoline-6-sulfonic acid
DMSO: Dimethyl sulfoxide
DNA: Deoxyribonucleic acid
DPPH: 2,2'-Diphenyl-1-picrylhydrazyl
DW: Dry weight
EC₅₀: The effective concentration
EDTA: Ethylenediaminetetraacetic acid
FeCl₃: Ferric chloride test
GLDH: Glutamate dehydrogenase
GRA: Granulocytes
HGB: Hemoglobin
HPLC: High performance liquid chromatography
IC₅₀: The half maximal inhibitory concentration
MCF-7: Michigan cancer foundation-7
NO•: Nitric oxide
O₂•⁻: Superoxide anion radical
OH•: Hydroxyl ion
PBS: Phosphate-buffered saline
pH: Potential of hydrogen
PLT: Platelets
RBC: Red blood cell
RO•: Alkoxy
ROO•: Peroxyl
ROS: Reactive oxygen species
SOD: Superoxide dismutase
SPF: Sun protected factor
TCA: Trichloroacetic acid
TPC: Total protein content
WBC: White blood cell
WHO: World Health Organizatio

SOMMAIRE

Acknowledgment	
Dedications	
ABSTRACT	
الملخص	
Résumé	
List of Figures	
List Of Tables	
List Of Abbreviation	
Sommaire	
Introduction	
Part I: Bibliographic part	
Chapter I: <i>Hammada scoparia</i> (pomel) Iljin	
1. Chenopodiaceae family	8
2. <i>Hammada scoparia</i>	8
3. Synonyms and Nomenclatures	8
4. Taxonomic Classification	8
5. Ecology and Distribution	9
6. Botanical Discription	9
7. Ethnomedicinal Uses	9
8. Phytochemical Constituents	10
9. Previous studies of Biological Activities of <i>Hammada scoparia</i>	10
9.1 .Antioxidant activity	11
9.2 .Antibacterial activity	11
9.3 .Antidiabetic activity	11
9.4 .Antileukemic activity	11
Chapter II: Zinc Oxide Nanoparticles	
1. Nanotechnology	13
2. Zinc Oxide Nanoparticles	13
3. ZnO NPs synthesis methods	13
3.1 .Physical synthesis methods	13
3.2 Chemical synthesis methods	14
3.3 Green synthesis methods	14
4. Characterizations of ZnO nanoparticles	14
4.1. UV-visible spectroscopy	14
4.2. Fourier Transform Infrared Spectroscopy (FTIR)	14
4.3. X-ray diffraction	15
4.4. Scanning electron microscopy (SEM)	15
4.5. Energy Dispersive Spectroscopy (EDS)	15
5. Biological activities of ZnO nanoparticles	15

5.1. Antimicrobial activity	15
5.2. Anticancer Activity	16
5.3. Anti-inflammatory Activity	16
Chapter III: Evaluated Biological activities	
1. Antioxidant activity	18
1.1. Antioxidant compounds	18
1.2. Antioxidant mechanisms	19
2. Anti-inflammatory activity	19
2.1. Inflammation	19
2.2. Inflammation and protein denaturation	19
3. Photoprotective activity	19
3.1. Solar radiation effect on the skin	19
3.2. Photoprotection	20
3.3. Photoprotective of secondary metabolites	20
4. Antidiabetic Activity	20
4.1. Diabetes Mellitus	20
4.2. Diabetes Mellitus indices	20
4.2.1. Postprandial Hyperglycemia	20
4.2.2. Glycated Hemoglobin (HbA1c)	21
4.3. Mechanisms of Action of Antidiabetic Agents	21
4.3.1. Biguanides	21
4.3.2. Sulfonylureas	21
4.3.3. Non-sulfonylurea Insulin Secretagogues (Glinides)	21
4.3.4. GLP-1 Receptor Agonists	21
4.3.5. DPP-4 Inhibitors (Gliptins)	21
4.3.6. α -Glucosidase Inhibitors	22
4.4. Phytotherapy for Diabetes	22
5. Probiotics activity	22
5.1. Probiotics	22
5.2. Prebiotics	22
5.3. Synbiotic	22
5.4. Probiotic role on human Health	22
5.5. Probiotics mechanisms	23
5.5.1. Production of antimicrobial substances	23
5.5.2. Enhancement of intestinal immune system	23
5.6. Properties and criteria for selecting probiotic strains	23
5.6.1. Resistance to gastric acidity	23
5.6.2. Resistance to bile salts	23
5.6.3. Adhesion to epithelial cells	24
5.6.4. Antibiotic resistance	24
6. Anti-cancer Activity	24
6.1. Cancer	24

6.2. Cancer cells characteristics	24
6.3. Treatment	24
6.4. Biological Target in Cancer Treatment	25
6.4.1. Cancer cell lines	25
6.4.2. DNA of cancer cell	25
6.4.2.1. Covalent Interaction with DNA (Alkylating Agents)	25
6.4.2.2. Non-covalent Interaction	25
a. Intercalation Binding	25
b. Groove Binding	26
6.4.2.3. Electrostatic Interactions	26
6.4.2.4. DNA-Degrading Agents	26
5.6. Cancer Phytotherapy	26
7. Wound Healing Activity	26
7.1. Wound Definition	26
7.2. Modes of Wound Healing	26
7.2.1. Primary Intention Healing	26
7.2.2. Secondary Intention Healing	26
7.2.3. Tertiary Intention Healing	27
7.3. Mechanisms of Wound Healing	27
7.3.1. Hemostasis	27
7.3.2. Inflammation	27
7.3.3. Proliferation	28
7.3.4. Remodeling	28
7.4. Wound Healing Treatment	28
7.4.1. Healing dermatological ointments and creams	28
7.4.2. Wound Healing Phytotherapy	28
Part II: Experimental part	
Chapter I: Material & Methods	
1. Materials	31
1.1. Plant material	31
1.2. Milk samples	31
1.3. Blood samples	31
1.4. Cells	32
1.5. Animals	32
1.6. Chemicals	32
2. Methods	32
2.1. Phytochemical analysis of <i>H. Scoparia</i>	32
2.1.1. Phytochemical Screening	32
2.1.1.1. Alkaloids	32
2.1.1.2. Flavonoids	33
2.1.1.3. Terpenoids	33
2.1.1.4. Saponins	33

2.1.1.5. Tannins	33
2.1.1.6. Cardiac glycosides	33
2.1.1.7. Mucilages	33
2.1.1.8. Anthocyanins	33
2.1.1.9. Leuco-anthocyanins	34
2.1.1.10. Steroids	34
2.2. Aqueous extract preparation	34
2.2.1. Extraction yield	34
2.2.2. Preparation of extract fractions	34
2.3. Colorimetric analysis	35
2.3.1. Total phenolics content (TPC)	35
2.3.2. Total flavonoid contents (TFC)	36
2.3.3. Total tannins content (TTC)	36
2.4. Chromatographic Analysis	36
2.4.1. HPLC Analysis	36
2.4.2. LC-MS-MS Analysis	37
2.5. Green synthesis of calcinated and uncalcinated ZnO-NPs	37
2.6. Characterization of ZnO-NPs	38
2.6.1. UV-visible spectroscopy	38
2.6.2. Fourier Transform Infrared Spectroscopy (FTIR)	38
2.6.3. X-ray diffraction	39
2.6.4. Scanning electron microscopy (SEM)	39
2.6.5. Energy Dispersive Spectroscopy (EDS)	40
2.7. <i>In vitro</i> biological activities	40
2.7.2. Antioxidant activity	40
2.7.1.1. ABTS radical scavenging assay	40
2.7.1.2. DPPH radical scavenging assay	41
2.7.1.3. Ferric-reducing antioxidant power (FRAP) assay	41
2.7.2. Photoprotective activity	42
2.7.3. Anti-inflammatory activity	42
2.7.4. Anti-diabetic activity	43
2.7.4.1. Non-enzymatic hemoglobin glycosylation	43
2.7.4.2. Inhibition of α -glucosidase enzyme	44
2.7.5. Probiotic Activity	44
2.7.5.1. Characterization of probiotic properties	44
2.7.5.2. Phenotypic characterization	45
2.7.5.3. Molecular identification	45
2.7.5.4. Synbiotic effect Evaluation	46
2.7.6. Anticancer Activity	46
2.7.6.1. DNA interaction study	46
2.7.6.2. UV-visible spectroscopic DNA/BSA interaction study	49
2.7.6.3. Cytotoxicity activity	50

2.7.6.3.1. Cell Culture	50
2.7.6.3.2. MTT Assay	51
2.7.7. <i>In vivo</i> Wound Healing activity <i>In vivo</i> Wound Healing activity	51
2.7.7.1. Elaboration of wound healing creams	51
a. Ingredients used in this cream	51
b. Formulation of Wound healing cream	52
c. Physical analyzes of formulated cream	52
2.7.7.2. Biological evaluation of creams	53
2.7.7.3. Histological study	54
2.7.8. Statistical analysis	55
Chapter II: Results	
I. Results	57
1. Phytochemical screening of major secondary metabolites	57
2. Yields of <i>Hammada scoparia</i> (Pomel) Iljin Extract	57
3. Colorimetric analysis	58
3.1. Total polyphenol content	58
3.2. Total flavonoid content	58
3.3. Condensed tannin content	59
4. LC-MS-MS Analysis	59
5. Green synthesis of ZnO-NPs	61
6. Characterization of ZnO-NPs	62
6.1. XRD analysis of photosynthesized ZnO-NPs	62
6.2. UV-visible spectroscopy	63
6.3. Scanning Electron Microscopy (SEM)	63
6.4. Energy Dispersive X-ray Spectroscopy (EDX).	63
6.5. Fourier transforms infrared analysis (FT-IR)	66
7. <i>In vitro</i> biological activities	66
7.1. Antioxidant activity	66
7.1.1. ABTS radical scavenging assay	66
7.1.2. DPPH radical scavenging assay	67
7.1.3. Ferric-reducing antioxidant power (FRAP) assay	67
7.2. Photoprotective activity	67
7.3. Anti-inflammatory activity	68
7.4. Anti-diabetic activity	68
7.4.1. Non-enzymatic hemoglobin glycosylation	68
7.4.2. Inhibition of α -glucosidase enzyme	69
7.5. Probiotic Activity	70
7.5.1. Probiotic characterization	70
7.5.1.1. Phenotypic characterization	70
7.5.1.2. Molecular identification	72
7.5.2. Synbiotic effect Evaluation	75
7.6. Anticancer Activity	76

7.6.1. BSA/DNA with Samples interaction study	76
7.6.1.1. Cyclic Voltametry interaction study	76
a. Binding constants	76
b. Binding free energy	79
7.6.1.1. Electronic Spectroscopy Interaction Study	79
a. Binding constants	80
b. Binding free energy	81
7.6.2. Cytotoxicity activity	82
7.7. <i>In vivo</i> Wound Healing activity of of <i>H.Scoparia</i> extract / ZnO-NPs	83
7.7.1. Physical analyzes of formulated cream	83
7.7.2. <i>In vivo</i> evaluation of creams	83
7.7.3. Hematological Parameters	86
7.7.4. Inflammation Parameters	88
7.7.5. Histological study	89
Chapter III: Discussion	
General conclusion & Perspectives	120
References	124
Annexes	158

Introduction

INTRODUCTION

The field of nanotechnology has seen a rapid expansion over the past few decades, particularly due to its potential to revolutionize various industries by allowing the manipulation of materials at the atomic or molecular scale. Miniaturization, often referred to as "the art of making things smaller," is at the core of this transformative science. This trend aims to uncover new behaviors of matter, enhance functionality, and improve efficiency across numerous fields, from medicine to electronics. As the world gravitates towards more compact, faster, and cost-effective solutions, nanoparticles (NPs) have become one of the most sought-after materials due to their distinctive properties and applications. When scaled down to the nanometer range, materials exhibit novel physicochemical characteristics that differ significantly from their bulk counterparts, such as increased surface area, reactivity, and enhanced mechanical, optical, and thermal properties (Bayda *et al.*, 2019).

Nanotechnology, specifically the use of nanoparticles, has already demonstrated immense promise in the field of medicine. In particular, NPs have been used as tools for drug delivery, wound healing, diagnostic imaging, and as therapeutic agents in the treatment of various diseases, including cancers, autoimmune disorders, and infections. Their small size allows them to easily penetrate biological membranes and interact with cells and tissues, making them highly effective in diagnosing and treating diseases at the molecular level. Furthermore, the high surface area-to-volume ratio of NPs enables enhanced interaction with biological molecules, improving the bioavailability of drugs and allowing for more precise targeting of disease sites, which minimizes side effects and optimizes therapeutic efficacy (Yetisgin *et al.*, 2020).

Among the numerous types of nanoparticles, zinc oxide (ZnO) nanoparticles have gained significant attention due to their biocompatibility, low toxicity, and wide range of applications. ZnO nanoparticles are used in various industries, including medicine, cosmetics, and electronics. Their versatility stems from their excellent properties, such as UV absorption, antibacterial activity, and anti-inflammatory effects. These properties make ZnO nanoparticles an ideal candidate for use in wound healing, as well as in the development of therapeutic ointments, sunscreens, and other personal care products (Zouhair, 2007). Additionally, the use of ZnO nanoparticles in controlled drug delivery systems is another promising application, where their unique properties allow for the targeted release of drugs in a controlled and sustained manner, enhancing the effectiveness of the drug while reducing systemic toxicity.

As the demand for safer, more sustainable, and eco-friendly manufacturing methods increases, green synthesis has emerged as a popular and promising alternative to traditional chemical synthesis methods. Green synthesis utilizes natural resources, particularly plant extracts, to produce nanoparticles in a way that is both environmentally friendly and cost-effective. This method offers several advantages, such as being free from toxic chemicals, reducing energy consumption, and providing better control over nanoparticle characteristics like size, shape, and dispersion. Plants have long been a source of medicinal and bioactive compounds, and their extracts are rich in antioxidants, polyphenols, and flavonoids, which can aid in the stabilization and reduction of metal ions into nanoparticles. By utilizing plant-based resources, green synthesis not only reduces the ecological footprint of nanoparticle production but also produces nanoparticles with improved biological activity due to the synergistic effects of the plant's secondary metabolites (Iravani, 2011).

Numerous plants have already been investigated for their potential in green synthesis, with several species showing promising results in the synthesis of ZnO nanoparticles. For example, *Cynara scolymus* (Rajapriya *et al.*, 2019), *Crataegus microphylla* (Naghizadeh *et al.*, 2020), and *Zingiber officinale* (Ali *et al.*, 2020) have all been successfully used to produce ZnO nanoparticles with enhanced properties. These plant extracts contain compounds such as polyphenols, flavonoids, and alkaloids, which not only facilitate the reduction of metal salts into nanoparticles but also improve their stability and biological activity. The increasing number of plant species being explored for this purpose highlights the vast potential of green synthesis in developing novel, eco-friendly nanomaterials for a wide range of applications, particularly in the fields of medicine and biotechnology.

Given these advancements, it is clear that the combination of nanotechnology and green synthesis represents a powerful approach for the future of nanomedicine. By harnessing the potential of plant extracts and sustainable synthesis methods, researchers are poised to develop innovative and effective treatments for various diseases while also minimizing the environmental impact of nanoparticle production. As the field continues to evolve, the development of plant-based ZnO nanoparticles could play a pivotal role in advancing the next generation of therapeutic agents, medical devices, and diagnostic tools (Naghizadeh *et al.*, 2020).

Hammada scoparia, a member of the Chenopodiaceae family, is a plant that has garnered significant attention in traditional medicine, particularly within North African cultures. Its

therapeutic potential has been well-documented for a variety of ailments, including cancer, hepatitis, inflammation, and obesity prevention (Ezzeddine *et al.*, 2016). With a rich history of medicinal use, this plant contains a variety of bioactive compounds, including polyphenols, flavonoids, and alkaloids, which are believed to contribute to its healing properties. These compounds have shown promise in reducing the severity of numerous diseases, offering a natural and holistic approach to health management. Given the growing demand for environmentally sustainable and safe alternatives in modern medicine, the green synthesis of nanoparticles has emerged as an exciting field of research.

Zinc oxide (ZnO) nanoparticles, in particular, have gained considerable interest due to their unique physicochemical properties, such as their high surface area, biocompatibility, and versatile applications in drug delivery, wound healing, and disease treatment. In this context, utilizing *Hammada scoparia* as a green source for the synthesis of ZnO nanoparticles presents a valuable opportunity to develop eco-friendly and cost-effective alternatives to traditional chemical synthesis methods. By leveraging the plant's natural phytochemicals, this approach not only ensures the safe production of ZnO nanoparticles but also preserves the beneficial properties of the plant itself (Bayda *et al.*, 2019).

The primary objective of this study is to explore the green synthesis of ZnO nanoparticles from *Hammada scoparia*, focusing on both calcined and non-calcined forms of ZnO. Calcining the nanoparticles at high temperatures can alter their structural properties, potentially enhancing their stability and performance in various applications. Therefore, the study aims to compare and contrast the properties of these two forms of ZnO nanoparticles, examining factors such as crystal structure, size, morphology, and surface area. The biological activities of the synthesized nanoparticles will also be a key focus of this research, with a particular emphasis on their potential for wound healing, anti-inflammatory effects, and antimicrobial properties.

In pursuit of these objectives, the study will proceed with the following research axes:

1. **Phytochemical Analysis of *Hammada scoparia*:** The first step of the study will involve a detailed phytochemical analysis of *Hammada scoparia* to identify the bioactive compounds present in the plant extract. This will help determine which components of the plant contribute to the reduction and stabilization of metal ions during the green synthesis process of ZnO nanoparticles.
2. **Synthesis of Calcined and Non-Calcined ZnO Nanoparticles:** The next step will involve the preparation of both calcined and non-calcined ZnO nanoparticles through

the green synthesis method, using *Hammada scoparia* extract as a reducing and stabilizing agent. The calcined form will undergo high-temperature treatment to investigate the effect of heat on the structural and functional properties of the nanoparticles.

3. **Characterization of the Nanoparticles:** The synthesized nanoparticles will be thoroughly characterized using a variety of advanced techniques, such as X-ray diffraction (XRD), scanning electron microscopy (SEM), and other spectroscopic methods. These techniques will help identify the crystallographic structure, morphology, particle size, and distribution of the ZnO nanoparticles, providing essential insights into their properties.
4. **Evaluation of Biological Activities:** The next phase of the research will focus on assessing the biological activities of the green-synthesized ZnO nanoparticles. This will include *in vitro* studies to evaluate their potential for antioxidant, antiinflammatory activity, photoprotective, antidiabetics and synbiotic properties. Additionally, the plant extract itself will be tested to determine its individual contribution to these biological activities.
5. ***In Vivo* Wound Healing Study:** Finally, an *in vivo* study will be conducted to assess the wound healing potential of both the *Hammada scoparia* extract and the green-synthesized ZnO nanoparticles (both calcined and non-calcined). This study will aim to determine whether the nanoparticles enhance wound closure and tissue regeneration, with a particular focus on their healing efficacy compared to the plant extract alone.

By integrating the green synthesis approach with the therapeutic potential of *Hammada scoparia*, this study aims to contribute to the growing body of knowledge on plant-based nanomaterials and their applications in medicine. The successful synthesis and characterization of ZnO nanoparticles could lead to the development of novel, environmentally friendly, and biocompatible treatments for a range of medical conditions, particularly those involving inflammation and wound healing.

This thesis is divided into two parts. The first part includes a chapter focused on nanotechnology. The second part consists of a presentation of the studied plant and a chapter detailing the evaluated biological activities.

The second part will cover the experimental evaluations of the biological activities examined in this study. Three chapters "Materials & Methodes", "Results", and "Discussion" are presented before summarizing the work in a general conclusion and suggesting potential avenues for future research based on these findings.

Part I:

Bibliographic part

Chapter I:

Hammada scoparia (Pomel)

Iljin

1. Chenopodiaceae family

The Chenopodiaceae family, comprising 98 genera and roughly 1,400 species, is often utilized in traditional medicine and plays a significant role in daily life (Gelin *et al.*, 2003). These plants commonly thrive in desert and semi-desert regions, salt marshes, saline coastal or inland areas, and ruderal environments. Many species within the Chenopodiaceae family are vital to dry or ruderal ecosystems (Heklau *et al.*, 2012).

2. *Hammada scoparia* (Pomel) Iljin

Hammada scoparia is, a species belonging to the Chenopodiaceae family, is renowned for its therapeutic properties in traditional North African medicine, including the treatment of cancer, hepatitis, inflammation, and the prevention of obesity (Ezzeddine *et al.*, 2016). The importance of natural substances in mitigating the severity of diseases is well recognized.

3. Synonyms and Nomenclatures

Hammada scoparia, also known scientifically as *Hammada scoparia* (Pomel) Iljin, has a complex taxonomic history with various synonyms, including *Haloxylon scoparium* (Pomel) Bge., *Haloxylon articulatum* ssp. *scoparium* (Pomel) Batt., and *Arthrophytum scoparium* (Pomel) Iljin. These names reflect its evolutionary and morphological traits that have led to reclassification over time (Bouaziz *et al.*, 2016; Édouard *et al.*, 2010). In traditional Algerian settings, it is commonly known as “Rimth” (Taïr *et al.*, 2016). Recognizing these synonyms and regional names is essential for accurate research and traditional medicinal use.

4. Taxonomic Classification

Kingdom: Plantae;

Subkingdom: Tracheobionta;

Phylum: Spermatophytes;

Superdivision: Angiosperms;

Division: Magnoliophyta;

Class: Magnoliopsida;

Subclass: Caryophyllidae;

Order: Caryophyllales;

Family: Chenopodiaceae;

Genus: Hammada;

Species: *Hammada scoparia* (Pomel) Iljin (Boucherit *et al.*, 2018) .

5. Ecology and Distribution

Hammada scoparia is a plant species that exhibits a preference for salty soils and thrives in arid to semi-arid environments. Its ecological distribution spans several regions across North Africa, including Morocco, Algeria, Libya, and Egypt. Additionally, it is found in Lebanon, Syria, Palestine, Western Sahara, southern Spain, and extends into portions of Iran and Turkey. In these habitats, *H. scoparia* plays ecological roles, such as soil stabilization and contributing to biodiversity resilience in arid landscapes (Karous *et al.*, 2020; Nounah *et al.*, 2019).

6. Botanical Discription

Hammada scoparia, a grey-brown woody shrub of the Chenopodiaceae family, grows up to 1 meter and is noted for its unique morphology and resilience (El-Shazly & Wink, 2003). This shrub has tiny, triangular, articulated leaves and slender, fleshy branches that change color with the seasons, ranging from dark green to red (Hafidha *et al.*, 2017; Boucherit *et al.*, 2018). Its solitary or clustered flowers have 5 sepals, wings, stamens, and 2 carpels, and its branches bear small, lenticular seeds in winter if conditions are humid. The plant's deep, mixed root system, extending 40 cm to 1.2 m, helps stabilize soil and reduce erosion, making *H.scoparia* beneficial for soil preservation (Boucherit *et al.*, 2018). This adaptability supports its use in both medicinal and environmental applications.

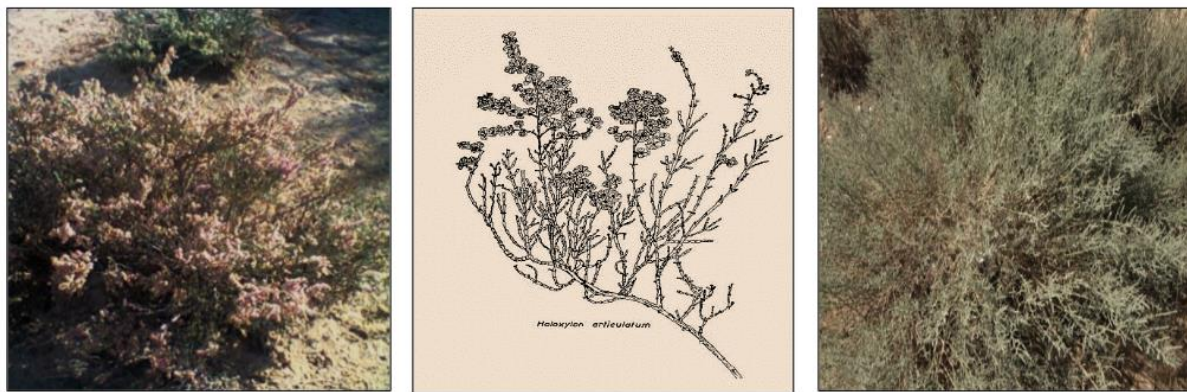


Figure 1. *Hammada scoparia* species (Benkherara *et al.*, 2021 ; Lachkar *et al.*, 2021 ; Ozenda, 2004), respectively.

7. Ethnomedicinal Uses

Hammada scoparia, a plant from the Chenopodiaceae family, is highly valued in North African traditional medicine for its wide range of therapeutic applications. It is traditionally used to prevent hepatitis, reduce inflammation, and manage obesity, with studies supporting its effectiveness in these areas (Ezzeddine *et al.*, 2016). Additionally, *H. scoparia* is known for its anti-cancer and antidiabetic properties, with extracts showing promise in the treatment of cancer and diabetes through methods such as decoctions, infusions, and cataplasms

(Boulanouar *et al.*, 2013; Saidi *et al.*, 2015; Bouaziz *et al.*, 2016; Hamza *et al.*, 2019; Taïbi *et al.*, 2020). Beyond these serious conditions, *H. scoparia* is used to treat hypertension, dermatitis, scabies, gastroenteritis, and food poisoning, while also promoting wound healing (Eddouks *et al.*, 2002; El-Hadri, 2019; Karous *et al.*, 2020). Its versatility makes it a valuable plant in traditional medicine for a variety of health issues.

8. Phytochemical Constituents

The phytochemical composition of *H. scoparia* has been the subject of extensive research, revealing a rich array of bioactive molecules. Among its notable constituents, the plant is particularly abundant in alkaloids and flavonoids, known for their biological activities. Table 1 highlights the principal compounds extracted and identified from *H. scoparia*:

Table 1. Phytochemical compounds identified from *Hammada scoparia*.

Class	Compound	Plant Part	Reference
Alkaloids	Carnegine (1)	Leaves	(Bouaziz <i>et al.</i> , 2016)
	N-methylisosalsoline (2)		
	Salsolidine (3)	Aerial Parts	(El-Shazly & Wink, 2003)
	β -carboline (4)		
Flavanols triglycerides	Isorhamnetin 3-O- β -D xylopyranosyl-(1 ^{'''} 3 ^{'''})- α L-rhamnopyranosyl-(1 ^{'''} 6 ^{'''})- β -D galactopyranoside	Leaves	(Salah <i>et al.</i> , 2002)
	Isorhamnetin 3-O- β -D apiofuranosyl-(1 ^{'''} 2 ^{'''}) [α L-rhamnopyranosyl-(1 ^{'''} 6 ^{'''})] - β -D Galactopyranoside		
	Isorhamnetin 3-O- α -L rhamnopyranosyl-(1 ^{'''} 2 ^{'''}) [α -L rhamnopyranosyl-(1 ^{'''} 6 ^{'''})] - β -D Galactopyranoside		
Flavone	Chrysoeriol	Stems	(Chao <i>et al.</i> , 2013)
Phenol	Catechol		
	Coumaric Acid		
	Cinnamic Acid		
Phenolic Acids	Caffeoylquinic Acid		
	Catechic acid		
	Syringic acid		
	Vanillic acid		
	Benzoic acid		

9. Previous studies of Biological Activities of *Hammada scoparia*

The biological activity of *Hammada scoparia* has been investigated extensively, as summarized in Table 2:

Table 2: Biological activities of *Hammada scoparia*.

Plant part	Activity	Reference
Aerial parts	Antioxidant	(Boulanouar <i>et al.</i> , 2013)
Leaves & stems		(Bouaziz <i>et al.</i> , 2016 ; Nounah <i>et al.</i> , 2019)
Aerial parts	Antidiabetic	(Benkherara <i>et al.</i> , 2021; Zerriouh, 2014)
Leaves & stems	Antimicrobial	(Bouaziz <i>et al.</i> , 2016 ; Nounah <i>et al.</i> , 2019)
Aerial parts		(Fatehi <i>et al.</i> , 2018 ; Lamchouri <i>et al.</i> , 2012)
Leaves	Antileukemic	(Bourogaa <i>et al.</i> , 2011)

9.1 .Antioxidant activity

H.scoparia is rich in phenolic compounds, making it an effective natural source of antioxidants. Its hydroalcoholic leaf extracts show strong antiradical activity, with a direct correlation between phenol content and antioxidant capacity (Nounah *et al.*, 2019; Bouaziz *et al.*, 2016). This antioxidant activity is attributed to its metal-reducing and chelating abilities, as well as its capacity to scavenge peroxy radicals (Boulanouar *et al.*, 2013).

9.2 .Antibacterial activity

H. scoparia has demonstrated strong antibacterial activity, particularly in its hydroethanolic and methanolic extracts, with inhibition zones of 8-30 mm against both Gram-positive and Gram-negative bacteria (Bouaziz *et al.*, 2016; Licá *et al.*, 2018). The alkaloid extract is notably effective, with minimum inhibitory concentration (MIC) values of 0.125-0.5 mg/ml and minimum bactericidal concentration (MBC) values of 0.25-2 mg/ml, showing strong action against *Citrobacter freundii* and *Acinetobacter baumannii*. (Nounah *et al.*, 2019).

9.3 .Antidiabetic activity

H. scoparia shows potential as an antidiabetic treatment, particularly through its methanolic extract, flavonoids, and alkaloids, which effectively inhibit α -amylase activity—a key enzyme in controlling postprandial hyperglycemia. Studies by Benkherara *et al.* (2021) and Zerriouh (2014) indicate that these components could be valuable in developing diabetes therapies.

9.4 .Antileukemic activity

Researchers are exploring *Hammada scoparia* extracts as a novel approach to overcoming CAM-DR in leukemia. CAM-DR occurs when leukemic cells resist chemotherapy by attaching to surfaces, like the extracellular matrix, making them harder to eliminate. *Hammada scoparia*, particularly its flavonoid component rutin, has been shown to induce apoptosis in adherent leukemic cells, helping to counteract CAM-DR and potentially improve chemotherapy effectiveness (Ezzeddine *et al.*, 2016).

Chapter II:
Zinc Oxide Nanoparticles

1. Nanotechnology

Nanotechnology is the branch that involves synthesizing, engineering and utilizing materials ranging in size from 1 to 100 nm, known as nanomaterials. (Joudeh and Linke, 2022). Nanoparticles possess unique physical and chemical properties due to their high surface area and nanometer size (Khan *et al.*, 2019). Nanoparticles are generally called particles controlled or tricked at the atomic level. The intrinsic properties of metal nanoparticles such as zinc oxide NPs are mainly characterized by their dimension, composition, morphology, and crystallinity. Reducing the size to the nanoscale can transform their chemical, mechanical, technological, architectural, morphological, and optical properties (Sirelkhatim *et al.*, 2015).

2. Zinc Oxide Nanoparticles

Zinc is an essential trace element found in muscles, bones, skin, and hard tissues of teeth (Pushpalatha *et al.*, 2022). Zinc oxide nanoparticles (ZnO NPs) are the second most abundant metal oxide after iron. They are inexpensive, safe, and easy to prepare (Lakshmipriya and Gopinath, 2021). ZnO NPs are an odorless white powder (Figure 2) with a molecular weight of 81.38 g/mol. Its many applications are due to its unique optical, morphological, catalytic, and photochemical properties, which can be easily modified according to needs by changing the size, doping with additional compounds, or adjusting the synthesis conditions (Pushpalatha *et al.*, 2022). ZnO presents a set of properties that allow its use in various applications, such as the pharmaceutical field. These properties are much more interesting than the solids in the nanometric state (Özgür, *et al.*, 2005).



Figure 2. Zinc Oxide Nanoparticles and powder (Azom, 2011; Azonano, 2013).

3. ZnO NPs synthesis methods

3.1 .Physical synthesis methods

Much work on the physical synthesis of zinc oxide has been published. These methods require high temperatures and the implementation of heavy infrastructure. These methods include vapour condensation, laser, and jet pyrolysis (Sun *et al.*, 2004).

3.2 Chemical synthesis methods

Chemical methods are more straightforward to implement, less expensive, and generally allow reasonable morphology control. The most relevant and encountered methods in the literature are sol-gel, Solvothermal/hydrothermal, electrodeposition, and precipitation (Pillai *et al.*, 2003).

3.3 Green synthesis methods

The synthesis of ZnO nanoparticles traditionally relies on physical and chemical methods, which often require high pressure, temperature, and energy, and can be costly and harmful (Ameen *et al.*, 2015; Chen & Ma, 2016). Chemical methods can also leave toxic residues, posing challenges for medical applications (Fan *et al.*, 2015; Parashar *et al.*, 2009). To address these issues, green synthesis methods using plant extracts and microorganisms have gained popularity. These methods are more cost-effective, environmentally friendly, and sustainable, as they minimize the use of toxic chemicals and waste production. Green synthesis, using plant-based materials, is simpler, reproducible, and yields stable nanoparticles, with phenolic compounds often playing a key role in the process (Mohanpuria, Rana & Yadav, 2008).

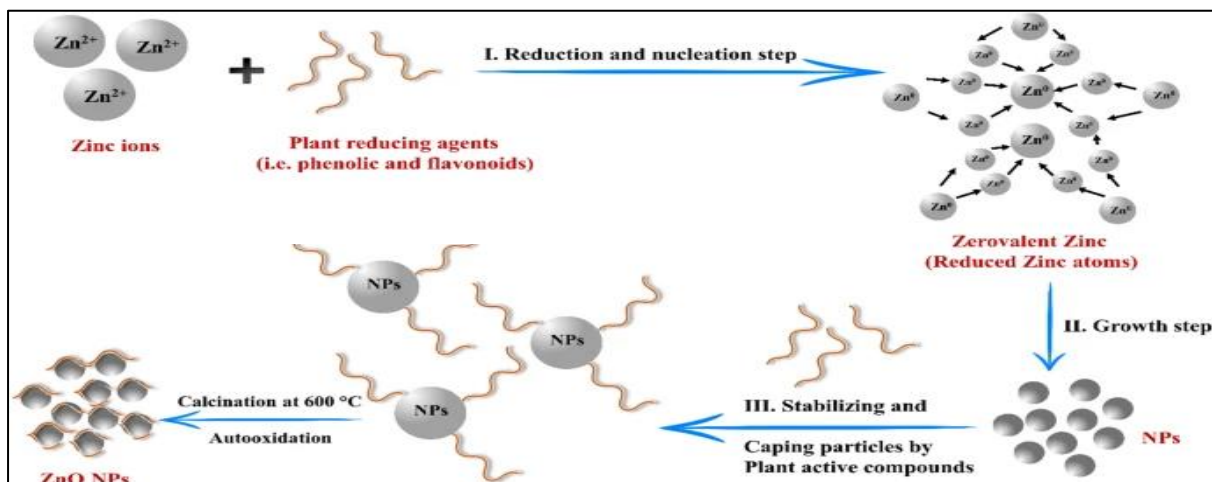


Figure 3. green synthesis mechanism of ZnONPs using plant extract (Abdelbaky *et al.*, 2023).

4. Characterizations of ZnO nanoparticles

The biosynthesized ZnO NPs can be characterized using different analytical techniques.

4.1. UV-visible spectroscopy

This technique measures light absorption across 200-1400 nm wavelengths, indicating the transitions of electrons from ground to excited states. Absorbance follows the Beer-Lambert law.

4.2. Fourier Transform Infrared Spectroscopy (FTIR)

FTIR identifies chemical bonds within compounds by observing vibrational transitions, producing spectra with distinct absorption bands characteristic of specific bond types.

4.3. X-ray diffraction

Ideal for powdered samples, XRD identifies crystal structures by analyzing diffraction patterns of X-rays scattered off the sample. Peaks in the pattern reveal details like crystal size, shape, and phase according to Bragg's law.

4.4. Scanning electron microscopy (SEM)

SEM scans a sample's surface with high-energy electrons to visualize surface morphology in high resolution. It generates 3D images but requires the sample to be coated with a conductive layer (Salman, 2020).

4.5. Energy Dispersive Spectroscopy (EDS)

EDS is utilized to gain insight into the elemental composition of metal nanoparticles, offering a foundational comprehension of the sample (Brongersma *et al.*, 2007).

5. Biological activities of ZnO nanoparticles

5.1. Antimicrobial activity

ZnO-NPs are considered a powerful and non-toxic antibacterial agent (Figure 4). Most of the conflicting activities have focused on the use of ZnO-NPs for coatings or nanocomposites. Various studies have also demonstrated and confirmed the antimicrobial effects of natural biological compounds. The size of the nanoparticles (Yamamoto, 2001; Cha & Chinnan, 2004).

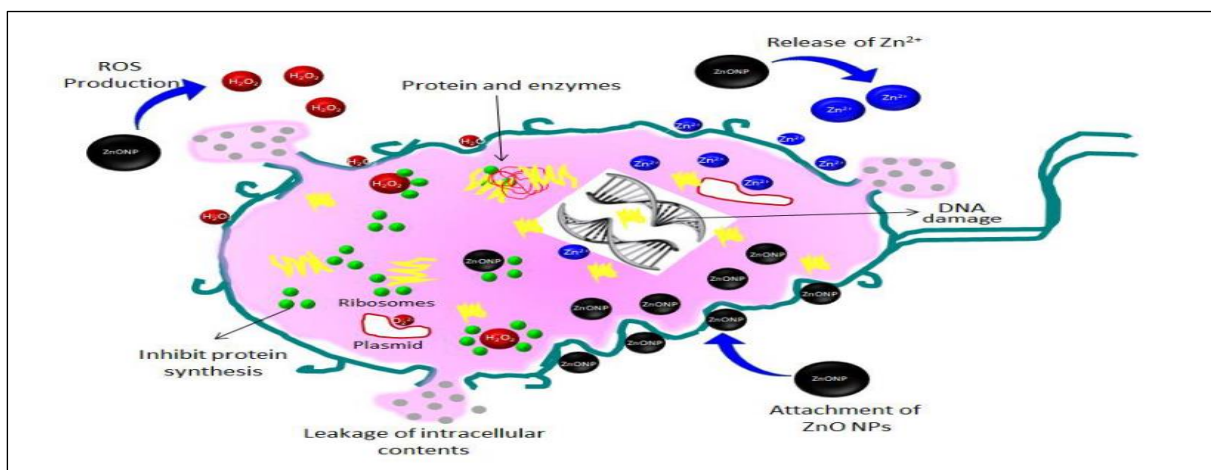


Figure 4. Schematic illustration shown Zinc oxide nanoparticles' antibacterial mechanism (Hamrayev, Shameli, & Korpayev, 2021).

ZnO-NPs exhibit strong antifungal properties, particularly effective against fungal pathogens that affect both agriculture and the food industry. Research has shown that ZnO-NPs can enhance the efficacy of fungicides, especially against fungi like *P. expansum* and plant pathogens such as *A. alternata*, *A. niger*, *B. cinerea*, *F. oxysporum*, and *P. expansum*.

(Rajakumar *et al.*, 2018). They also show significant antifungal activity against *C. albicans*, with MIC of 128 $\mu\text{g/ml}$ and fungicidal effects at 256 $\mu\text{g/ml}$ (Rajeshkumar *et al.*, 2018). ZnO-NPs inhibit fungal growth of *Aspergillus* and *Penicillium* at 30 $\mu\text{g/ml}$ (Randa *et al.*, 2015), and effectively reduce the growth of *Candida* isolates by 90% at MIC and by 99.9% at MFC (Rangeela *et al.*, 2019).

5.2. Anticancer Activity

ZnO-NPs offer a promising alternative to traditional cancer therapies, which can cause side effects and may not effectively target resistant cells (Noor, 2018; Doan *et al.*, 2020). Known for their biocompatibility, ZnO-NPs work by generating ROS that damage cancer cell mitochondria, inducing cell death (Olbert *et al.*, 2017). Studies show ZnO-NPs effectively inhibit various cancer cells, including A549 lung cancer cells and rhabdomyosarcoma RD cells, while showing minimal toxicity to healthy cells (Mishra *et al.*, 2017; Barui *et al.*, 2018; Rafique *et al.*, 2020).

5.3. Anti-inflammatory Activity

ZnO-NPs have gained attention for their anti-inflammatory properties. ZnO-NPs exhibit their anti-inflammatory effects through several mechanisms, including inhibiting pro-inflammatory cytokine release, suppressing myeloperoxidase activity, downregulating inducible nitric oxide synthase (iNOS) expression, blocking the NF- κ B pathway, and reducing mast cell degranulation (Agarwal *et al.*, 2019). Additionally, ZnO-NPs synthesized with Amla fruit extract have shown significant anti-inflammatory activity, with effects ranging between 80–90% (Sadhasivam *et al.*, 2020).

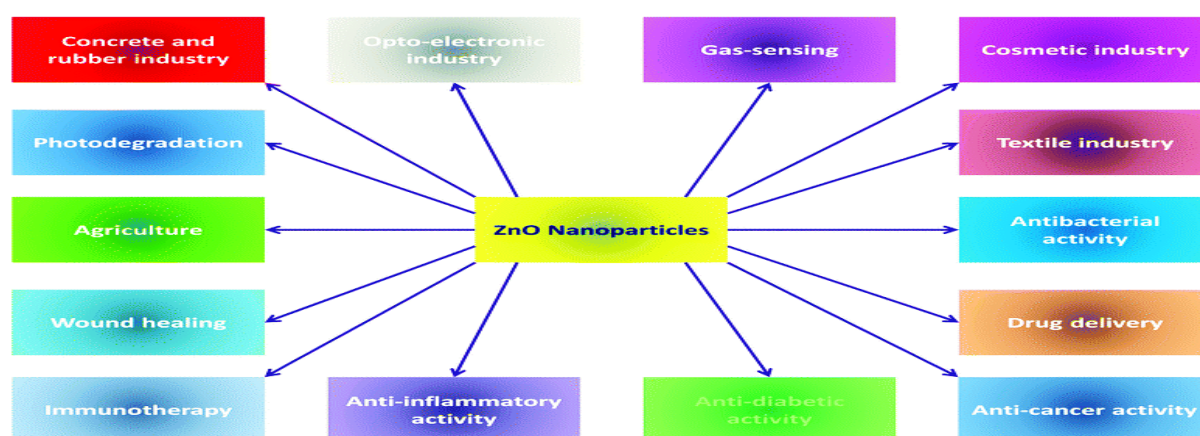


Figure 5. ZnO Nanoparticles activities and applications (Raha & Ahmaruzzaman, 2022).

Chapter III:

Evaluated Biological activities

1. Antioxidant activity

Oxidative stress occurs when ROS exceed the body's antioxidant defenses, leading to damage in cells, lipids, proteins, and DNA. This imbalance is linked to various diseases, including atherosclerosis, diabetes, and cancer (Zhang *et al.*, 2019). ROS can be generated during metabolism or due to external factors like pollution and UV exposure. Free radicals contribute to this stress, accelerating aging and degenerative conditions (Sayed, 2018).

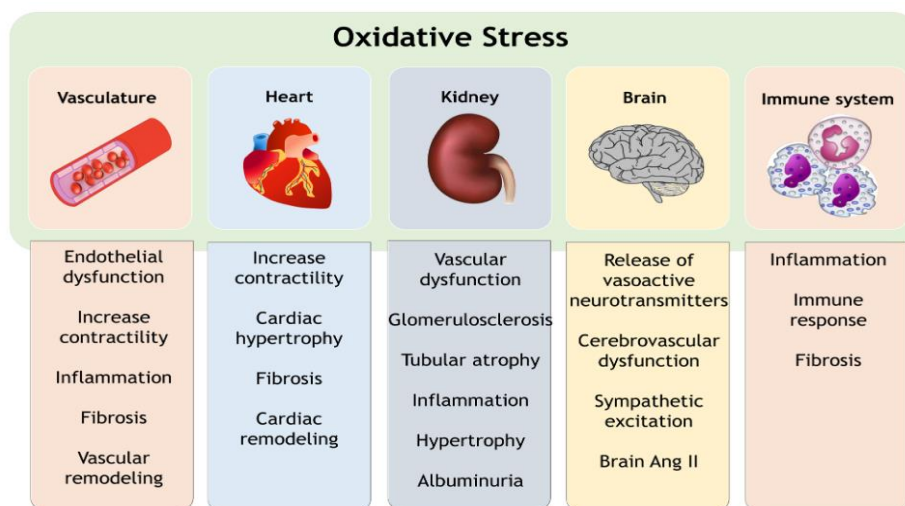


Figure 6. Functional effects of oxidative stress in regulatory systems and organs (Griendling *et al.*, 2021).

Antioxidants are substances that protect the body from the harmful effects of oxidative stress (Ouibrahim, 2015). The food industry increasingly values antioxidants in developing functional foods, as they help prevent degenerative diseases caused by free radicals and enhance the shelf life of these products (Peters, 2016). To assess the antioxidant potential of a compound or extract, the DPPH (diphenylpicrylhydrazyl) free radical scavenging test is commonly used, as DPPH is a stable free radical with an unpaired electron on a nitrogen atom (Dahmane *et al.*, 2017).

1.1. Antioxidant compounds

Antioxidants are essential in combating oxidative damage from ROS in both food and the human body. They work by neutralizing free radicals, preventing oxidation, and thus preserving food and safeguarding against chronic diseases. These include vitamins C and E, glutathione, and synthetic agents like BHT and BHA used in the food industry. Plant-derived antioxidants, found in fruits and vegetables, also provide significant health benefits by reducing oxidative stress and helping manage related conditions (Gulcin, 2020; Francenia *et al.*, 2019).

1.2. Antioxidant mechanisms

Antioxidant mechanisms operate through several strategies:

- Inhibition of free radical generation
- Direct scavenging of free radicals
- Conversion of harmful free radicals into less toxic forms
- Prevention of the synthesis of more harmful metabolites
- Interruption of the propagation of secondary oxidants in a chain reaction
- Restoration of damaged molecules
- Activation of the body's innate antioxidant defense mechanisms (Hunyadi, 2019).

2. Anti-inflammatory activity

2.1. Inflammation

Inflammation is a biological defense mechanism triggered by harmful agents like infections or injuries, involving immune cells that protect against pathogens. It can be acute, marked by increased blood flow and immune cell migration, or chronic, involving persistent tissue damage and repair. The process affects the vascular system, immune response, and various cell types, with symptoms such as redness, warmth, swelling, pain, and potential loss of function. Cellular changes occur in response to infection (Sá *et al.*, 2013; Azab *et al.*, 2016; Esho *et al.*, 2021).

2.2. Inflammation and protein denaturation

Inflammation is triggered by the release of arachidonic acid, which is converted into prostaglandins and leukotrienes through cyclooxygenase and lipoxygenase pathways (Khan *et al.*, 2015 ;Esho *et al.*, 2021). Denatured proteins also contribute to inflammation, linked to conditions like rheumatoid disorders, cataracts, and Alzheimer's disease. Targeting protein denaturation may offer therapeutic potential for these diseases (Osman *et al.*, 2016).

3. Photoprotective activity

3.1. Solar radiation effect on the skin

UV radiation, including UVC, UVB, and UVA, affects skin health in different ways. UVC is mostly absorbed by the ozone layer but can cause harm if it reaches the skin, leading to carcinogenic and mutagenic effects (Araújo & Souza, 2008). UVB, which causes erythema, DNA damage, and cancer, is highly energetic but less penetrating (Simis & Simis, 2006). UVA penetrates deeper into the skin, contributing to aging, cancer, and photosensitivity (Balogh *et al.*, 2011). Peak UV radiation occurs between 10-11 am and 4-5 pm, increasing the risk of skin damage (Toffetti & De Oliveira, 2006). While prolonged exposure raises skin cancer risk (Chiari-Andréo *et al.*, 2020), moderate sun exposure offers benefits like vitamin D3 production and improved mood (Juzeniene & Moan, 2012).

3.2. Photoprotection

Sunscreens, introduced in 1928 and regulated by the FDA in 1978, protect the skin from UV radiation through active photoprotective agents and base ingredients like moisturizers and preservatives (Toffetti & De Oliveira, 2006; Flor *et al.*, 2007). Their effectiveness depends on factors like absorption spectrum and agent concentration, preventing sunburn and skin cancer (Toyoshima *et al.*, 2004). Sunscreen filters are either organic (chemical), which absorb UV radiation, or inorganic (physical), like titanium dioxide and zinc oxide, which reflect UV light. With increasing concerns about health and environmental risks, there is a growing shift toward using natural ingredients in sunscreens (Korkina *et al.*, 2018).

3.3. Photoprotective of secondary metabolites

Secondary metabolites with photoprotective properties are gaining popularity in the cosmetic industry due to sustainability concerns and safety issues with synthetic ingredients (Mota *et al.*, 2020). Plants like *Psidium guajava* and *Scutellaria baicalensis* have shown potential in enhancing sunscreen efficacy by increasing SPF, thanks to their phenolic and flavonoid content (Seok *et al.*, 2016; Livia *et al.*, 2018). *Lippia sericea* extract was found to have superior photoprotective properties due to its high phenol content (Polonini *et al.*, 2014). Additionally, incorporating polyphenols from cinnamic or benzoic acids can improve UVA and UVB protection in sunscreens (Wolf *et al.*, 2001).

4. Antidiabetic Activity

4.1. Diabetes Mellitus

Diabetes mellitus, type 2, is characterized by high blood glucose levels due to impaired insulin secretion and resistance. Inhibiting α -D-glucosidase, which breaks down carbohydrates in the intestine, can help slow glucose absorption, potentially preventing diabetes and obesity (Zhu *et al.*, 2014). Type 2 diabetes increases cardiovascular risks, including heart disease and stroke. Effective glycemic control is crucial to prevent complications, with treatments aimed at improving insulin secretion, glucose utilization, reducing liver glucose production, or inhibiting intestinal glucose absorption (Barau *et al.*, 2016).

4.2. Diabetes Mellitus indices

4.2.1. Postprandial Hyperglycemia

Postprandial hyperglycemia results from rapid carbohydrate absorption and/or inadequate inhibition of hepatic glucose production after meals. It is influenced by the diet's glycemic index and the rate of gastric emptying. This condition worsens metabolic imbalance and contributes significantly to elevated glycosylated hemoglobin levels (Scheen, 2002).

4.2.2. Glycated Hemoglobin (HbA1c)

Glycated hemoglobin (HbA1c) reflects average blood glucose levels over the past 2-3 months and is used to monitor diabetes control. A level of 6.5% or higher, measured by HPLC, is a diagnostic criterion for diabetes (American Diabetes Association, 2008). HbA1c results from glucose binding to hemoglobin and accumulates in red blood cells over their 120-day lifespan, providing a historical record of blood glucose levels (Procopiu, 2006; Gillery, 2014).

4.3. Mechanisms of Action of Antidiabetic Agents

4.3.1. Biguanides

Metformin, the only biguanide class drug, lowers blood glucose levels by activating AMPK (AMP-dependent Protein Kinase), which regulates energy metabolism. AMPK activation decreases hepatic glucose production by inhibiting gluconeogenesis and enhances glucose uptake and utilization in skeletal muscles. Since metformin does not stimulate insulin secretion, it does not cause hypoglycemia (Barau *et al.*, 2016).

4.3.2. Sulfonylureas

Hypoglycemic sulfonamides stimulate insulin secretion by pancreatic β cells by sensitizing them to glucose action. They bind to the SUR protein (Sulfonyl Urea Receptor) of ATP-dependent potassium channels and induce their closure. This results in depolarization of β cells, leading to insulin secretion (Barau *et al.*, 2016).

4.3.3. Non-sulfonylurea Insulin Secretagogues (Glinides)

Repaglinide is the only marketed molecule in this class. It does not belong to the sulfonamide family but also binds to the SUR protein, at a site distinct from sulfonylureas. It leads to the closure of ATP-dependent potassium channels on the membrane of β cells. The resulting cellular depolarization initiates insulin secretion (Barau *et al.*, 2016).

4.3.4. GLP-1 Receptor Agonists

These drugs are synthetic peptides with amino acid sequences like GLP-1. Currently, two molecules are available, exenatide and liraglutide. They stimulate insulin secretion by activating the GLP-1 receptor on β pancreatic cells in a glucose-dependent manner and exhibit increased stability or resistance to DPP-4 action (Barau *et al.*, 2016).

4.3.5. DPP-4 Inhibitors (Gliptins)

Gliptins are inhibitors of DPP-4, the enzyme responsible for GLP-1 inactivation. Sitagliptin is a competitive inhibitor, while vildagliptin and saxagliptin bind to the enzyme covalently. This

inhibition allows GLP-1 to remain in the bloodstream longer, resulting in increased insulin secretion and decreased postprandial hyperglycemia (Barau *et al.*, 2016).

4.3.6. α -Glucosidase Inhibitors

Acarbose and miglitol are competitive inhibitors of intestinal α -glucosidases, selectively inhibiting glucose absorption in the intestine. This action reduces postprandial hyperglycemia without increasing insulin secretion, preventing hypoglycemia. For optimal effect, these drugs are recommended to be taken at the beginning of meals (Barau *et al.*, 2016).

4.4. Phytotherapy for Diabetes

Since ancient times, herbal remedies have been widely used to help manage diabetes; more than 1200 different plants have been described in traditional diabetes treatment (Eddouks *et al.*, 2007). Among all plants tested in vitro, 80% show potential anti-diabetic properties (Oubré *et al.*, 1997). In other cases, certain hypoglycemic medicinal plants induce the regeneration of pancreatic β cells (Kanter *et al.*, 2003).

5. Probiotics activity

5.1. Probiotics

A probiotic is a living microorganism that, when ingested in adequate quantities, has a beneficial effect on health. Probiotics primarily consist of bacteria and yeasts that are naturally present or reintroduced into the resident intestinal flora (Gaggia *et al.*, 2010).

5.2. Prebiotics

Prebiotics differ from probiotics as they are not microorganisms. Instead, they are non-digestible food-derived molecules that promote the growth and activity of specific intestinal bacteria, serving as an energy source for both the gut microbiota and probiotics. Prebiotics are commonly found in foods like wheat, rye, leeks, onions, and bananas (Rapha lle, 2015).

5.3. Synbiotic

A symbiotic mixture combines a probiotic with its specific prebiotic substrate, such as a suspension of *Bifidobacterium* and fructo-oligosaccharides. The goal of this combination is to enhance the survival and persistence of the probiotic in the digestive tract by utilizing the prebiotic to support its growth (Rapha lle, 2015).

5.4. Probiotic role on human Health

The health benefits of probiotics, especially those found in traditional fermented dairy products, have been recognized for centuries. Recently, interest in probiotics has grown,

particularly regarding their positive impact on digestive health and gut flora balance. However, the expansion of probiotics has been hindered by regulations on health claims (Naimi, 2014).

5.5. Probiotics mechanisms

5.5.1. Production of antimicrobial substances

Probiotics can restrict pathogen growth through indirect antimicrobial effects by producing compounds like bacteriocins, organic acids, and hydrogen peroxide. Bacteriocins, such as nisin from *Lactococcus lactis*, are protein compounds that inhibit closely related bacterial strains by disrupting their outer membranes (Klaenhammer, 1998; Fooks and Gibson, 2002). Organic acids like lactic and acetic acid, produced by lactobacilli and bifidobacteria, lower intestinal pH, inhibiting acid-sensitive pathogens (Servin, 2004). Additionally, some lactic acid bacteria produce hydrogen peroxide (H₂O₂), which, along with lactic acid, inhibits the growth of pathogens such as *E. coli*, *Candida albicans*, and viruses (Ouweland and Vesterlund, 2004).

5.5.2. Enhancement of intestinal immune system

Probiotics interact with the immune system to strengthen the host's defense against enteropathogens. They stimulate both adaptive immunity, including the production of IgA antibodies (Shu and Gill, 2002), and innate immunity, such as the activation of macrophages and monocytes (Oelschlaeger, 2010).

5.6. Properties and criteria for selecting probiotic strains

For a microorganism to be considered a potential probiotic, it must be non-pathogenic and safe for consumption (Dunne *et al.*, 2001). A key requirement is its ability to adhere to the epithelial cells of the intestine, with Lactobacillus species, for example, showing better adherence to HT-29 and Caco-2 intestinal cell lines than Bifidobacterium (Guarner & Schaafsma, 1998; Thornton, 1996).

5.6.1. Resistance to gastric acidity

The survival of bacteria in gastric juice hinges on their capacity to withstand low pH levels. Survival time may vary from one to four hours depending on individual factors and diet. Hence, some scholars suggest that probiotic strains must endure a pH of 2.5 in a culture medium for at least four hours (Ammor & Mayo, 2007).

5.6.2. Resistance to bile salts

Probiotics' survival in the small intestine depends largely on bile salt tolerance. After withstanding stomach acidity, these bacteria encounter bile salts in the duodenum, which act as detergents. Probiotics counter this by enzymatically hydrolyzing bile salts, reducing their solubility and emulsifying effects (Ammor & Mayo, 2007; Gu *et al.*, 2008).

5.6.3. Adhesion to epithelial cells

Adherence to the intestinal epithelium is essential for probiotics, enabling colonization and serving as a primary defense against pathogens, as shown in various *in vitro* and *in vivo* studies (Palomares *et al.*, 2007; Reyes *et al.*, 2011). Probiotics can also attach to the mucous layer covering enterocytes and other microorganisms in the gut (Lamoureux, 2000).

5.6.4. Antibiotic resistance

LAB inherently possess resistance to numerous antibiotics owing to their structural and physiological characteristics. Research by Temmerman *et al.* (2003) revealed that 68.4% of isolated probiotics exhibit resistance to one or more antibiotics. For instance, *Lactobacillus* strains have shown resistance to Kanamycin (81%), tetracycline (29.5%), erythromycin (12%), and chloramphenicol (8.5%) (Denohue, 2004).

6. Anti-cancer Activity

6.1. Cancer

Cancer is a genetic disease characterized by uncontrolled cell proliferation (Cattaly *et al.*, 2004). The process of cancer formation is termed carcinogenesis or tumorigenesis, during which normal cells undergo transformation into cancerous cells (Helena *et al.*, 2020).

6.2. Cancer cells characteristics

Cancer cells exhibit resistance to cell death, insensitivity to growth-inhibiting signals, immune evasion, and uncontrolled proliferation without external growth cues. They also promote blood vessel formation, migrate, and form metastases, largely due to genomic instability that disrupts energy metabolism and other processes (Hanahan *et al.*, 2011) (Figure 7).

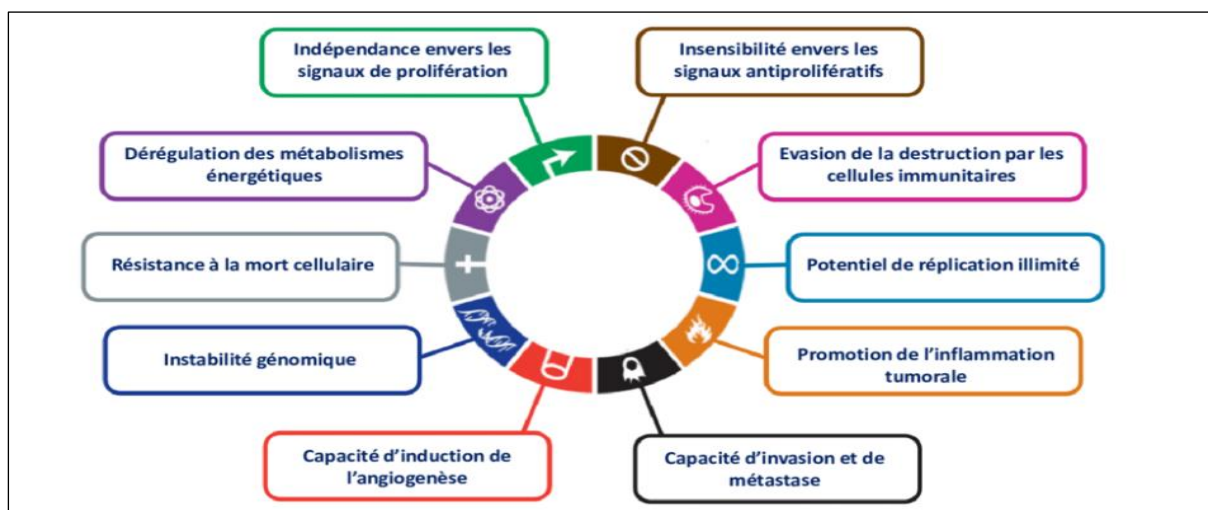


Figure 7. Characteristics of Cancer Cells (Hanahan *et al.*, 2011).

6.3. Treatment

Managing cancer represents one of the most intricate facets of medical care. Therapeutic plans consider the type of cancer, including its location, stage, genetic characteristics, as well as the specific traits of the individual being treated (Morere *et al.*, 2001). The objective of anticancer agents is to obliterate tumor cells by interfering with one or multiple pharmacological targets.

6.4. Biological Target in Cancer Treatment

- Genetic material (DNA, RNA).
- Proteins.
- The mitotic spindle.
- Signaling pathways during different phases of the cell cycle (Morel *et al.*, 2010).

Anticancer molecules can interfere with DNA in three different ways (Piccart *et al.*, 2003):

- By binding to DNA (alkylating agents).
- By disrupting DNA repair systems (intercalators, topoisomerase inhibitors).
- By blocking the biosynthesis of DNA constituents (antimetabolites).
- Other anticancer agents include particles that disrupt the mitotic spindle, hindering cell division (Piccart *et al.*, 2003).

6.4.1. Cancer cell lines

Research on organic drugs in cancer treatment shows that some highly cytotoxic compounds are effective in vitro against multiple cancer cell lines, such as breast, prostate, lung, colon, and leukemia, though few have been tested in vivo. The targeted delivery of these compounds via antibodies, known as the "magic bullet" concept (Monneret, 2010).

6.4.2. DNA of cancer cell

Chemical agents are necessary to inhibit DNA replication within the cellular nucleus. Therefore, investigating the interaction of chemical molecules with the double helix facilitates a better understanding of drug mechanisms, thereby enhancing their efficacy (Despax, 2014).

6.4.2.1. Covalent Interaction with DNA (Alkylating Agents)

Alkylating agents attach alkyl groups to DNA's nucleophilic sites, particularly targeting nitrogen atoms in purine and pyrimidine bases, such as adenine, cytosine, and guanine (Madonna, 2010). These agents, severely damaging DNA and hindering mitosis, ultimately leading to cell death as repair mechanisms fail to correct the damage (Madonna, 2010).

6.4.2.2. Non-covalent Interaction

a. Intercalation Binding

DNA's conformational flexibility allows aromatic molecules to intercalate between its base pairs, increasing separation and partially unwinding the double helix (Gago, 1998). Stabilized

by hydrogen bonding, hydrophobic interactions, and charge transfer, this intercalation process is exploited in chemotherapy to inhibit DNA replication in cancer cells (Sirajuddin *et al.*, 2013).

b. Groove Binding

Certain small compounds bind to the minor groove of DNA. They possess multiple aromatic cycles, such as pyrrole, furan, or benzene, thereby promoting van der Waals interactions. Moreover, these drugs can form hydrogen bonds with bases, typically with adenine's N3 and thymine's O₂. These interactions are specific to regions rich in AT (Sirajuddin *et al.*, 2013).

6.4.2.3. Electrostatic Interactions

The negatively charged of the DNA helix can interact with positively charged organometallic molecules through Coulombic interactions or via a phosphate-oxygen bond (Despax, 2014).

6.4.2.4. DNA-Degrading Agents

Some agents induce DNA fragmentation. These compounds cause breaks in the nucleotide sequence and accumulation of cells in the G₂ phase of the cell cycle (Pottier, 2003). The study of molecule-DNA binding can be detected through various techniques: UV-visible spectroscopy, voltammetric methods (Shafaqat *et al.*, 2013).

6.5. Cancer Phytotherapy

Medicinal plants treat benign conditions, while natural anticancer drugs have advanced through generations, with recent approvals including mTOR inhibitors and compounds from *Saussurea costus*, which show varied anticancer effects (Monneret, 2010; Chabosseau & Derbré, 2016).

7. Wound Healing Activity

7.1. Wound Definition

A skin wound refers to any disruption in the integrity of the skin. In clinical practice, wounds pose significant challenges, with both immediate and delayed complications contributing to morbidity and mortality (Chhabra *et al.*, 2017). Wounds can be categorized based on their origin, bacteriological aspects, and histological and clinical progression (Le Bronec, 2005).

7.2. Modes of Wound Healing

7.2.1. Primary Intention Healing

This approach to wound healing involves the straightforward and rapid closure of the wound, often through suturing, potentially following trimming (Ferraq, 2007).

7.2.2. Secondary Intention Healing

In cases where there is significant loss of tissue or extensive surface wounds leading to substantial defects, the healing process becomes more intricate. Granulation tissue gradually

fills in from the wound edges to facilitate repair, often resulting in noticeable scarring. This mode of healing is referred to as secondary intention healing (Chhabra *et al.*, 2017).

7.2.3. Tertiary Intention Healing

Tertiary healing, involves a delay in primary wound closure typically occurring after 4 to 6 days. This approach is implemented when the secondary intention healing process is intentionally halted, and the wound is closed through mechanical means. Typically, this occurs subsequent to the formation of granulation tissue (Chhabra *et al.*, 2017).

7.3. Mechanisms of Wound Healing

The mechanism of wounds healing is a meticulously orchestrated phenomenon, tightly regulated both spatially and temporally (Hamdan *et al.*, 2017). The mechanism of wound healing is unfolding through four sequential yet interlacing phases: hemostasis, inflammation, proliferation, and tissue remodeling, as depicted in Figure 6 (Srivastava *et al.*, 2024).

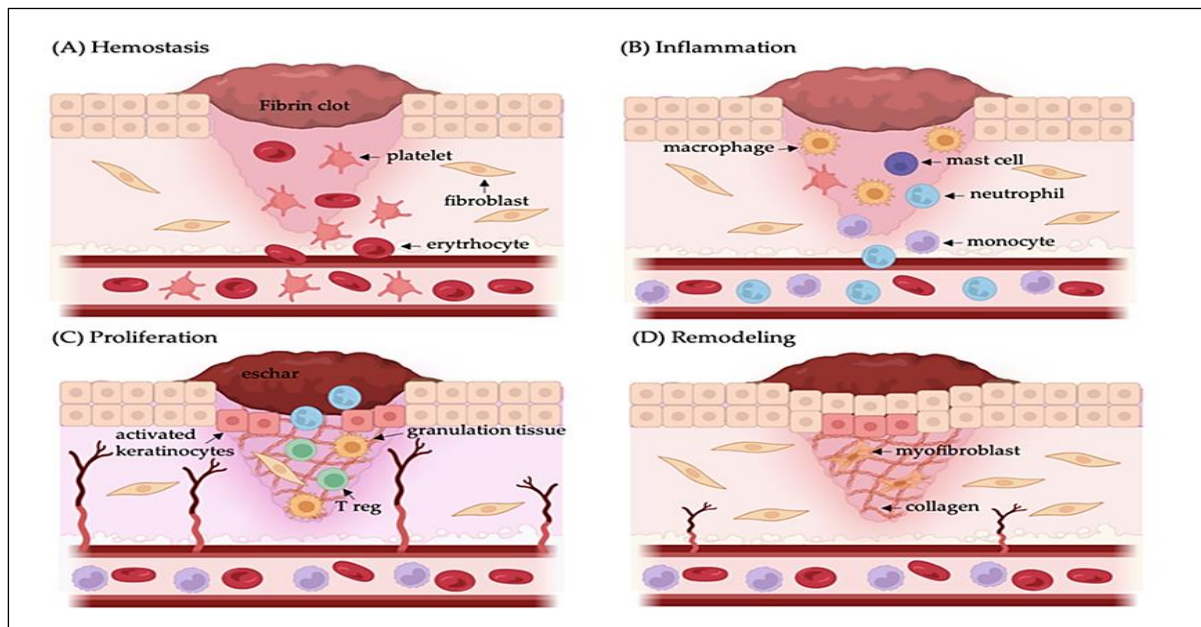


Figure 8. the stages of skin healing, showcasing the cells and molecules pivotal in restoring a robust barrier (Srivastava *et al.*, 2024).

7.3.1. Hemostasis

The initiation of hemostasis promptly follows wound formation, involving vasoconstriction, platelet aggregation, and clot formation (Srivastava *et al.*, 2024). This clot formation serves a dual purpose: halting local hemorrhaging and swiftly filling the tissue deficit through the coagulation cascade (Lebonvallet *et al.*, 2018). Concurrently, cytokines and growth factors facilitating the recruitment of inflammatory cells to the wound site (Srivastava *et al.*, 2024).

7.3.2. Inflammation

After initial vasoconstriction, vasodilators and chemoattractants attract neutrophils and macrophages to the wound, where they clear bacteria and debris. Macrophages release growth factors to recruit fibroblasts and endothelial cells, aiding in tissue repair. The inflammatory phase, lasting up to 4 days, is marked by redness, swelling, pain, and warmth (Moulin, 2001).

7.3.3. Proliferation

The proliferative phase of wound healing involves three key processes: granulation, contraction, and reepithelialization. Granulation begins after the inflammatory phase, where cells proliferate and migrate to form granulation tissue, rich in collagen and other proteins, which supports cell migration and blood vessel formation for nutrient delivery (Moulin, 2001).

7.3.4. Remodeling

The final phase of the healing process, known as the maturation process or remodeling, culminates in the formation of the ultimate scar (Lebonvallet *et al.*, 2018). This phase is characterized by the restructuring of newly developed connective tissue alongside adjustments affecting the epidermis and its appendages, including the restoration of vascularization and nerve supply (Bensegueni & Cherif., 2017).

7.4. Wound Healing Treatment

7.4.1. Healing dermatological ointments and creams

Dermatological formulations play a pivotal role in facilitating the healing, among these are: *Cicaderma*, designed to expedite skin repair and pave the way for subsequent therapeutic interventions to enhance healing outcomes (Morin *et al.*, 2012).

Cicatryl, a pharmacological agent renowned for its wound-healing properties, acting to stimulate skin regeneration processes (Beroual *et al.*, 2017).

Madecassol, recognized for its wound-healing capabilities, particularly in mitigating acute radiation reactions owing to its anti-inflammatory properties (Chen *et al.*, 1999).

7.4.2. Wound Healing Phytotherapy

In vivo studies highlight the wound healing benefits of several plant species. *A. herba-alba* and *A. absinthium* have shown efficacy in promoting wound closure (Merkantia, 2017; Benkhaled *et al.*, 2020). The pods of *A. nilotica* also expedite healing, particularly for burn injuries (Darré *et al.*, 2014). *K. crenata* and *T. imperati* have been found to accelerate the healing process and reduce wound size (Ernest *et al.*, 2019; Nejari *et al.*, 2019). Additionally, *P. lentiscus* L. has demonstrated similar wound-healing effects (Khedir *et al.*, 2017).

Part II:

Experimental part

Chapter I:

Material & Methods

1. Materials

1.1. Plant material

The aerial parts of the *Hammada Scoparia* (Pomel) Ilijin were gathered in November 2021, in Southeastern Algeria precisely in the province of Biskra ($34^{\circ} 51' 0''$ N $5^{\circ} 43' 59.999''$ E). The plant material was identified by Professor Hammel Tarek (Department of Biology, Faculty of Science University of Badji Mokhtar - Annaba, Algeria). After collection and transport, the aerial part was washed with flowing water to remove dust. Then, it was dried in shadow at room temperature, powdered, and stored for further use.

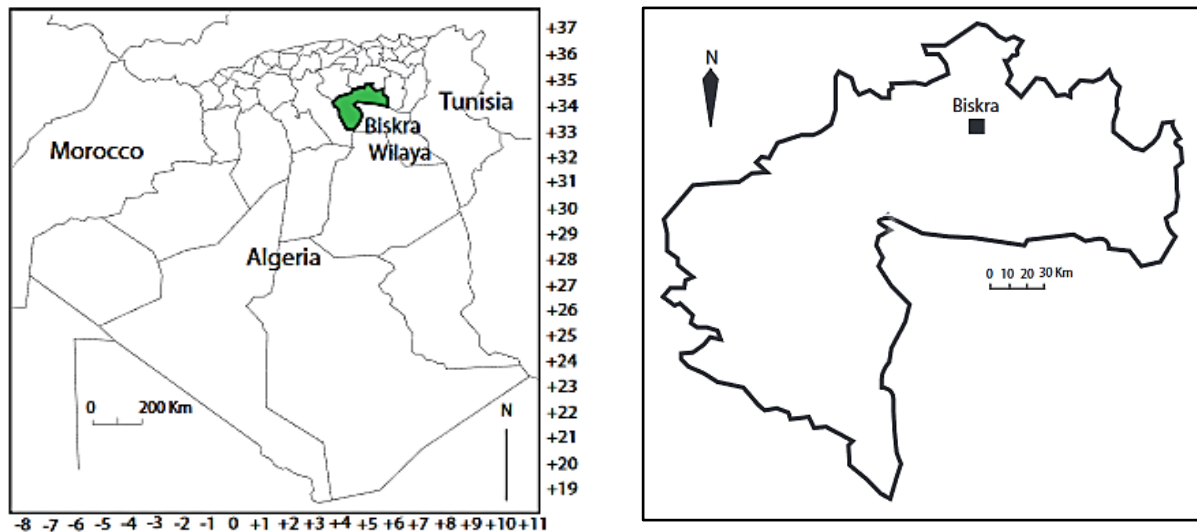


Figure 9. Map of the Wilaya of Biskra and position of study station (Moussi *et al.*, 2011).

1.2. Milk samples

The raw milk samples used in the research were aseptically collected from goats, having a traditional semi-extensive breeding system in southeastern Algeria (El Oued), during January 2023. The sample was collected in a sterilized glass bottle and kept cool with ice packs and other refrigerants during transport to the Microbiology Laboratory at El Oued University. (Distance of 20 min). bacterial species were procured using M17 prepared agar plates. The microbiological, physical, and biochemical characteristics were investigated using a series of tests (Sachin *et al.*, 2023).

1.3. Blood samples

Blood samples were meticulously collected from both chickens and humans on the same working day. For each species, blood was drawn into specialized blood collection tubes pre-filled with EDTA, an anticoagulant used to prevent clotting and maintain the quality of the samples. Once collected, the blood samples were promptly stored at a controlled temperature

of 4°C to ensure their stability and to preserve the cellular and plasma components for subsequent analysis.

1.4. Cells

MCF-7 cell lines which was an human breast cancer cell line are used in the cytotoxicity assessment. MCF-7 cells are useful for *in vitro* breast studies because they retained several ideal characteristics. These cell lines were sourced from Institut of Arid Region (IRA), located in Medenine, Tunisia.

1.5. Animals

A total of 35 adult male albino rats, weighing 160-200g, were obtained from Pasteur Institute, Algeria. They were placed and kept in the animal house of the Molecular and Cellular Biology Department, University of El-Oued, Algeria. Animals were adapted for 15 days under the same laboratory conditions of photoperiod (12 h light/12 h dark) with relative humidity and room temperature (22°C) of standard rats. Food and tap water were available for the duration of the experiments (Southon & Johnson , 1984).

1.6. Chemicals

Chemicals utilized in this study were procured from Prolabo (USA), Biochem chemopharma Co (France), and Sigma-Aldrich (USA). MRS broth, Mueller Hinton Agar for the bacteria culture from condalab (Spain). API 10S strip (Carbohydrate fermentation patterns) used from bioMérieux (France). The antibiotics Amoxicillin®, Gentamicin®, and Penicillin® were employed in the experiment. Medications such as Aspirin®, Metformine®, Acarbose® and DoucePlus® were also included in the analysis.

2. Methods

2.1. Phytochemical analysis of *H. Scoparia*

2.1.1. Phytochemical Screening

The identification and detection of active constituents in the plant extract of *H. Scoparia* were conducted through chemical tests as outlined below:

2.1.1.1. Alkaloids

For alkaloid analysis, 1 mL of the extract was divided into two test tubes. The medium was acidified with a few drops of HCl, and Mayer's reagent was added to one tube while Wagner's reagent was added to the other. The appearance of a white or brown precipitate in the respective tubes confirmed the presence of alkaloids (Gontijo *et al.*, 2017).

2.1.1.2. Flavonoids

To test for flavonoids, 5 mL of the extract was combined with 5 mL of dilute ammonia and 1 mL of H₂SO₄ in a test tube. The presence of a yellow coloration indicated the presence of flavonoids (Sharma *et al.*, 2020).

2.1.1.3. Terpenoids

In a test tube, 5 mL of plant extract was mixed with 2 mL of chloroform and 3 mL of strong sulfuric acid. The development of a reddish-brown tint indicated the presence of terpenoids (Harborne, 1998).

2.1.1.4. Saponins

A volume of 10 mL of the aqueous extract was added to a test tube, shaken for 15 s, and left to stand for 15 min. The presence of persistent foam higher than 1 cm indicated the presence of saponins (Edeoga *et al.*, 2005).

2.1.1.5. Tannins

In a test tube, 5 mL of extract was mixed with 1 mL of a 2% aqueous solution of ferric chloride (FeCl₃). The presence of tannins was confirmed by a greenish or bluish-black coloration (Sharma *et al.*, 2020).

2.1.1.6. Cardiac glycosides

A mixture of 2 mL of chloroform and 1 mL of the extract was carefully treated with H₂SO₄. The presence of a reddish-brown color indicated the presence of the glycone part of a cardiac glycoside (Yam *et al.*, 2009).

2.1.1.7. Mucilages

A volume of 3 mL of methanol was combined with 1 mL of the aqueous extract at 60°C. The formation of a flocculent precipitate upon stirring indicated the presence of mucilage (Kiendrebeogo *et al.*, 2016).

2.1.1.8. Anthocyanins

The aqueous extract was treated with a few drops of hydrochloric acid followed by ammonia (NH₄OH). A change in color to red indicated the presence of anthocyanins (Wadood *et al.*, 2013).

2.1.1.9. Leuco-anthocyanins

A volume of 5 mL of the infusion was mixed with 4 mL of hydrochloric alcohol (Ethanol / pure HCl 3v / 1v) and heated in a water bath at 50°C for a few minutes. The appearance of a cherry red color indicated the presence of leuco anthocyanins (Bate-Smith, 1954).

2.1.1.10. Steroids

1 mL of the extract received 5 drops of concentrated H₂SO₄. The presence of steroids was confirmed by the development of a red color (Trease and Evans, 1989).

2.2. Aqueous extract preparation

Fifty grams of powdered *H. Scoparia* was soaked in 500 mL of distilled water over one night at ambient temperature. Wattman paper N°1 was used to filter the mixture, and the residues were macerated for another two days with the same solvent and volume. The filtrates were collected and concentrated with rotatory vapor (Buchi R-300H) under low pressure and a temperature of 40 °C. The yield was calculated, and the extract was stored for further studies (Souri *et al.*, 2008).

2.2.1. Extraction yield

The extraction yield was assessed using the method mentioned by Muniyandi *et al.* (2019). It was calculated using the following formula:

$$\text{Extraction Yield (\%)} = (M_1 / M_0) \times 100,$$

Where M₁ represents the mass in grams of the resulting dry extract, and M₀ represents the mass in grams of the plant material processed.

2.2.2. Preparation of extract fractions

Aqueous extract fractions (Figure 10) was conducted following the Bruneton method (1993), with slight modifications, which relies on the varying solubility of polyphenols in organic solvents. The aqueous extract was fractionated using three organic solvents of different polarities: ethyl acetate and n-butanol. Apart from the aqueous fraction (F0), three additional fractions were obtained: the ethyl acetate fraction (F1), the n-butanol fraction (F2), and the aqueous fraction (F3). These different extracts were preserved until further use.

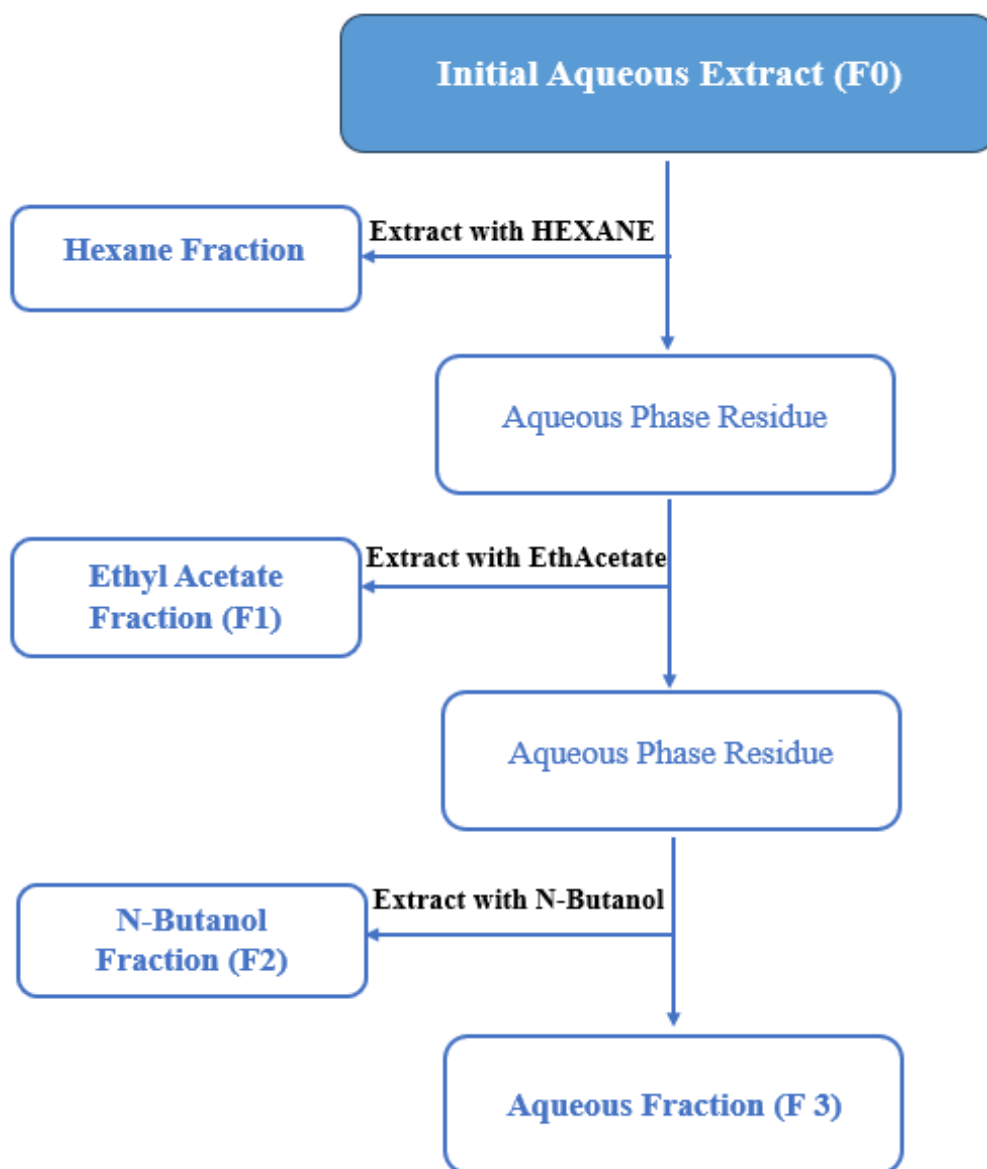


Figure 10. Sequential fractionation of aqueous extract using organic solvents

2.3. Colorimetric analysis

2.3.1. Total phenolics content (TPC)

Total phenolics content of the *H. Scoparia* extract was calculated using the colorimetric Folin-Ciocalteu technique using a spectrophotometer (Labindia Analytical UV-VIS 2000), as described by Singleton *et al.* (1999). In summary, 200 μ l of extract and 1 mL of Folin dilution reagent (1:10) were mixed. After 5 min, 800 ml sodium carbonate (7.5% w/v) was added. After 60 min of incubation, the absorbance was measured at 765 nm. For calibration, gallic acid solutions with concentrations ranging from 20 to 200 μ g/mL were used for blotting the curve

of standard absorbance and the amounts in the samples, and a dose-response linear regression was created. TPC was measured and represented as mg gallic acid equivalent/g dry extract using gallic acid as standard.

2.3.2. Total flavonoid contents (TFC)

The estimation of Total flavonoid contents of *H. Scoparia* aqueous extract was quantified by the typical colorimetric experiment using $AlCl_3$ as a reagent and quercetin as standard. For calibration, quercetin solutions with concentrations ranging from 20 to 200 μ /mL were used to plot the curve of standard absorbance and the amounts in the samples, a dose-response linear regression was created. Total flavonoids were quantified in mg of quercetin equivalents per g of the dry extract (Quettier-Deleu *et al.*, 2000). 1 mL of the $AlCl_3$ solution is mixed with 1 mL of the sample or the standard. Absorbance is measured at 430 nm after 30 minutes of incubation. The results are expressed in milligrams equivalent of quercetin per gram of extract, calculated from the calibration equation derived from the quercetin standard.

2.3.3. Total tannins content (TTC)

The estimation of Total tannins content of the aqueous extract was done according to Schofield *et al.* (2001) using the vanillin-HCl method. In a 1:1 ratio, the extract was combined with the reagent's vanillin 4% (w/v) and HCl 8% (v/v). Absorbance was measured at 500 nm using catechin as the reference. For calibration, catechin solutions with concentrations ranging from 20 to 200 μ g/mL were used for plotting the curve of standard absorbance and the amounts in the samples, and a dose-response linear regression was created. The results were expressed as mg catechin equivalents/g dry extract.

2.4. Chromatographic Analysis

2.4.1. HPLC Analysis

Reverse-phase high-performance liquid chromatography and scanning instruments were used to identify the active components. RP-HPLC with a UV-Visible detector (Shimadzu LC20 AL) was used to investigate the presence of phenolic content in the crude extract. Shim-pack VP-ODSC18 (4.6 mm, 250 mm, 5 μ m) analytical column, UV-Visible detector SPD 20 A, and universal injector (Hamilton 25 l) were all incorporated into the system (Shimadzu). Non-polar aliphatic residues were used in the RP-HPLC experiments, and the mobile phase was made up of a gradient elution of acetonitrile and acetic acid (0.1%). The flow rate employed in this study was 1 mL/min, and the injection volume was 450 μ L. The sample and standard injection

volumes were 20 ml, and the monitoring wavelength was 268 nm. Various substances were determined by comparing their UV absorption and retention time to standards.

2.4.2. LC-MS-MS Analysis

The qualitative analysis of polyphenols in the aqueous and ethyl acetate fractions of each algal methanolic extract was carried out using the UPLC-SI-MS Shimadzu 8040 Ultra-High Sensitivity system, equipped with UFMS technology and a Nexera XR LC-20AD binary pump. Polyphenol standards were optimized using column-free direct injection. Electrospray ionization (ESI) conditions included CID gas at 230 KPs, a conversion dynode set at -6.00 Kv, interface temperature at 350°C, DL temperature at 250°C, nebulizing gas flow at 3.00 L/min, heat block at 400°C, and drying gas flow at 15.00 L/min. All standards were prepared in methanol at a concentration of 500 µg/L. The ion trap mass spectrometer operated in both negative and positive ions using the MRM mode (multiple reaction monitoring). The mobile phase comprised water, 0.1% formic acid, and 70% methanol, with a flow rate set at 0.4 mL/min and an injection volume of 5 µL. Separation of phenolic compounds in each fraction was achieved using a C18 Ultra-force column (100 mm length, 2.5 mm diameter, 1.8 µm particle size; Restek) with an oven temperature maintained at 25°C. Isocratic elution was performed using a mixture of 0.1% formic acid and methanol (30:70, v/v) at a flow rate of 0.4 mL/min, and the injection volume was 5 µL.

2.5. Green synthesis of calcinated and uncalcinated ZnO-NPs

The ZnO-NPs were synthesized according to the method described by Sachin *et al.* (2023) with modification, a typical method combined 50 mL of an *H. Scoparia* extract with 100 mL of (0.1M) zinc acetate dihydrate ($Zn(C_2H_3O_2)_2 \cdot 2H_2O$) solution mixed in 250 mL flasks (Figure 11). This mixture was stirred and heated at 70 °C on the hot plate for 1 hour. The resulting precipitates were centrifuged at 4000 rpm for 10 min and washed with double-distilled water 2 to 3 times. The dried ZnO-NPs were divided into two groups, one was left uncalcinated, and the second calcinated at 500°C for 4 h. The two ZnO-NPs were kept at 4°C for future experimental use.

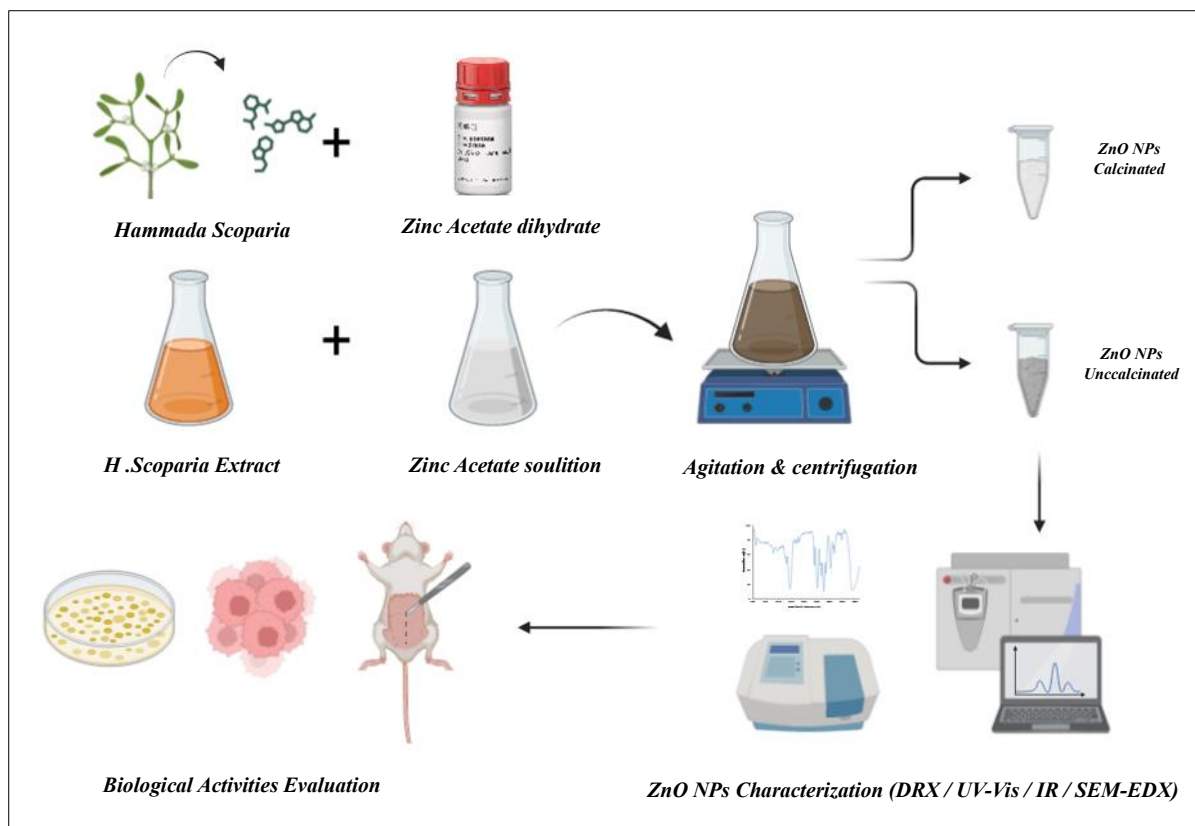


Figure 11 : The green synthesis method of zinc oxide nanoparticles using *H.scoparia* extract.

2.6.Characterization of ZnO-NPs

2.6.1. UV-visible spectroscopy

UV/Visible spectroscopy (Shimadzu-00463) was used to assess the bio-reduction and optical properties of ZnO-NPs samples. The optical properties of the ZnO- NPs samples in the UV and visible ranges were studied by UV-visible absorption spectroscopy. Electron spectroscopy is an absorption spectroscopy concerning transitions from the ground to an excited state. It consists of measuring the attenuation of an incident light ray of intensity (I_0) as a function of the wavelength when it passes through a homogeneous medium of thickness (l) containing an absorbing species (Truffault, 2010). The technique consists of detecting and quantifying the intensity of radiation whose wavelength varies between 200 and 1400 nm; the sample can absorb, transmit, or reflect the photons emitted. The Beer-Lamber law governs Absorbance.

2.6.2. Fourier Transform Infrared Spectroscopy (FTIR)

Fourier transform infrared spectroscopy (Thermo Fischer Scientific-USA, Nicolet iS10) was utilized to demonstrate and reveal the functional groups and Zn-O bonds generated in the produced nanoparticles, with spectra ranging from 400 to 4000 cm^{-1} . Fourier transform infrared spectroscopy provides insight into the nature of chemical bonds and can be used to identify compounds. Indeed, this technique characterizes vibrational transitions within

molecules or crystals and produces spectra comprising adsorption bands whose position is characteristic of the vibration bonds of the compound studied. There are different types of vibration: elongation (Symmetric or antisymmetric), angular deformation, rocking, out-of-plane movement, or torsion. The most common are elongation, angular deformation, and out-of-plane movement.

2.6.3. X-ray diffraction

The XRD method is best appropriate for powdered samples, which are freshly prepared after drying the samples' respective colloidal solutions. Using XRD equipment (Bruker D8 Advance, Texas, US), the position and intensity of peaks in a sample are compared to patterns in various diffraction databases, allowing the composition of nanoparticles to be quantified (Mourdikoudis *et al.*, 2018).

The principle of operation of the XRD method includes the dispersing of X-rays due to the revolution of electrons in the nucleus of the atom when the rays hit the nanoparticles. Dispersed X-rays are reflected in different directions, causing interference patterns. These patterns are destructive or constructive (Fultz and Howe, 2013), but only dispersed X-rays that go through constructive interaction give rise to diffraction. Characterization of nanoparticles by XRD begins with identifying the phase of the sample material. The type of crystal in the sample is determined by a search and match process, which is carried out in regions where high peak intensities are observed. The different XRD peak configurations are the result of different atom arrangements. In an XRD approach, interference occurs when the light of a given wavelength highlights a periodic structure having a predetermined spacing. The principle of XRD follows Bragg's law ($n\lambda = 2d\sin\theta$), where λ , n , d , and θ respectively denote the X-ray wavelength, integer, plane spacing, atomic, and the half-angle of diffraction. Therefore, information can be obtained regarding sample crystal defects, crystal size, crystal phase, shape anisotropy, deformation, and texture by evaluating the diffraction peaks' width, shape, and position (Widjonarko, 2016).

2.6.4. Scanning electron microscopy (SEM)

The morphology of the surface and zinc and oxygen distribution in the sample were verified by SEM-EDAX experiments (Carl Zeiss, Germany, Gemini 300). SEM is an electron microscope that generates images of the sample top surface by scanning it with a stream of high-energy electrons. The external surface structure of the materials was studied using the scanning electron microscopy (SEM) approach. SEM provides information on surface

morphology and material composition. The SEM technique has several advantages in dimensional morphological analysis, but the information regarding the distribution size and average population is limited. Studying a nanoparticle solution using SEM requires drying it to a powder before mounting it on a sample holder and coating the sample surface with a conductive metal, such as using a cathode sputtering device. The external surface sample is examined when a high-spirited flow of electrons is incident on it. The high-resolution enlarged images produced when the narrow electron beam reveals details smaller than 1-5 nm produce a characteristic three-dimensional image to understand the structure of the surface sample (Salman, 2020).

2.6.5. Energy Dispersive Spectroscopy (EDS)

EDS is utilized to gain insight into the elemental composition of metal nanoparticles, offering a foundational comprehension of the sample (Brongersma *et al.*, 2007).

2.7. *In vitro* biological activities

2.7.1. Antioxidant activity

2.7.1.1. ABTS radical scavenging assay

The ABTS, or 2,2'-azino-bis(3-ethylbenzothiazoline-6-sulfonic acid), is an organic chemical compound with a molecular formula of $C_{18}H_{18}N_4O_6S_4$ and a molecular weight of approximately 514.62 g/mol. It finds application in assessing the antioxidant capacity of plant extracts.

The ABTS* free radical scavenging method was used to determine the reducing power of the aqueous extract of *H. Scoparia* and two ZnO-NPs (Pellegrini *et al.*, 1999). The stock solution was made by combining 7 mM ABTS and 2.4 mM potassium persulfate. This reagent was refrigerated for at least 16 h. The reagent was diluted with 50% ethanol before use. The samples with various concentrations (6.25, 12.5, 25, and 50 $\mu\text{g/mL}$) were mixed with 1 mL of ABTS solution, and the absorbance was determined at 734 nm after 7 min of incubation, and then the percentage of ABTS inhibition was calculated using the following formula:

$$\text{ABTS inhibition (\%)} = [(A_{\text{Control}} - A_{\text{Sample}}) / A_{\text{Control}}] \times 100$$

A_{control} refers to the absorbance measured in the control solution, which contains all reagents except the sample, while A_{sample} refers the absorbance measured in the sample.

2.7.1.2. DPPH radical scavenging assay

The DPPH, an abbreviation for 2,2-diphenyl-1-picrylhydrazyl, is categorized as an organic compound. It has a chemical formula of $C_{18}H_{12}N_5O_6$ and a molar mass of 394.32 g/mol. Presenting as a soluble crystalline powder when dissolved in water, it exhibits a dark hue and comprises molecules featuring stable free radicals.

The method for evaluating the DPPH scavenging activity of *H. Scoparia* aqueous extract was adapted from a previously published protocol by Yarrappagaari *et al.* (2020). Briefly, 1 mL of 0.1 mM DPPH dissolved in methanol was mixed with various concentrations (25, 50, 100, and 150 $\mu\text{g/mL}$) of the extract. A control was prepared by mixing 1 mL of methanol with 1 mL of DPPH, while ascorbic acid was used as a standard. The mixture was incubated in the dark for 30 min, after which the absorbance was measured at 517 nm using a UV-Vis spectrophotometer. The following equation was used to calculate the percentage of DPPH inhibition:

$$\text{DPPH inhibition (\%)} = [(A_{\text{Control}} - A_{\text{Sample}}) / A_{\text{Control}}] \times 100$$

A_{control} refers to the absorbance measured in the control solution, which contains all reagents except the sample, while A_{sample} refers the absorbance measured in the sample.

2.7.1.3. Ferric-reducing antioxidant power (FRAP) assay

The ferricyanide, characterized by the chemical formula $[\text{Fe}(\text{CN})_6]^{3-}$, is typically found in its primary salt form, potassium ferricyanide, $\text{K}_3\text{Fe}(\text{CN})_6$. This compound manifests as a red crystalline solid and is commonly employed as an oxidizing agent within organic chemistry. Iron readily converts to ferrocyanide $[\text{Fe}(\text{CN})_6]^{4-}$ through reduction, generating a ferrous complex Fe^{2+} . Notably, this redox process is reversible and does not entail the cleavage of Fe–C bonds.

The FRAP assay was used to determine the total antioxidant capacity of *H. Scoparia* aqueous extract and two ZnO-NPs. The extract concentrations of 50, 100, 150, and 200 $\mu\text{g/mL}$ were mixed with 1250 μl of 1% (m/v) potassium ferricyanide and 1250 μl of 0.2 M phosphate buffer (pH 7). The reaction mixture was incubated for 30 min at 50°C. Next, 1250 μl of 10% (m/v) TCA was added to the mixture, which was then centrifuged at 6500 rpm for 10 min. The supernatant was collected, and 1250 μl of distilled water and 250 μl of ferric chloride reagent were added to it. The absorbance was measured at 700 nm (Nyayiru *et al.*, 2020). Ferric-reducing antioxidant power (FRAP) values were calculated using the following formula:

$$\text{FRAP values} = [100 - (A_{\text{Control}} \times 100) / A_{\text{Sample}}]$$

A_{control} refers to the absorbance measured in the control solution, which contains all reagents except the sample, while A_{sample} refers the absorbance measured in the sample.

2.7.2. Photoprotective activity

The SPF value provides an indication of how well a sunscreen or similar substance can protect skin from UVB rays, which are primarily responsible for sunburn and contribute to skin cancer risk. Higher SPF values indicate greater protection. Thus, the assessment of *H. Scoparia* aqueous extract and ZnO-NPs helps to understand their capability in absorbing harmful UV rays and their potential application in sunscreens and other protective formulations.

The effectiveness of *H. Scoparia* aqueous extract and two ZnO-NPs against UV rays was assessed in vitro using UV-Visible spectrophotometry to determine the sun protection factor (SPF). The SPF was calculated based on the method described by Aida *et al.* (2022), by measuring the difference between the spectroscopic readings of the aqueous extract and ZnO-NPs (500 µg/mL) in the range of 290 nm- 320 nm, using the following formula:

$$\text{SPF}_{\text{Spectrophotometric}} = \text{CF} \sum_{\lambda 290}^{\lambda 320} EE(\lambda) \times (\lambda) \times \text{Abs}(\lambda)$$

Where CF: correction factor (=10); EE: erythemal effect spectrum; I: solar intensity spectrum; Abs: absorbance of the sample. The results obtained were compared with the categories of sunscreens mentioned in Table 3, according to Schalka *et al.* (2011).

Table 3. Categories of sunscreens based on the value of the SPF.

Protection Level	SPF Value
Maximum	>50
High	30-50
Medium	15-30
Low	02-15

2.7.3. Anti-inflammatory activity

To study the potential anti-inflammatory effects of *H. Scoparia* extract and two ZnO-NPs, the albumin denaturation assay was utilized as described by Alhakmani *et al* (2014), with Aspirin® serving as a control. To perform this assay, a reaction mixture of 500 µl of various concentrations of *H. Scoparia* extract or the standard (ranging from 100 to 500 µg/mL) and 700 µl of phosphate-buffered saline (pH 6.4) was combined with 500 µl of fresh egg albumin. The reaction mixture was then incubated for 15 min at $27 \pm 1^\circ\text{C}$. Denaturation of albumin was induced by heating the mixture in a hot bath at 70°C for 10 min. After cooling, the absorbance

at 660 nm was measured using distilled water as a blank. The experiment was carried out in triplicate. The inhibition percentage of egg Albumin denaturation was calculated using the following formula:

$$\text{Albumin Denaturation Inhibition (\%)} = [(A_{\text{Sample}} - A_{\text{Control}}) / A_{\text{Control}}] \times 100$$

A_{control} refers to the absorbance measured in the control solution, which contains all reagents except the sample, while A_{sample} refers the absorbance measured in the sample.

2.7.4. Anti-diabetic activity

2.7.4.1. Non-enzymatic hemoglobin glycosylation

Haemoglobin Preparation

Blood was obtained from a healthy human volunteer and added to a blood bottle containing an anticoagulant. Hemolysate was then prepared using the hypotonic lysis method as outlined by Adisa *et al.* (2004). The collected red blood cells underwent three washes with a 0.14M NaCl solution. Subsequently, one volume of the red blood cell suspension was lysed using two volumes of 0.01M phosphate buffer (pH 7.4) and 0.5 volume of CCl_4 . Following centrifugation at 2300 rpm for 15 minutes at room temperature, the hemolysate was separated from debris. The upper layer, enriched with haemoglobin, was isolated and transferred into sample bottles for storage at refrigerated temperatures until further use as per the method described by Adisa *et al.* (2004).

Hemoglobin glycosylation assay

The assay for non-enzymatic glycosylation of hemoglobin to investigate the antidiabetic activity of *H.Scoparia* extract and uncalcined and calcined ZnO-NPs involved colorimetric measurement at 520nm. Glucose (2%), haemoglobin (0.06%), and Gentamycin (0.02%) solutions were prepared in phosphate buffer (0.01 M, pH 7.4). One milliliter of each solution was mixed, followed by the addition of various concentrations of the *H.Scoparia* extract / ZnO-NPs. The mixture was then incubated in darkness at room temperature for 72 hours. The degree of haemoglobin glycosylation was subsequently measured colorimetrically at 520nm. Metformine[®] served as the standard drug for the assay. All tests were conducted in triplicate (Chaudhari *et al.*, 2013). The percentage inhibition (I%) was computed using the formula:

$$I \% = [(A_c - A_s) / A_c] \times 100$$

Where A_c represents the absorbance of the control and A_s represents the absorbance of the sample (Manikandan *et al.*, 2016).

2.7.4.2. Inhibition of α -glucosidase enzyme

The inhibition of the α -glucosidase enzyme was assessed by incubating a solution containing starch substrate (2% w/v maltose or sucrose), 1 ml of 0.2 M Tris buffer at pH 8, and various concentrations of plant extract for 5 minutes at 37°C. The reaction was initiated by adding 1 ml of α -glucosidase enzyme (1 U/ml) and further incubated for 40 minutes at 35°C. To halt the reaction, 2 ml of 6N HCl was added. Subsequently, the color intensity was measured at 540 nm (Manikandan *et al.*, 2016).

To determine the 50% Inhibitory Concentration (IC₅₀), the concentration of plant extracts needed to scavenge 50% of the radicals was calculated based on the percentage scavenging activities at five different extract concentrations. The percentage inhibition (I%) was computed using the formula:

$$I \% = [(Ac - As) / Ac] \times 100$$

Where Ac represents the absorbance of the control and As represents the absorbance of the sample (Manikandan *et al.*, 2016).

2.7.5. Probiotic Activity

2.7.5.1. Characterization of probiotic Properties

Test of Acid tolerance

The acid resistance test was performed according to the method described by Kiani *et al.* (2021a). with slight modifications. Simply, two MRS broth (Man, Rogosa and Sharpe broth) were prepared with pH 2 and pH 4; 9 mL of each MRS broth were mixed with 1 mL of the MRS preculture with and without *H. scoparia* extract and the two ZnO-NPs, the mixtures incubated at 37 °C for 3 h. Finally, the measurement of the optical density of samples at 600 nm with a spectrophotometer. The acid tolerance was estimated by using the following equation:

$$\text{Acid Tolerance (\%)}: [OD_{0h} / OD_{3h}] \times 100\%$$

OD_{0h} refers to the Optical density measured on the Time 0, while OD_{3h} refers the Optical density measured after 3h of incubation.

Test of Bile tolerance

The bile salt tolerance test was performed according to the method described by Kiani *et al.* (2021b). Simply, 1 mL of MRS preculture with and without *H. scoparia* extract were added to

9 mL of fresh MRS broth with 0.3% (w/v) bile oxgall and incubated for 3 h at a temperature of 37 °C. A spectrophotometer was used to measure the growth rate at 600 nm. Finally, the bile tolerance was estimated by the following equation:

$$\text{Bile Tolerance (\%)}: [A_{0h} / A_{3h}] \times 100\%$$

A_{0h} refers to the Optical density measured on the Time 0, while A_{3h} refers the Optical density measured after 3h of incubation.

Test of cell surface hydrophobicity

Hydrophobicity was determined by the method mentioned in the study of Rodríguez-S'anchez *et al.* (2021). The precultures with and without *H. scoparia* extract were centrifuged at 4500×g for 10 min, washed twice using sterile phosphate buffer saline (PBS), and the pellets were resuspended in 3 mL of PBS and the initial absorbance at 600 nm (A_0) was measured using a spectrophotometer. Then, 1 mL of xylene was added to each bacterial suspension then mixed using a vortex for 2 min. The mixtures were allowed to separate into two phases by decantation for 1 h at a temperature of 10°C, 37°C, and 45°C and the absorbance of the aqueous phase (A_1) was measured by a spectrophotometer. The test was carried out in triplicate and calculated as:

$$\text{Hydrophobicity (\%)} = (1 - A_1/A_0) \times 100$$

2.7.5.2. Phenotypic characterization

The isolated bacterial strains were characterized by morphological, physiological, and biochemical characterization as described by Chukeatirote *et al.* (2015) with slight modifications. These involved the examination of Gram-staining, catalase activity test, and ability to grow at different NaCl concentrations of 2%, 4%, and 6%, and grow at different temperatures of 10°C, 37°C, and 45°C for 7 days. In addition, the bacteria were identified at the species level by analyzing their phenotypic characteristics and carbohydrate fermentation patterns using the API 10S strip.

2.7.5.3. Molecular identification

DNA has been recovered from overnight LAB cultures using the NucleoSpin Soil kit (Macherey-Nagel, USA). The 16S rRNA gene was amplified using the primers 27F (5'-AGAGTTTGATCCTGGCTCAG-3') and 1492R (5'-GGTACCTTGTTACGACTT-3') as previously reported by Sukara *et al.* (2014) with slight modification. PCR mixes have been set as follows: initially denatured at 96°C for 4 min; then 35 cycles of 94°C for 30 s, 57°C for 30s, 72°C for 1min 30s, and the final extension was set for one cycle of 5 min at 72°C. Gel

electrophoresis using 1% agarose gel 1xTE buffer for 45 min was used to verify the existence of certain DNA products produced by PCR. Amplified DNA was purified, sequenced, and BLASTN with NCBI. LAB isolates were identified using 98–100% similarity. The neighbor-joining approach was used to generate the phylogenetic tree and phylogenetic analysis, MEGA 11 was used.

2.7.5.4. Synbiotic effect Evaluation

By conducting these comprehensive tests, the test aimed to explore the potential benefits of combining *H. Scoparia* aqueous extract and ZnO-NPs with *Bacillus* probiotics, contributing to the development of enhanced probiotic formulations.

Different preculture were prepared with different concentrations of *H. Scoparia* aqueous extract or ZnO-NPs (500; 1000; 2000 µg/ml) in MRS broth and used for the test of the enhancement of *Bacillus* strains to study their effect on the isolated strain in each test of the Probiotic characteristics. After incubation of 24 h the test of Acid tolerance, Bile tolerance, and Test of cell surface hydrophobicity were carried out to determine the synbiotic effect of *H. scoparia* and ZnO-NPs (Kiani *et al.*, 2021a; Kiani *et al.*, 2021b; Rodríguez-S'anchez *et al.*, 2021).

2.7.6. Anticancer Activity

2.7.6.1. DNA interaction study

DNA Extraction

The isolation of DNA from blood can be achieved using various techniques, different protocols, and a wide range of commercially available kits (Filote *et al.*, 2022) . The chosen DNA extraction technique should be able to provide pure DNA samples ready for use in studying anticancer activity with the studied compounds.

In this study, we isolated DNA from chicken blood using salting-out techniques (Gaaib, Nassief, and Al-assi, 2011; Miller, Dykes, and Polesky, 1988). The advantage of this technique is that it avoids the use of toxic and corrosive organic solvents and only utilizes standard chemicals that can be obtained from any commercial supplier, and it does not require specialized equipment or biochemical knowledge (Nasiri *et al.*, 2005; Rivero *et al.*, 2006). The DNA purification protocol is based on protein precipitation at high salt concentration. The traditional protocol involves initial cell disruption and digestion with sodium dodecyl sulphate, followed by the addition of high salt concentrations, typically 6 M sodium chloride. The mixture is then centrifuged to allow proteins to precipitate to the bottom, with the supernatant

containing the transferred DNA into a new flask. DNA is then precipitated using cold ethanol (Howe,1997). The steps involved in DNA extraction are summarized in Figure 12.

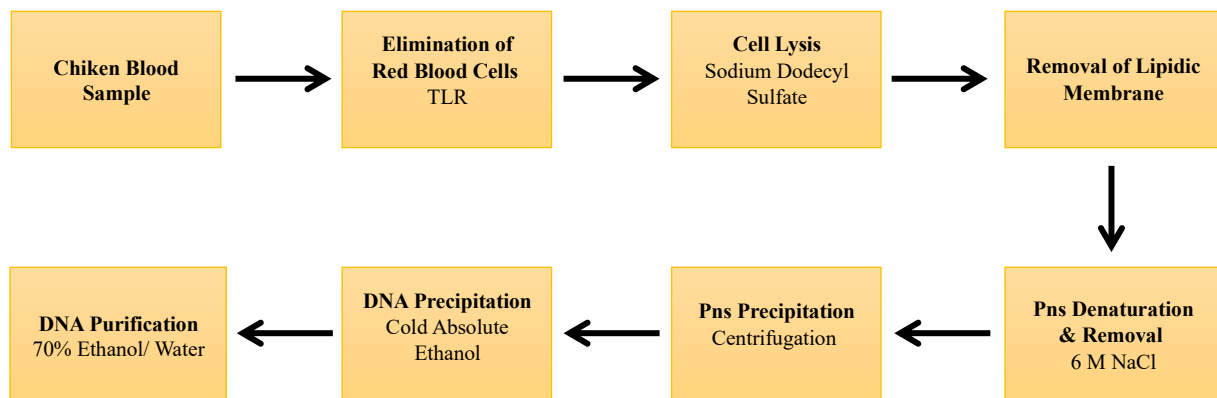


Figure 12. Steps Involved in DNA Extraction

DNA is extracted from chicken blood using salting-out techniques. Chicken blood differs from human blood in that red blood cells are also nucleated and contain much more DNA than non-nucleated mammalian blood. This allows for obtaining chicken DNA in sufficient quantity and quality using relatively simple extraction techniques. Therefore, during DNA purification from chicken blood, there is more DNA material compared to working with human blood (Javanrouh *et al.*, 2020).

Extraction Procedure

5 ml of whole chicken blood sample is placed in a 20 ml flask, then 10 ml of TLGR (Red Blood Cell Lysis Buffer) was added to the blood and the resulting mixture was cooled in an ice bath for 20 minutes, then centrifuged at 2500 rpm for 15 minutes at room temperature. This step was repeated 3 to 4 times until the red colour of the blood disappeared, then the flask was left to dry for 5 minutes.

The white blood cells were removed by adding 2 ml of TLGB buffer and vortexed for 3 minutes. Subsequently, cell lysis was carried out by adding 150 μ L of sodium dodecyl sulphate solution and centrifuged at 172 rpm for 90 minutes at 55°C. After centrifugation, 3 ml of 6 M sodium chloride solution was added, and the resulting mixture was vortexed for 6 minutes and then centrifuged at 1300 rpm for 10 minutes. The liquid phase was recovered, and 2 volumes of cold isopropanol were added, followed by centrifugation at 1300 rpm for 30 minutes at room temperature. DNA was then recovered from the isopropanol layer, washed several times with 70% ethanol, and characterized using UV-Vis spectroscopy.

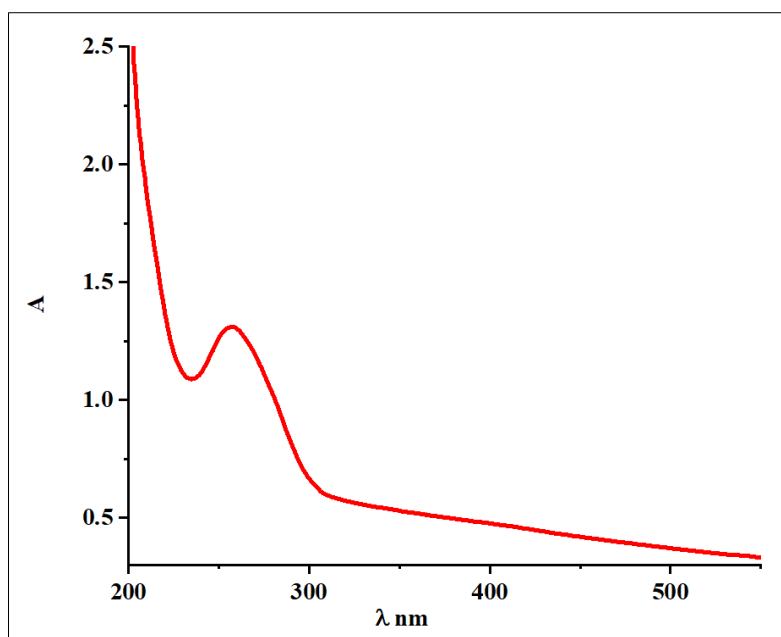


Figure 13. UV-Vis spectrum of the isolated DNA.

UV-Vis spectroscopy can be used to detect protein contamination in extracted DNA (Saab *et al.*, 2007). Proteins exhibit two absorption peaks in the UV region: the first peak is located between 190-210 nm, attributed to electronic transitions in the peptide backbone, and the second peak is situated at 280 nm (Figure 13) due to absorption by the aromatic amino acids tyrosine, tryptophan, and phenylalanine (Khennoufa *et al.*, 2021).

Estimation of DNA Purity

The isolated DNA cannot be used without further purification as it contains contaminating RNA and proteins. Therefore, the DNA is rehydrated in distilled water, and this dissolution requires continuous agitation overnight at 42°C. The concentration and purity of the DNA can be determined by measuring ultraviolet light absorption. DNA has maximum and minimum absorption at 260 nm and 234 nm, respectively (Telfer *et al.*, 2013). The purines and pyrimidines in the nucleic acid are responsible for these absorptions. At 260 nm, double-stranded DNA has a specific absorption coefficient of $0.02 (\mu\text{g/ml})^{-1}\text{cm}^{-1}$ (Griffiths and Chacon-Cortes, 2014). Additionally, the ratio of A_{260}/A_{280} can detect nucleic acid purity relative to protein contamination, as proteins have maximum absorption at 280 nm. Highly purified DNA samples have a 260/280 nm ratio of (1.7-1.9), so below (1.7), a significant amount of protein impurities may be present in the sample (Whitlock *et al.*, 2008). The A_{260}/A_{230} ratio is determined to confirm that the sample is free from carbohydrates, peptides, ethanol, or any other organic compounds, and it is generally greater than 1.5 (Ning *et al.*, 2009).

Therefore, good quality DNA should have:

$$\frac{A_{260}}{A_{280}} = 1.7 - 2 \quad \text{and} \quad \frac{A_{260}}{A_{230}} > 1.5$$

In the present study, UV-Vis spectroscopy was used to estimate the purity of the isolated DNA. The absorbance values of the DNA solution obtained were measured at 230, 260, and 280 nm to determine the concentration and purity of the extracted DNA. The dissolved DNA can be stored at 4°C for a few days or at -20°C for longer-term storage (Heckel *et al.*, 2017). The absorbance values were taken from Figure 13 and listed in Table 4. The values obtained for the various absorbance ratios indicate the high purity of the isolated DNA.

Table 4. Absorbance Ratio of Isolated DNA

A_{230}	A_{260}	A_{280}	A_{260}/A_{230}	A_{260}/A_{280}
1.116	1.301	1.021	1.166	1.724

The quantity of DNA was determined by absorption spectroscopy using the molar extinction coefficient value of 6600 M⁻¹cm⁻¹ at 260 nm (Schöppler *et al.*, 2011).

2.7.6.2. UV-visible spectroscopic DNA/BSA interaction study

Cyclic Voltammetric Measurements

The apparatus used for voltammetric measurements is a Potentiostat/Galvanostat Model PGZ301 (Radiometer Analytical SAS) connected to a three-electrode electrochemical cell, A glassy carbon electrode with a diameter of 5.2 mm²; A mercury/mercurous chloride/saturated KCl reference electrode; A platinum auxiliary electrode with a diameter of 3 mm². All of this is controlled by a Pentium IV microcomputer (CPU 4.0 GHz and RAM 2 GB) equipped with VoltaMaster4 software, version 7.08.

The reaction between the studied compounds and the DNA/BSA takes place in the electrochemical cell. The reaction medium is a DMSO.

Before each measurement, the working electrode is polished using p4000 abrasive paper. After polishing, the electrode is washed with ultra-pure water and dried with air. The surface of the electrode thus appears mirror-like. Then, the electrochemical cell is equipped with the reference electrode and the auxiliary electrode, as well as the working electrode. The cell is filled with 10 ml of a solution consisting of DMSO solution containing the studied compounds. Nitrogen gas is bubbled through the solution for 10 to 15 minutes to remove oxygen from the cell. A variable potential is applied at a fixed scan rate and at a temperature of 28 ± 2°C. The obtained

voltammogram is analysed to access the interaction parameters between the studied compounds and the DNA/BSA.

Spectroscopic Measurements

UV-Vis measurements were performed using a UV-Vis spectrometer (Shimadzu 1800) and a quartz cell with a volumetric capacity of 5 ml. Data acquisition was carried out with a Pentium IV microcomputer (CPU 4.0 GHz and RAM 2 GB) equipped with UV probe software version 2.34 (Shimadzu). The data is processed using OriginLab 9.0 software.

The electronic spectra of the studied compounds in the DMSO solution were obtained in the absence and presence of increasing concentrations of DNA/BSA.

2.7.6.3. Cytotoxicity activity

2.7.6.3.1. Cell Culture

Cell cultures were obtained from the National Centre for Cell Sciences (NCCS) in Pune. The culture medium and Trypsin Phosphate Versene Glucose (TPVG) solution were brought to room temperature through thawing. Tissue culture bottles were examined under an inverted microscope for signs of growth, cell degeneration, pH levels, and turbidity. Upon reaching 80% confluency, subculturing was initiated. The bottle openings were wiped clean using cotton soaked in spirit to remove any adhering particles.

Following this, the growth medium was discarded, and 4-5 ml of Minimal Essential Media (MEM) without Fetal Calf Serum (FCS) was gently added and rinsed by tilting. Dead cells and excess FCS were washed away, and the medium was discarded again. TPVG was added over the cells, followed by incubation at 37°C for 5 minutes to disaggregate the cells, resulting in individual suspension cells. Then, 5ml of 10% MEM was added to FCS using a serological pipette. Passaging was performed using a serological pipette. After passaging, the cells were split into ratios of 1:2 and 1:3 for cytotoxicity studies using the plating method.

The MCF-7 breast cancer cells were cultured in Dulbecco's Modified Eagle's Medium (DMEM) supplemented with 10% Fetal Bovine Serum (FBS), 100U penicillin, and 100 µg/ml streptomycin. Incubation was carried out at 37°C with a 5% CO₂ atmosphere. Normal breast (MCF-7) cells were cultured in a 1:1 mixture of DMEM and Ham's F12 medium, supplemented with 20 mg/ml epidermal growth factor (EGF), 100 µg/ml cholera toxin, 0.01 mg/ml insulin, 500 µg/ml hydrocortisone, and 5% chelex-treated horse serum. Purified berberine and tamoxifen were dissolved in dimethyl sulfoxide (DMSO) and used for the bioassays.

2.7.6.3.2.MTT Assay

The cytotoxic effects of the *H. scoparia* and ZnO-NPs samples on MCF7 cells were assessed using the MTT (3-(4,5-dimethylthiazol-2yl)-2,5-diphenyl tetrazolium bromide) assay, following the method described by Horiuchi *et al.*,(1988). Cells were seeded at a density of 1×10^5 cells/well in 96-well plates with 0.2 ml of medium per well. After the designated incubation period, the medium was carefully aspirated from the wells, and each well was washed with MEM without FCS (Fetal Calf Serum) for 2-3 times. Subsequently, 200 μ l of MTT solution (5mg/ml) was added to each well, and the plates were incubated for 6-7 hours in a 5% CO₂ incubator to assess cytotoxicity. Following incubation, 1ml of DMSO (solubilizing reagent) was added to each well, mixed thoroughly using a micropipette, and allowed to stand for 45 seconds. The presence of viable cells was indicated by the development of a purple color due to the formation of formazan crystals. The suspension was then transferred to a spectrophotometer cuvette, and the optical density (OD) values were measured at 595nm, with DMSO serving as the blank. The cell viability (%) was calculated using the formula:

$$\text{Cell viability (\%)} = \text{Mean OD/Control OD} \times 100\%.$$

The concentration required for a 50% inhibition of viability (IC₅₀) was determined graphically by plotting a standard graph with the concentration of the drug on the X-axis and relative cell viability on the Y-axis.

2.7.7. *In vivo* Wound Healing activity

2.7.7.1. Elaboration of wound healing creams

a. Ingredients used in this cream

H.scoparia/ZnO-NPs extract. dissolving extracts in water to form the aqueous phase.

Sweet almond oil. is renowned for its skin benefits, boasting a plethora of nutrients and recognized for its anti-inflammatory properties.

Emulsifying-Wax. serves as a common component in lotions and creams, contributing to their smooth texture and preventing separation.

Glyceryl stearate and Peg 100. produced through the esterification of glycerin and stearic acid. then combined with Peg 100, it enhances the final stability of the emulsion, thereby improving its capacity to absorb additional ingredients like essential oils and colorants.

Vitamin E. in cosmetics acts as an antioxidant, safeguarding the formula from oxidation. Moreover, it mitigates the impact of free radicals induced by sunlight and pollutants.

b. Formulation of Wound healing cream

This study aimed to enhance the formulation of a water-in-oil type healing cream, composed primarily of two phases (Figure 14): a fatty phase consisting of sweet almond oil, and an aqueous phase containing distilled water and *H.scoparia* extract /ZnO-NPs. Emulsification between these phases was achieved using E-wax and Glyceryl stearate with peg 100. Additionally, Vitamin E was incorporated as a preservative.

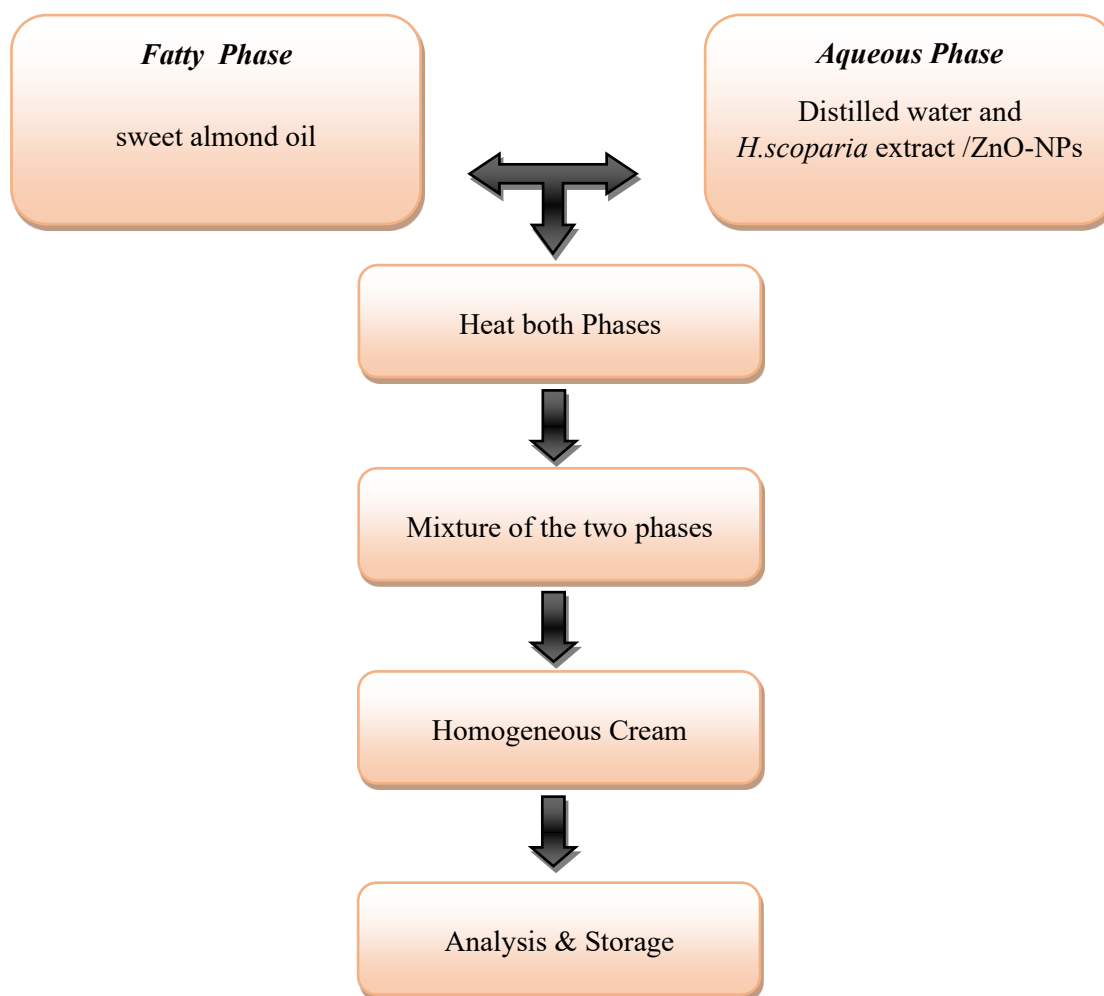


Figure 14: Cream preparation process

c. Physical analyzes of formulated cream*pH test*

The pH measurement of the cream is measured by diluting a quantity of the samples with water, then filtered with Watman N°4 filter paper (Anchisi, Maccioni, and Sinico, 2001). The pH analysis is carried out at a temperature of 20°C. using a pH meter (HANNA-HI 8424).

Stability test

This test was carried out on the sample after centrifugation at 3000 rpm, for 30 min and at room temperature. The degree of separation of the two phases is expressed by the total percentage of stability, i.e. (100 = stable, 0 = unstable).

2.7.7.2. Biological evaluation of creams

Experimental design

Wistar albino rats served as an experimental model for creating wounds. The rats came from Institut Pasteur, and the experiment was carried out in the laboratory of the molecular and cellular biology department. The animals were divided into seven groups, each comprising 05 rats:

- *Group I:* The rats were not exposed to any wound induction and did not receive any cream treatment for 13 days ;
- *Group II:* The rats were exposed to wound induction, and left without cream treatment;
- *Group III:* The rats were exposed to wound induction, and received base cream treatment for 13 days;
- *Group IV:* The rats were exposed to wound induction, and received 5% *H. scoparia* cream treatment for 13 days;
- *Group V:* The rats were exposed to wound induction, and received 5% ZnO-NPs-C cream treatment for 13 days;
- *Group VI:* The rats were exposed to wound induction, and received 5% ZnO-NPs-NC cream treatment for 13 days;
- *Group VII:* The rats were exposed to wound induction, and received 5% DOUCE PLUS[®] cream treatment for 13 days;

Pharmaceutical Treatments used

DOUCE PLUS[®] is a dermal ointment that combines the benefits of cod liver oil and zinc oxide. This soothing formula is designed to nourish and protect the skin, while providing anti-inflammatory and healing properties. It can be used to relieve skin irritation and promote soft, healthy skin.

Induction of wounds

The wounds were made on the skin of the dorsal region of each animal; the choice of this region is motivated by ease of access, both for making the wound and for monitoring the progress of healing and taking measurements. The wounds were made on the previously shaved back of

each animal. The depilated region is disinfected with 70° surgical alcohol and the area to be cut is traced in a rounded shape and the traced area is cut out using a pair of scissors and pliers.

Application of treatments

Just after wound induction, the animals in the treated batches each received a topical application of the product intended for their respective batch. Treatments were applied once every 24 hours for each rat. Treated or untreated wounds were not protected by a dressing.

Evaluation of cicatrisation process

After photographing them, the dimensions (length, width) of the excision wounds are measured every 3 days during the trial period (15 days). The percentage of the evolution of wound cicatrisation is calculated using the following formula (Lodhi *et al.*, 2006):

$$\text{Wound Healing (\%)} = (\text{cicatrised wound surface} / \text{initial wound surface}) \times 100$$

Sacrifice and Blood Collection

After a 16-hour fasting period and completion of each treatment, rats were euthanized under light anesthesia with 94% chloroform. Blood samples were collected into pre-marked and numbered EDTA tubes for each rat. The blood was then centrifuged at 2500 rpm for 10 minutes, and the resulting serum was stored at -20°C until biochemical analysis.

2.7.7.3. Histological study

Preparation of Tissue Samples

Skin tissue samples were obtained from the wound sites of all Wistar albino rats to create histological sections for monitoring the stages of wound healing.

Block preparation

The skin fragments previously fixed in 10% formalin are placed in cassettes which are then placed in an automated machine. The organ fragments are first dehydrated by submersion in ethanol baths at increasing concentrations (60%, 70%, 80%, and 100%). The samples undergo two baths of xylene and two others of melted paraffin. Xylene occupies the place of water and therefore facilitates the penetration of paraffin since the latter is hydrophobic. The duration of the baths is 24 hours. Using an embedding device, the skin samples are placed in metal molds and covered with melted paraffin. After cooling, the blocks are ready for cutting.

Making cuts and coloring

The blocks are placed in the microtome in order to make sections 3 µm thick. Using very fine forceps, the sections are placed on slides which are then deparaffinized by heating in an oven for one hour. To highlight the layers of the skin, the sections are first rehydrated by successive

submersion in the following baths: xylene bath (5 min), ethanol bath (5 min). After rinsing in distilled water (5 min), the rehydrated sections are placed in a hematoxylin bath (5 to 6 min). The excess dye is removed by a water bath with a few drops of ammonium hydroxide (NH_4OH), then they are put in an eosin bath (5 min) to color the cytoplasm and the excess dye. dye is removed by ethanol. The slides thus stained are covered with lamellae and are suitable for microscopic observation.

2.7.8. Statistical analysis

The results are presented as the mean \pm standard error of the mean (Mean \pm SEM). Group comparisons were conducted using one-way ANOVA. Statistical analysis was performed using EXCEL (Version 2007). Significant differences between means were determined using Duncan's multiple range test (DMRT) at a significance level of $p=0.05$ with SPSS (Statistical Package for Social Sciences) version 29 software. Differences were considered significant at $p\leq 0.05$.

- Significant (* $P \leq 0.05$).
- Highly significant compared with the control (** $P \leq 0.01$).
- Very highly significant compared with the control (***) $P \leq 0.001$.

Chapter II:

Results

I. Results

1. Phytochemical screening of major secondary metabolites

The results obtained from the various preliminary biochemical tests carried out on the aerial part of the plant species *Hammada scoparia* (Pomel) Iljin or Broomstick from the region of Sidi Khaled Wilaya of Biskra in South-East Algeria are indicated in the table below.

Table 5. Different Phytochemical of the aerial part of *Hammada scoparia* (Pomel) Iljin.

Phytochemical	<i>H. scoparia</i>
Polyphenols	+
Alkaloids	+
	Mayer
	Wagner
Flavonoids	+
Terpenoids	+
Saponins	+
Tannins	+
Cardiac glycosides	+
Mucilage	+
Anthocyanins	+
Leuco-anthocyanins	-
Steroids	+

–, absence of phytochemicals; +, presence of phytochemical

The phytochemical test results demonstrate the extract's richness in several active ingredients. The chemical contents of *H. Scoparia* include polyphenols, tannins, flavonoids, alkaloids, saponins, glycosides, and steroids (Table 5).

2. Yields of *Hammada scoparia* (Pomel) Iljin Extract

aqueous extractions from the aerial part of *Hammada scoparia* (Pomel) Iljin was utilized to calculate the yield of each extract. The yield, expressed in mg/g of dry plant matter. The recorded values have been represented in the following table (Table 6).

Table 6. Yields of Aqueous extracts of *Hammada scoparia* (Pomel) Iljin.

Extract	Yields
<i>H. scoparia</i>	24.6± 1.47

3. Colorimetric analysis

The phenolic compound content was determined by measuring the absorbance of the plant extract solution and comparing it with reference solutions containing various concentrations of

phenolic acids and other compounds. The results of the colorimetric analysis for total polyphenols, total flavonoids, and total tannins are presented in Table 7.

Table 7. Phenolic compound contents in aqueous extract of the species *Hammada scoparia*.

Assay	Total phenol (mg GAE/ gEx)	Total flavonoid (mgQE/gEx)	Total tannin (mgCE/gEx)
Content	141.61 ± 0.53	67.88 ± 0.71	54.47 ± 0.86

3.1. Total polyphenol content

From the Figure 15 below of the gallic acid calibration curve established with a determination coefficient ($R^2 = 0.997$) and from the linear regression equation ($y = 0.0103x + 0.0561$), we were able to calculate the total polyphenol content. A very high content of the order of 141.61 ± 0.53 mg GAE/ gEx of total polyphenols was recorded in the extract of the aerial part of the plant species *Hammada scoparia* (Pomel) Iljin from the southeast region Algerian (Table 6).

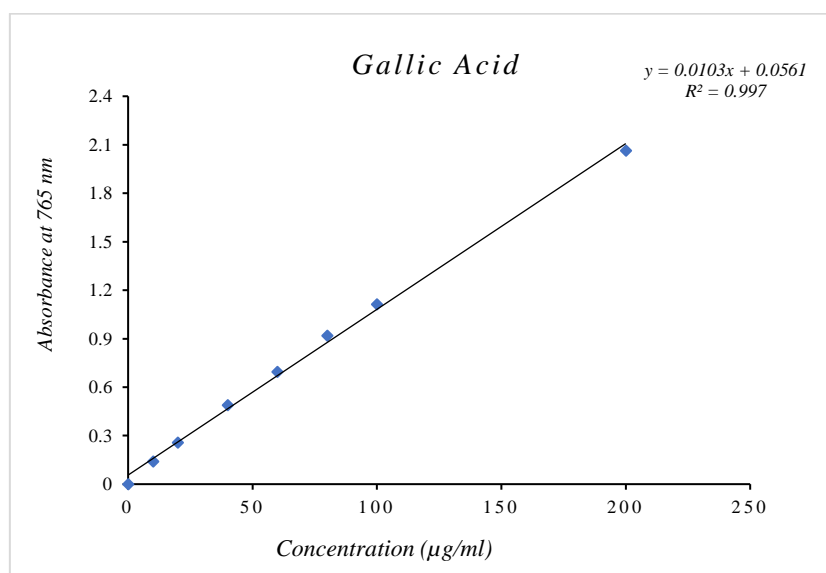


Figure15. Calibration curve of Gallic acid for determination of total phenolic content.

3.2.Total flavonoid content

From Table 6, the the aqueous extract of the aerial part of the plant species *Hammada scoparia* (Pomel) Iljin from the southeast region Algerian to be riche in total flavonoids with a content equal to 67.88 ± 0.71 mg QE/ gEx , which comparing with reference calibration curve ($y = 0.0112x - 0.0227$; $R^2 = 0.9934$) (Figure16) containing various concentrations of Quercetin.

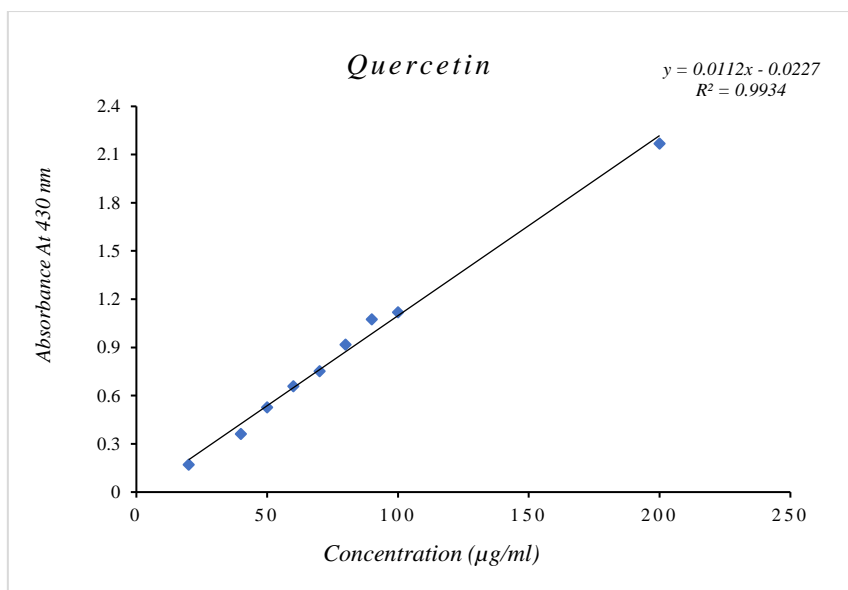


Figure 16. Calibration curve of Quercetin for determination of total flavonoids content.

3.3. Condensed tannin content

Concerning the condensed tannins of this plant species, a content of the order of 54.47 ± 0.86 mg CE/ gEx was recorded (Table 7) in the aqueous extract using the linear regression equation of the calibration curve for catechin ($y = 0.0018x - 0.0097$; $R^2 = 0.9994$) (Figure 17).

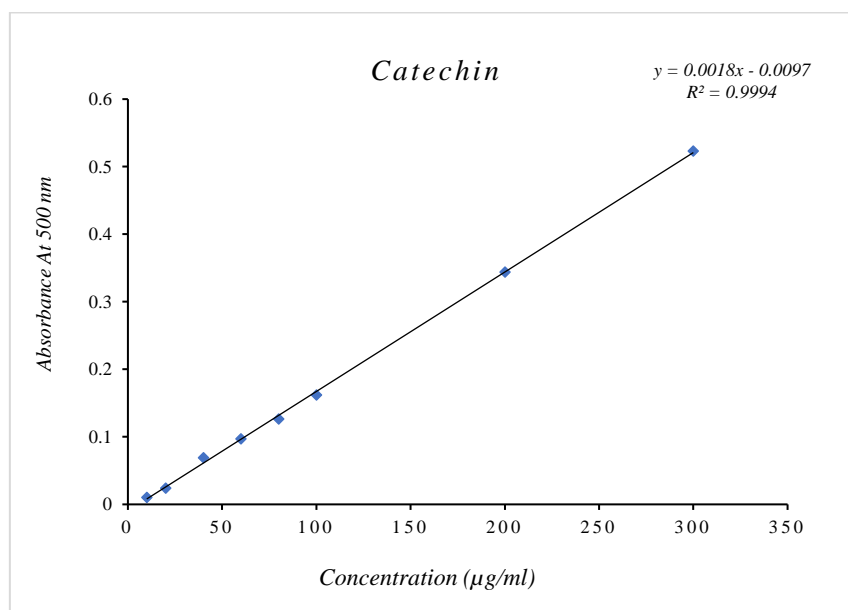


Figure17. Calibration curve of Catechin for determination of condensed tannins content.

4. LC-MS-MS Analysis

The initial analysis conducted via LC/MS of the aqueous extract of the aerial part of the plant species *Hammada scoparia* (Pomel) Iljin from the southeast region Algerian identified a total

of 28 compounds, spanning various groups of secondary metabolites such as phenol acids, simple phenols, saponins, tannic compounds, flavonoid compounds, among others. A comprehensive characterization of these compounds is provided in Appendix No. 2. However, it's worth noting that the complexity of the analysis resulted in the separation of approximately 127 distinct products. Chromatogram profiles obtained from the HPLC/UV-visible analysis of the aqueous extract is depicted in Figures 18.

The chromatogram profile of the aqueous extract unveiled the presence of 21 phenolic compounds (Table8). By evaluating retention times and peak areas, the nature of these compounds was discerned. Rutin emerged as the most abundant, constituting a major peak at 28.288 %, succeeded by Naringenin (13.662 %), Gallic Acid (11.037 %), Valinin (9.436 %), and Hydroxy-Comarin (6.006%). Among the less dominant compounds, including Beta-Carotene, Ferulic Acid, Salicylic Acid, Caffeic Acid, and ascorbic acid, their quantitative significance varied between 2.8% and 3.7%. Ferulic acid, myricetin, and quercetin exhibited lower prominence, with contents ranging from 0.785 % to 2.101%, these compounds possess notable biological activities, particularly in terms of their antioxidant, antiseptic, analgesic, and anti-inflammatory properties, potentially rivaling those detected at higher concentrations.

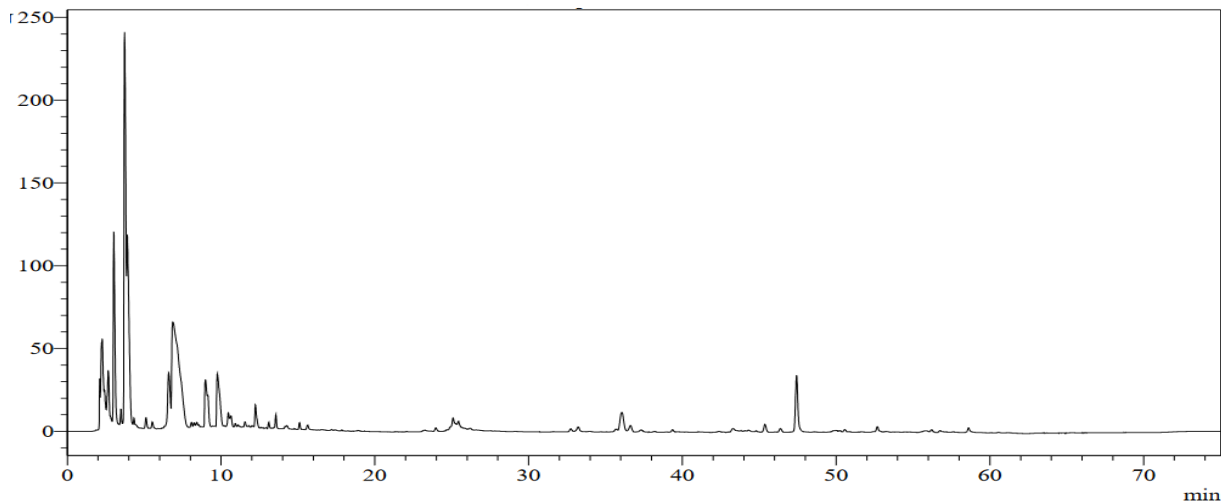


Figure18. HPLC/UV chromatogram profile of the aqueous extract of *Hammada scoparia*.

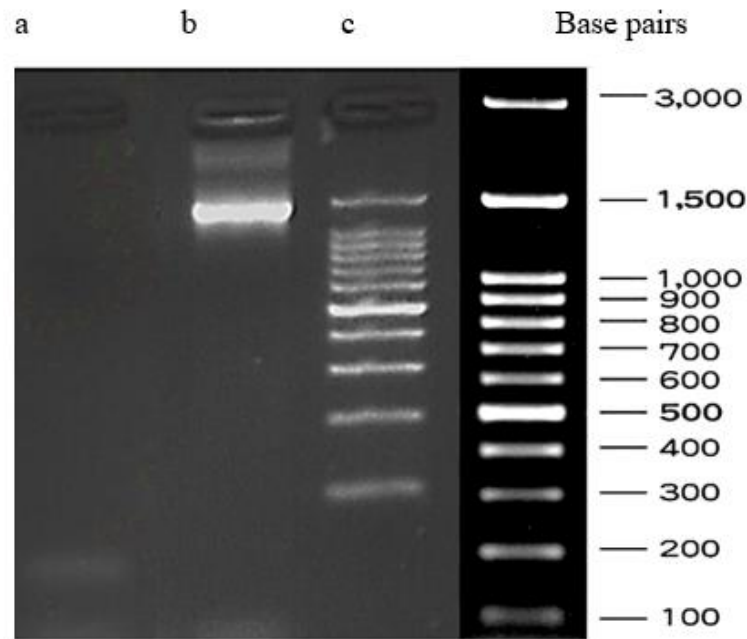


Figure 25. PCR amplification of 16S rRNA region of isolated LAB strain; a: Negative Control, b: Amplified 16S rRNA of the isolated strain, c: Molecular marker + 100 bp DNA ladder.

The 16S rRNA gene sequencing identified the isolated strain to be *Bacillus pumilus* (confidence degree, $E = 0.0$, homology = 99.14%). The neighbor-joining approach was used to estimate the evolutionary history. The greatest composite likelihood approach was used to determine the tree. A phylogenetic tree (Figure 26) was constructed using 51 bacterial nucleotide sequences, of which one sequence of the 16S rRNA gene was amplified from the *Bacillus* isolated strain. The nBLAST alignments tool was used to acquire 50 sequences that represented the most similar aligns from the NCBI GeneBank database.

Table 20. Cytotoxic effects of the *Hammada scoparia* extract, uncalcined ZnO-NPs, and calcined ZnO-NPs samples on MCF7 cells using the MTT assay

Samples	IC ₅₀ (µg/mL)
<i>Hammada scoparia</i>	186.028 ± 0.027
Uncalcined ZnO-NPs	<IC ₅₀
Calcined ZnO-NPs	<IC ₅₀

7.7. *In vivo* Wound Healing activity of of *H.Scoparia* extract / ZnO-NPs

7.7.1. Physical analyzes of formulated cream

The results concerning the Physical analyses of formulated cream used in this study are mentioned in Table 21. The pH analysis is carried out at a temperature of 25°C using a pH meter (HANNA-HI 8424). The degree of separation of the two phases is expressed by the total percentage of stability, i.e. (100 = stable, 0 = unstable).

Table 21. Physical analyzes of formulated cream

Color	Odor	Texture	pH	Stability
White	No	Humid	6.8	100

The results represented in Table 20 offer insights into the properties of a skin cream formulation which described as white appears neutral. Its lack of odour suggests it is formulated without added fragrances, making it potentially suitable for individuals with sensitivities to scented products. The texture is labelled as "humid," indicating a moisture-rich consistency that may provide hydration and comfort upon application to the skin. With a pH value of 6.8, the cream falls within the slightly acidic range, which is often preferred for skincare products as it is closer to the skin's natural pH, promoting compatibility and minimizing the risk of irritation. Moreover, the cream demonstrates excellent stability, scoring a rating of 100, suggesting it is robust and resistant to degradation over time, ensuring its efficacy and longevity. Overall, these characteristics suggest that the cream is well-suited for skin applications, offering hydration, comfort, and stability for daily use.

7.7.2. *In vivo* evaluation of creams

Various creams were applied to the wounds in all groups, and then the wound dimensions were measured after every three days to observe the wounds macroscopically, and then the healing rate was calculated each time to observe the speed of the healing effect of the creams carried out in this study using *H. scoparia* extract and biosynthesized zinc oxide nanoparticles (ZnO-NP-UC and ZnO-NP-C) and DOUCE Plus compared to the negative control groups on the

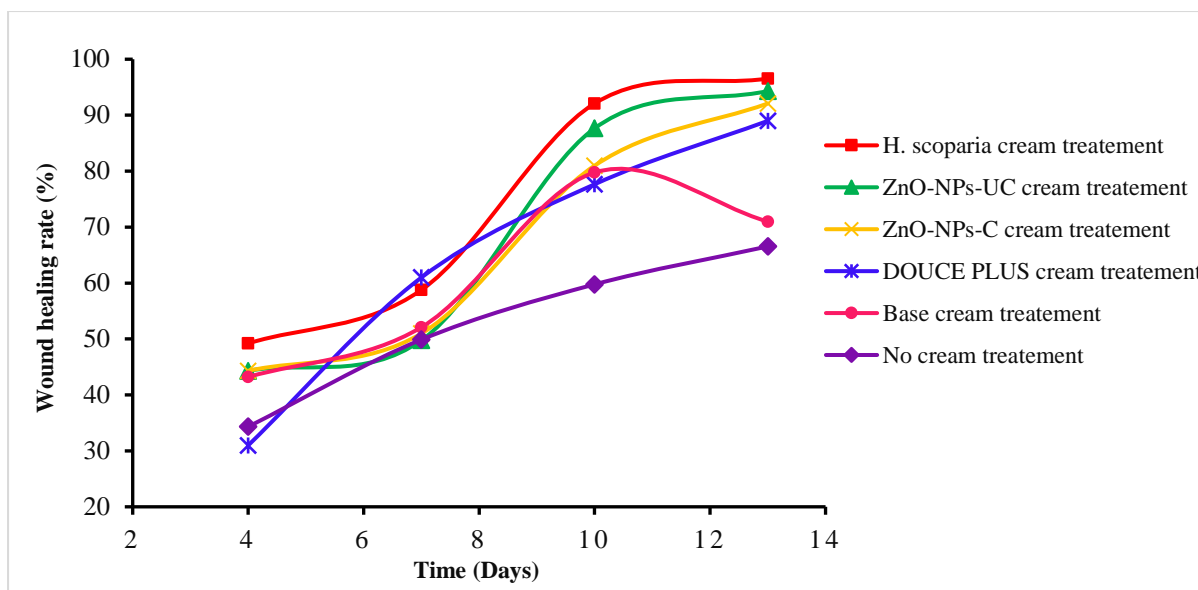


Figure 34. Wound healing rate at day 4, day 7,10, and day 13 *in vivo* treatment of different cream treatment formulations; n = 5.

7.7.3.Hematological Parameters

On day 13 of the study, the hematological parameters were analyzed across various treatment groups, shedding light on the effects of different creams on blood composition. The mean levels of red blood cells (RBCs) varied slightly among the groups (Figure 35), with the *H. scoparia* cream showing the highest mean level at $5.2 \times 10^6/\mu\text{L}$, followed closely by ZnO-NPs-C cream and Base cream. Conversely, the DOUCE PLUS cream exhibited the lowest mean RBC level at $4.8 \times 10^6/\mu\text{L}$. Similarly, white blood cell (WBC) levels (Figure 36) showed marginal differences, with ZnO-NPs-UC cream and DOUCE PLUS cream displaying the highest mean levels, while the No cream group exhibited the lowest. Blood platelet (PLT) levels (Figure 37), an essential factor in clotting, also varied across groups, with *H. scoparia* cream demonstrating the highest mean level at $250 \times 10^3/\mu\text{L}$. Overall, these findings provide insights into how different topical treatments may influence hematological parameters.

Chapter III:
Discussion

The phytochemical screening of *Hammada scoparia* from Biskra, Algeria, identified polyphenols, alkaloids, flavonoids, terpenoids, saponins, tannins, cardiac glycosides, mucilage, anthocyanins, and steroids, with leuco-anthocyanins absent. Compared to Benkhrara *et al.* (2021), which detected similar compounds but not polyphenols and cardiac glycosides, these differences might be due to extraction methods or environmental conditions, highlighting *H. scoparia*'s medicinal potential.

These molecules exhibit a wide range of properties. Polyphenols, for example, have been linked to a reduced risk of several chronic diseases, including cancer, diabetes, cardiovascular disease, and neurodegenerative disorders (Handore & Khandelwal, 2017; Rasouli *et al.*, 2017). They protect organisms against chronic pathologies by modulating various physiological processes, such as cellular redox potential, enzymatic activity, cell proliferation, and signal transduction pathways (Luca *et al.*, 2019). Additionally, flavonoids are known for their antioxidant and anti-inflammatory properties (Wang & Mazza, 2002). Alkaloids also possess therapeutic properties, including anti-inflammatory, antinociceptive, antitumor, antioxidant, and antimicrobial activities (Rosales *et al.*, 2020). Terpenoids are notable for their potential in treating inflammatory diseases (Hortelano *et al.*, 2020).

The study investigated the yield of aqueous extracts from the aerial parts of *Hammada scoparia* (Pomel) Iljin. The yields were recorded in milligrams per gram of dry plant matter (mg/g), showing the results of an overall mean of $24.6 \pm 1.47\%$.

Comparing these results with previous studies reveals interesting insights. Mezghani-Jarraya *et al.* (2009) reported a methanolic extract yield of 15.10% from the aerial parts of *Hammada scoparia* in Sfax, Tunisia. This is lower than the 24.6% yield obtained in the current study using aqueous extraction. The higher yield in the present study suggests that aqueous extraction may be more effective than methanolic extraction for this species, likely due to the higher solubility of certain phytochemicals in water.

Bouaziz *et al.* (2016) reported a methanolic extract yield of 6.15% from the same species and region. This is significantly lower than both the current study's aqueous extract yield and the yield reported by Mezghani-Jarraya *et al.* (2009). The lower yield could be attributed to differences in extraction efficiency, plant material quality, or extraction methods.

Bourogaa *et al.* (2012) reported an aqueous extract yield of 11% from *Hammada scoparia* in southern Tunisia, which is much lower than the 24.6% yield obtained in this study. Similarly, Taïr *et al.* (2016) found a low yield of 11% for aqueous extracts from the same species in

Naâma, northwestern Algeria. These results are consistent with each other but significantly differ from the current study's findings, highlighting potential regional or methodological variations.

Benkherara *et al.* (2021) reported a much higher aqueous extract yield of 44.44% from the same species in Biskra, southeastern Algeria. This yield is nearly double the yield obtained in the present study. The discrepancy could be due to regional differences in the plant's phytochemical composition, environmental factors, or specific extraction techniques employed. The high yield reported by Benkherara *et al.* suggests that the plants in Biskra might have a richer content of compounds, or that their extraction method was particularly efficient.

The current study's aqueous extract yield of 24.6% for *Hammada scoparia* is relatively high and consistent with certain previous studies while differing significantly from others. The comparison highlights the influence of extraction methods, solvents, and geographic variations on the yield of plant extracts. The substantial yield differences, particularly with the results from Benkherara *et al.* (2021) in Biskra, underscore the necessity of considering regional and methodological factors in phytochemical research. The findings indicate that aqueous extraction can be a highly effective method for extracting bioactive compounds from *Hammada scoparia*, potentially offering higher yields compared to methanolic extraction.

These distinctions stem from various factors, encompassing the geographical source, specific environmental conditions like temperature and humidity (Granger *et al.*, 1973), the particular plant species, organ utilized, growth stage, timing of harvest, methods employed for plant material preservation, and the specific partial drying approach. These differences are also influenced by the study's methodology and the extraction techniques utilized (Sefidkon *et al.*, 2007).

Phenolic compounds are commonly found in plant parts such as leaves, stems, barks, flowers, and fruits, and are recognized as natural antioxidants (Esmaeilzadeh *et al.*, 2022). *Hammada scoparia* is notably high in phenolic content within its aerial parts. Benkhrara *et al.* (2021) reported tannin and total flavonoid contents in the aqueous extract, which were notably different from the results obtained in this study. Specifically, they found tannin content (TTC) to be 2.576 ± 0.112 mg EC/g MVS and total flavonoid content (TFC) to be 12.955 ± 0.117 mg ER/g MVS in the raw aqueous extract. These discrepancies could be attributed to variations in extraction techniques, geographical locations, or plant characteristics.

formulations or combining them with organic and inorganic filters has generally shown positive results in modifying SPF values (Paixão *et al.*, 2023). Moreover, scientists are actively investigating natural compounds derived from plants that can absorb UV radiation and exhibit photoprotective properties. Polyphenols, particularly flavonoids, have been extensively studied for their ability to absorb radiation (Cefali *et al.*, 2016).

However, while all samples provide some degree of sun protection, VICHY® sunscreen and calcined zinc oxide nanoparticles stand out with higher SPF values, indicating superior UV radiation shielding. These findings underscore the importance of formulation technologies and processing techniques in developing effective photoprotective agents, crucial for mitigating the adverse effects of UV exposure on skin health.

The results of the anti-inflammatory activity evaluation, based on the capacity to inhibit albumin denaturation, demonstrated significant differences among the samples tested. Uncalcined ZnO nanoparticles (ZnO-NPs) exhibited the strongest inhibitory activity across various concentrations, with an IC_{50} of 77.070 $\mu\text{g/mL}$. This suggests that uncalcined ZnO-NPs are highly effective in preventing protein denaturation, which is a key marker of their anti-inflammatory potential. The high efficacy of uncalcined ZnO-NPs could be attributed to their unique structural and surface properties, which enhance their interaction with proteins involved in the inflammatory process. Calcined ZnO-NPs showed a significant inhibitory effect with an IC_{50} of 126.66 $\mu\text{g/mL}$. Although not as potent as the uncalcined form, calcined ZnO-NPs still demonstrated a good capacity to inhibit albumin denaturation. The process of calcination may alter the surface characteristics and possibly reduce the nanoparticles' ability to interact with and stabilize proteins, which could explain the reduced activity compared to the uncalcined form. Despite this, calcined ZnO-NPs still outperform the standard anti-inflammatory drug, Aspirin®, which had an IC_{50} of 154.93 $\mu\text{g/mL}$. This comparison underscores the potential of ZnO-NPs as effective anti-inflammatory agents.

The *Hammada scoparia* extract demonstrated the lowest anti-inflammatory activity among the samples tested, with an IC_{50} of 251.64 $\mu\text{g/mL}$. This indicates that while *Hammada scoparia* does possess some anti-inflammatory properties, it is significantly less effective than both forms of ZnO-NPs and even less effective than Aspirin®. The lower activity of *Hammada scoparia* could be due to the lower concentration or bioavailability of active compounds within the extract that are capable of inhibiting protein denaturation.

Algerian goat's milk could be a valuable addition to probiotic formulations (Gibson and Roberfroid, 1995; Kneifel, 2000).

The strain's resilience in different environmental conditions and its beneficial biochemical properties make it a strong candidate for further development and application in health-related fields. This study contributes valuable knowledge to the field of probiotics, emphasizing the importance of detailed characterization in identifying and utilizing beneficial bacterial strains. Several factors influence the colonization and survival of probiotic bacteria, including gastric pH, digestive enzymes, and bile acids. However, it is a significant challenge that the bacteria may not survive in sufficient numbers in the gastrointestinal tract and traditional fermented dairy products. Hence, providing probiotic living cells with a physical barrier against adverse environmental conditions is of vital importance, which has received considerable interest in recent times. This challenge highlights the importance of selecting robust strains and developing protective delivery systems to enhance their viability and effectiveness (Favaro-Trindade *et al.*, 2011; Chen *et al.*, 2007).

Currently, synbiotic, which are a combination of probiotics and prebiotics, are widely used to enhance the growth of intestinal microflora. They offer a higher likelihood of survival and attachment for beneficial microorganisms in the human gut compared to using prebiotics or probiotics alone. Therefore, it is crucial to identify a combination of natural sources of both prebiotics and probiotics to achieve health-related benefits (Tzounis *et al.*, 2011; Geier *et al.*, 2007). The results indicate that both *H. scoparia* extract and ZnO nanoparticles enhance the probiotic characteristics of *Bacillus pumilus* in different ways. For acid tolerance, all tested materials significantly improved the survival rate of *Bacillus pumilus* under highly acidic conditions, especially at higher concentrations. This indicates their potential for maintaining probiotic viability in the acidic environment of the stomach. In terms of bile tolerance, *H. scoparia* extract and ZnO nanoparticles (both uncalcined and calcined) significantly increased the tolerance of *Bacillus pumilus* to bile salts, which is crucial for survival and colonization in the small intestine.

Cell surface hydrophobicity, which relates to the ability of probiotics to adhere to intestinal cells, showed varying results. *H. scoparia* extract exhibited high hydrophobicity at lower concentrations but decreased at higher concentrations, whereas ZnO-NPs showed a moderate and decreasing trend with increasing concentrations. These findings suggest that while *H. scoparia* extract and ZnO nanoparticles both enhance the probiotic characteristics of *Bacillus*

collagen deposition, and showing fewer new blood vessels and less fibroblast activity compared to the treated samples

*General conclusion &
Perspectives*

In this study, we conducted a comprehensive exploration into the therapeutic potential of *Hammada scoparia* (Pomel) Iljin extract and zinc oxide nanoparticles (ZnO-NPs), synthesized using a green approach. Our investigation encompassed a wide range of biological activities, focusing on wound healing, antioxidant properties, anti-inflammatory effects, anti-diabetic potential, photoprotective activities, probiotic efficacy, and anticancer properties. Using albino rats as our *in vivo* model, we aimed to evaluate the efficacy of these substances both in controlled laboratory settings and in practical, therapeutic applications.

Hammada scoparia extract revealed a rich array of bioactive compounds, prominently including phenolic compounds like Rutin, Naringenin, Gallic Acid, and others. These compounds are known for their antioxidant and anti-inflammatory properties, which are critical in combating oxidative stress and inflammatory responses within biological systems. The green synthesis method employed for the ZnO-NPs utilized the aqueous extract of *Hammada scoparia*, ensuring an environmentally friendly approach. Characterization using UV-Vis spectrophotometry showed distinct absorption peaks at 362 nm for uncalcined and 376 nm for calcined ZnO-NPs, indicating their nanoparticulate nature suitable for biomedical applications. Additional analyses via FTIR, XRD, and SEM/EDS confirmed the crystalline structure, morphology, and surface characteristics of these nanoparticles. SEM images revealed spherical nanoparticles with average diameters of 36.12 ± 4.52 nm for uncalcined and 40.17 ± 6.43 nm for calcined ZnO-NPs, elucidating their physical attributes essential for therapeutic efficacy.

In vitro studies demonstrated that both *Hammada scoparia* extract and ZnO-NPs possess robust antioxidant properties. These findings were supported by their ability to scavenge free radicals and inhibit lipid peroxidation, which are pivotal in reducing oxidative damage to cells and tissues. Furthermore, the anti-inflammatory effects observed in our experiments highlight the potential of these substances in managing inflammatory conditions. The ability to suppress pro-inflammatory cytokines and enzymes underscores their therapeutic promise in diseases characterized by chronic inflammation.

In addition to their antioxidant and anti-inflammatory activities, *Hammada scoparia* extract and ZnO-NPs exhibited significant photoprotective properties. This capability is crucial for shielding skin cells from UV-induced damage, suggesting potential applications in skincare formulations and sunscreens.

The probiotic potential of *Hammada scoparia* extract and ZnO-NPs was also explored, particularly against *Bacillus pumilus*. The antimicrobial efficacy observed underscores their potential utility in wound care and infection management, where microbial control is critical for promoting healing and preventing complications.

In terms of antidiabetic activity, ZnO-NPs—especially the uncalcined variant—demonstrated noteworthy inhibition of hemoglobin glycosylation and α -glucosidase activity. These results suggest a role for ZnO-NPs in managing diabetes mellitus, potentially by regulating glucose metabolism and mitigating associated complications.

This studies further delved into the interaction between ZnO-NPs and biomolecules such as DNA and BSA. The results indicated electrostatic interactions between ZnO-NPs and these biomolecules, suggesting potential applications in drug delivery and therapeutic targeting. Moreover, both *Hammada scoparia* extract and ZnO-NPs exhibited significant cytotoxic effects against MCF7 breast cancer cells. The observed cytotoxicity, evaluated using the MTT assay, demonstrated dose-dependent inhibition of cancer cell viability, highlighting their potential as adjuncts in cancer therapy.

In *in vivo* wound healing study using albino rats with induced wounds, topical application of *Hammada scoparia* extract cream and ZnO-NP creams resulted in accelerated wound healing compared to control groups. Macroscopic evaluation showed reduced wound area and enhanced epithelialization in treated groups, indicative of improved healing rates. Histopathological examination confirmed enhanced collagen deposition, reduced inflammatory cell infiltration, and accelerated re-epithelialization in the presence of *Hammada scoparia* extract and ZnO-NPs. Hematological analyses further supported these findings, revealing improvements in blood parameters associated with systemic health in treated animals.

Perspective: This research represents a significant advancement in the fields of phytotherapy and nanotherapy, leveraging the bioactive constituents of *Hammada scoparia* extract and the unique properties of ZnO-NPs for therapeutic applications. The findings from our study offer promising avenues for future exploration and development:

1. **Formulation Development:** Further optimization of formulation techniques is essential to enhance the stability, bioavailability, and therapeutic efficacy of *Hammada*

scoparia extract and ZnO-NPs. Exploring novel delivery systems, such as nanoparticles and hydrogels, could facilitate sustained release and targeted delivery, thereby improving clinical outcomes in diverse therapeutic contexts.

2. **Mechanistic Insights:** Deeper investigations into the molecular mechanisms underpinning the observed biological activities are warranted. Elucidating how *Hammada scoparia* extract and ZnO-NPs modulate key signaling pathways involved in antioxidant defense, inflammation, and cellular metabolism could provide critical mechanistic insights necessary for optimizing therapeutic strategies.
3. **Clinical Translation:** The translation of these promising preclinical findings into clinical trials is paramount to validate their safety and efficacy in human subjects. Investigating their application in diverse clinical scenarios—such as chronic wound management, diabetic complications, and oncology—holds potential for developing novel therapeutic interventions and personalized medicine approaches tailored to individual patient needs.
4. **Environmental Considerations:** Given the green synthesis approach employed for ZnO-NPs, further studies should assess their environmental impact and biocompatibility profiles rigorously. Understanding these aspects is crucial for ensuring sustainable production practices and safe therapeutic applications, aligning with principles of eco-friendly nanotechnology.
5. **Interdisciplinary Collaborations:** Collaboration across disciplines—such as pharmacology, nanotechnology, biochemistry, and clinical medicine—is imperative to harness the full potential of *Hammada scoparia* extract and ZnO-NPs. Integrating diverse expertise can accelerate innovation and facilitate the development of multifaceted therapeutic strategies aimed at addressing complex health challenges.

In conclusion, this study underscores the promising therapeutic potential of *Hammada scoparia* extract and ZnO-NPs, offering new avenues for advancing medical applications in wound healing, cancer treatment, and various biological activities. Continued research and development efforts are essential to harness these findings effectively for the benefit of human health and to explore their broader implications in biomedical sciences.

References

- A. H. Battez, R. González, J. Viesca, J. Fernández, J. D. Fernández, A. Machado, *et al.*, "CuO, ZrO₂ and ZnO nanoparticles as antiwear additive in oil lubricants," *Wear*, vol. 265, pp. 422-428, 2008.
- A. Javanrouh and S. Jelokhani-niaraki, "DNA extraction from chicken blood using a modified Salting-out method," *Appl. Anim. Sci. Res. J.*, vol. 9, no. 34, pp. 3–10, 2020.
- A. Khennoufa, L. Bechki, T. Lanez, E. Lanez, and N. Zegheb, "Spectrophotometric, voltammetric and molecular docking studies of binding interaction of N-ferrocenylmethylnitroanilines with bovine serum albumin," *J. Mol. Struct.*, vol. 1224, p. 129052, 2021, <http://doi:10.1016/j.molstruc.2020.129052> .
- A. Samy, A.E. El-Sherbiny, A.A. Menazea, Green synthesis of high impact zinc oxide nanoparticles, *Egypt. J. Chem.* 62 (2019) 4e8.
- Aalami AH, Mesgari M, Sahebkar A. 2020. Synthesis and characterization of green zinc oxide nanoparticles with antiproliferative effects through apoptosis induction and microRNA modulation in breast cancer cells. *Bioinorg. Chem. Appl.* 2020, 1–17 .
- Abbes, N., Bekri, I., Cheng, M., Sejri, N., Cheikhrouhou, M., & Jun, X. U. (2022). Green synthesis and characterization of zinc oxide nanoparticles using mulberry fruit and their antioxidant activity. *Materials Science*, 28(2), 144-150.
- Abdelbaky, A. S., Mohamed, A. M., Sharaky, M., Mohamed, N. A., & Diab, Y. M. (2023). Green approach for the synthesis of ZnO nanoparticles using *Cymbopogon citratus* aqueous leaf extract: characterization and evaluation of their biological activities. *Chemical and Biological Technologies in Agriculture*, 10(1), 63.
- Adisa, R. A.; Oke, J.; Olomu, S. A. & Olorunsogo, O., Inhibition of human haemoglobin glycosylation by flavonoid containing leaf extract of *Cnestis ferruginea*. *Journal of the Cameroon Academy of Sciences* 4: 2004, 351-359.
- Agarwal, Happy, and Venkat Kumar Shanmugam. "Synthesis and Optimization of Zinc Oxide Nanoparticles Using *Kalanchoe Pinnata* Towards the Evaluation of Its Anti-Inflammatory Activity." *Journal of Drug Delivery Science and Technology* 54 (2019). <http://dx.doi.org/10.1016/j.jddst.2019.101291> .
- Ahmadi F, Ebrahimnezhad Y, Maheri N, Ghalehkandi GJ (2013) Effect of zinc oxide nanoparticles on the carcass traits and gut morphological of broiler chicks during starter phase. In: proceedings of the 3rd international conference of Nanotek and Expo, Hampton Inn Tropicana, Las Vegas, p 283

- Ahmed S., Annu Chaudhry S.A., Ikram S.; (2017). A review on biogenic synthesis of ZnO nanoparticles using plant extracts and microbes: A prospect towards green chemistry, *J. Photochem. Photobiol. B.*, 166: 272-284.
- Akhil K, Khan SS. 2017 Effect of humic acid on the toxicity of bare and capped ZnO nanoparticles on bacteria, algal and crustacean systems. *J. Photochem. Photobio. B* 167, 136–149.
- Alam, M. N., Bristi, N. J., & Rafiquzzaman, M. (2013). Review on in vivo and in vitro methods evaluation of antioxidant activity. *Saudi pharmaceutical journal*, 21(2), 143-152. <https://doi.org/10.1016/j.jsps.2012.05.002> .
- Ali M., Ikram M., Ijaz M., Hamid U.I., Avais M, Anjum A.A.; 2020. Green synthesis and evaluation of n-type ZnO nanoparticles doped with plant extract for use as alternative antibacterial. *Appl. Nanosci.*, 10: 3787-3803.
- Altemimi, A., Watson, D. G., Choudhary, R., Dasari, M. R., & Lightfoot, D. A. (2016) Ultrasound assisted extraction of phenolic compounds from peaches and pumpkins. *PLOS One*, 11(2), 1 -20.
- Ameen, S., M.S. Akhtar, and H.S. Shin, Highly dense ZnO nanowhiskers for the low-level detection of p-hydroquinone. *Materials Letters*, 2015. 155: p. 82-86.
- American Diabetes Association. (2008). Standards of medical care in diabetes-. *Diabetes Care*, 31(1): 12–54.
- Ammor M., Mayo B. (2007). Selection criteria for lactic acid bacteria to be used as functional starter cultures in dry sausage production. *Meat Science*.76:138-146.
- Anbukkarasi V, Srinivasan R, Elangovan N. 2015 Antimicrobial activity of green synthesized zinc oxide nanoparticles from *Embllica officinalis*. *Int. J. Pharm. Sci. Rev. Res.* 33, 110–115.
- Anchisi C., Maccioni A.M., Sinico C.D., 2001. Valenti. Stability studies of new cosmetic Formulations with vegetable extracts as functional agents. *Il Farmaco*56 : 427–431.
- Anitha R, Ramesh KV, Ravishankar TN, Kumar KHS, Ramakrishnappa T. 2018 Cytotoxicity, antibacterial and antifungal activities of ZnO nanoparticles prepared by *Artocarpus gomezianus* fruit mediated facile green combustion method. *J. Sci. Adv. Mat. Dev.* 3, 440451 .
- Ansari MA *et al.* 2020 *Cinnamomum verum* bark extract mediated green synthesis of ZnO nanoparticles and their antibacterial potentiality. *Biomolecules* 10, 1–15 .

- Araújo, T. S., & Souza, S. O. de (2008). Protetores solares e os efeitos da radiação ultravioleta. *Revista Scientia Plena* 4(1):1–7.
- Ashraf R, Riaz S, Kayani ZN, Naseem S (2015) Effect of calcination on properties of ZnO nanoparticles. *Mater Today Proc* 2(10):5468–5472.
- Atmaca S, Gul K, Cicek R (1998) The Effect of Zinc on Microbial Growth. *Tr J Medical Sciences* 28: 595.
- Azab, A., Nassar, A., Azab, A N. (2016). Anti-Inflammatory Activity of Natural Products. *Molecules*, 21(10), 1321. <https://doi.org/10.3390/molecules21101321> .
- Azizi S, Mohamad R, Bahadoran A, Bayat S, Rahim RA, Ariff A, Saad WZ. 2016 Effect of annealing temperature on antimicrobial and structural properties of bio-synthesized zinc oxide nanoparticles using flower extract of *Anchusa italic*. *J. Photochem. Photobiol. B* B.B. Aida, A. Zaater, B. Khezzani, F. Alia, Influence of soil type on the physicochemical and biological properties of bioactive compounds of *Portulaca oleracea* L. From Algerian Sahara, *Analele Universitat,ii din Oradea, Fasc. Biol. XXIX (1) (2022) 68-77*.
- Bader, J., Albin, A., and Stahl, U. (2012). Spore-forming bacteria and their utilisation as probiotics. *Benef. Microbes* 3, 67–75.
- Balogh, T. S, Velasco, M. V. R, Pedriali. C. A., Kaneko, T. A., & Baby, A. R. (2011). Proteção à radiação ultravioleta: recursos disponíveis na atualidade em fotoproteção. *Brazilian Annals of Dermatology* 86(4):732–742.
- Barani, D., Optimisation des conditions opératoires de synthèse verte de nanoparticules de ZnO à l'aide d'extrait des feuilles de *Phoenix Dactylifera*. L. 2020, Université Mohamed Khider-Biskra.
- Barau, C., Pons, S., Ghaleh, B., & Atkinson, C. (2016). Médicaments antidiabétiques. In *Pharmacologie Cardio-Vasculaire et Respiratoire* (pp. 179-186) .
- Barui, Ayan K., Rajesh Kotcherlakota, and Chitta R. Patra. "Biomedical Applications of Zinc Oxide Nanoparticles." In *Inorganic Frameworks as Smart Nanomedicines*, 239-78, 2018.
- Bate-Smith, E. (1954). Leuco-anthocyanins. 1. Detection and identification of anthocyanidins formed from leuco-anthocyanins in plant tissues. *Biochemical Journal*, 58(1), 122.
- Batool M, Khurshid S, Daoush WM, Siddique SA, Nadeem T. 2021 Green synthesis and biomedical applications of ZnO nanoparticles: role of PEGylated-ZnO nanoparticles as doxorubicin drug carrier against MDA-MB-231(TNBC) cells line. *Crystals* 11, 1–19 .

- Bayda S., Adeel M., Tuccinardi T., Cordani M., Rizzolio F.; (2019). The history of nanoscience and nanotechnology: From chemical–physical applications to nanomedicine. *Molecules.*, 25(1):1-15.
- Beasley DG, Meyer TA. Characterization of the UVA protection provided by avobenzone, zinc oxide, and titanium dioxide in broad-spectrum sunscreen products. *Am J Clin Dermatol.* 2010;11(6):413-421.
- Ben Salah H., Jarraya R., Martin M.T., Veitch N.C., Grayer R.J., Simmonds M.S.J. and Damak M. 2002. Flavonol Triglycosides from the leaves of *Hammada scoparia* (Pomel) Iljin. *Chem Pharm Bull.*, 50 (9), pp. 1268-1270.
- Benkhalel, A., Boudjelal, A., Napoli, E., Baali, F., & Ruberto, G. (2020). Phytochemical profile, antioxidant activity and wound healing properties of *Artemisia absinthium* essential oil. *Asian Pacific Journal of Tropical Biomedicine*, 10(11), 496.
- Benkherara, S., Bordjiba, O., Harrat, S., & Djahra, A. B. (2021). Antidiabetic potential and chemical constituents of *Haloxylon scoparium* aerial part, an endemic plant from Southeastern Algeria. *International Journal of Secondary Metabolite*, 8(4), 398-413.
- Benkherara, S., Bordjiba, O., Harrat, S., & Djahra, A.B. (2021). Antidiabetic Potential and Chemical Constituents of *Haloxylon scoparium* Aerial Part, An Endemic Plant from Southeastern Algeria. *International Journal of Secondary Metabolite*, 8(4), 398–412. <https://doi.org/10.21448/ijsm.990569>
- Bensegueni, A. and Cherif A. M. (2017). Effets cicatrisants de produits à base d’huile de lentisque (*Pistacia lentiscus* L.) sur les brûlures expérimentales chez le rat.
- Beroual, K., Agabou, A., Abdeldjelil, M. C., Boutaghane, N., Haouam, S., & Hamdi-Pacha, Y. (2017). Evaluation of crude flaxseed (*linum usitatissimum* L) oil in burn wound healing in new zealand rabbits. *African journal of traditional, complementary, and alternative medicines: AJTCAM*, 14(3), 280–286.
- Bouaziz, A., Mhalla, D., Zouari, I., Jlaiel, L., Tounsi, S., Jarraya, R., & Trigui, M. (2016). Antibacterial and antioxidant activities of *Hammada scoparia* extracts and its major purified alkaloids. *South African Journal of Botany*, 105, 89-96. <https://doi.org/10.1016/j.sajb.2016.03.012>
- Boucherit, H., Benabdeli, K., Benaradj, A., & Boughalem, M. (2018). Phytoecology of *Hammada scoparia* in the region of naâma (Western Algeria). *Botanica Complutensis*, 42, 93–99. <https://doi.org/10.5209/BOCM.61371>

- Boulanouar, B., Abdelaziz, G., Aazza, S., Gago, C., & Miguel, M.G. (2013). Antioxidant activities of eight Algerian plant extracts and two essential oils. *Industrial Crops and Products*, 46, 85–96. <https://doi.org/10.1016/j.indcrop.2013.01.020>
- Bourogaa E, Nciri R, Jarraya R, Racaud-Sultan C, Mohamed D, El Feki A (2012) Antioxidant activity and hepatoprotective potential of *Hammada scoparia* against ethanol-induced liver injury in rats. *Journal of physiology and biochemistry*, 69.
- Bourogaa E., Mezghani Jarraya R., Nciri R., Damak M. and Elfeki A. 2012. Protective effect of aqueous extract of *Hammada scoparia* against hepatotoxicity induced by ethanol in the rat. *Toxicol Ind Health.*, 30, pp. 113-122.
- Bourogaa, E., Bertrand, J., Despeaux, M., Jarraya, R., Fabre, N., Payrastre, L., Demur, C., Fournié, J.J., Damak, M., Feki, A. el, & Racaud-Sultan, C. (2011). *Hammada scoparia* flavonoids and rutin kill adherent and chemoresistant leukemic cells. *Leukemia Research*, 35(8), 1093–1101. <https://doi.org/10.1016/j.leukres.2010.12.011>
- Brongersma, H. H., Draxler, M., De Ridder, M., & Bauer, P. (2007). Surface composition analysis by low-energy ion scattering. *Surface Science Reports*, 62(3), 63-109.
- Bruneton J, Pharmacognosie, phytochimie, plantes médicinales. 2ème édition. Édition Tec et Doc .Paris, France. 1993.
- C. Filote, E. Lanez, V. I. Popa, T. Lanez, and I. Volf, “Characterization and Bioactivity of Polysaccharides Separated through a (Sequential) Biorefinery Process from *Fucus spiralis* Brown Macroalgae,” *Polymers (Basel)*, vol. 14, no. 19, p. 4106, 2022, <http://doi:10.3390/polym14194106> .
- C. Quettier-Deleu, B. Gressier, J.T. Vasseur, Phenolic compounds and antioxidant activities of buckwheat (*Fagopyrum esculentum* Moench) hulls and flour, *J. Ethnopharmacol.* 72 (2) (2000) 35-42, [https://doi.org/10.1016/S0378-8741\(00\)00196-3](https://doi.org/10.1016/S0378-8741(00)00196-3).
- Cattley R. C., & Radinsky B. R. (2004). *Cancer Therapeutics: Understanding the Mechanism of Action*. *Toxicologic Pathology*, 32(1_suppl), 116–121.
- Cefali, L. C., Ataide, J. A., Moriel, P., Foglio, M. A., & Mazzola, P. G. (2016). Plant-based active photoprotectants for sunscreens. *International journal of cosmetic science*, 38(4), 346-353.
- Chabosseau & Derbré, 2016. Cancer du sein : recommandations sur l’usage de la phytothérapie. *Actualités Pharmaceutiques*, 2016. 55(552): p. 45-49.
- Chao, H.C., Najjaa, H., Villareal, M.O., Ksouri, R., Han, J., Neffati, M., & Isoda, H. (2013). *Arthrophytum scoparium* inhibits melanogenesis through the down-regulation of

- tyrosinase and melanogenic gene expressions in B16 melanoma cells. *Experimental Dermatology*, 22(2), 131–136. <https://doi.org/10.1111/EXD.12089>
- Chaudhari, M. G., Joshi, B. B., & Mistry, K. N. (2013). In vitro anti-diabetic and anti-inflammatory activity of stem bark of *Bauhinia purpurea*. *Bulletin of Pharmaceutical and Medical Sciences (BOPAMS)*, 1(2), 139-150.
- Chen, M.J. and Chen, K.N., "Applications of probiotic encapsulation in dairy products", *Encapsulation and Controlled Release Technologies in Food Systems*, (2007), 83-112.
- Chen, Y. and S. Ma, Preparation and photoluminescence studies of high-quality AZO thin films grown on ZnO buffered Si substrate. *Materials Letters*, 2016. 162: p. 75-78.
- Chen, YJ, Dai, YS, Chen, BF, CHANG, A., CHEN, HC, LIN, YC, ... Et LAI, YJ (1999). L'effet de la tétrandrine et des extraits de *Centella asiatica* sur la dermatite aiguë de radiation chez le rat. *Bulletin biologique et pharmaceutique*, 22 (7), 703-706.
- Chhabra, S., Chhabra, N., Kaur, A., & Gupta, N. (2017). Wound Healing Concepts in Clinical Practice of OMFS. *Journal of maxillofacial and oral surgery*, 16(4), 403–423.
- Chiari-Andréo, B. G., Almeida, F. B., Yamasaki, P. R., Santos, J. L., Corrêa, M. A., Chin Chung, M. et al (2020). Can natural products improve skin photoprotection? *Rodriguésia* 71:e00672019.
- Chukeatirote E, Arfarita N, Niamsup P, Kanghae A. Phenotypic and genetic characterization of *Bacillus* species exhibiting strong proteolytic activity isolated from Terasi, an Indonesian fermented seafood product. *Journal of Northeast Agricultural University (English Edition)*. 2015, 1;22(4):15-22.
- Claudia Otero M, Ocaña VS, Elena N-M. Selection of probiotic microorganisms bacterial surface characteristics applied to selection of probiotic microorganisms. *Methods Mol Biol*. 2004;268:43
- Cole C, Shyr T, Ou-Yang H. Metal oxide sunscreens protect skin by absorption, not by reflection or scattering. *Photodermatol Photoimmunol Photomed*. 2016;32(1):5-10.
- Conklin, C.M.J., Bechberger, J.F., MacFabe, D., Guthrie, N., Kurowska, E.M., Naus, C.C., 2007 .Genistein and quercetin increase connexin43 and suppress growth of breast cancer cells. *Carcinogenesis* 28, 93–100.
- D. S. Cha and M. S. Chinnan, "Biopolymer-based antimicrobial packaging: a review," *Critical reviews in food science and nutrition*, vol. 44, pp. 223-237, 2004.
- Dahmane, D., Dob, T., Krimat, S., Nouasri, A., Metidji, H., & Ksouri, A. (2017). Chemical composition, antioxidant and antibacterial activities of the essential oils of medicinal

- plant *Ammodaucus leucotrichus* from Algeria. *Journal of Essential Oil Research*, 29(1), 48-55. <https://doi.org/10.1080/10412905.2016.1201015>.
- Darré, T., Metowogo, K., Lawson-Evi, P., Eklugadegbeku, K., Aklikokou, K. A., Napokoura, G., & Gbeassor, M. (2014). Effet topique de l'extrait hydroethanolique de l'acacia nilotica sur la cicatrisation cutanee des brulures de second degre. *European Scientific Journal*, 10.(30)
- Das, D., Nath, B. C., Phukon, P., & Dolui, S. K. (2013). Synthesis of ZnO nanoparticles and evaluation of antioxidant and cytotoxic activity. *Colloids and Surfaces B: Biointerfaces*, 111, 556-560.
- De Paola, M. V. R. V. & Ribeiro, M. E. (1998). Interação entre filtros solares. *Cosmetics & Toiletries*. 10:40–50.
- Debnath T, Kim DH, Lim BO. Natural products as a source of anti-inflammatory agents associated with inflammatory bowel disease. *Molecules* 2013 ;18 :7253-70.
- Denohue(2004).Safety of nevel probiotic bacteria. In: *Lactic acid bacteria: microbiological and functional aspects* (Salminen S., Wright A.V.et ouwehand A.) 3^eEd., Marcel Dekker, In New York. 531-546.
- Despax, S. (2014). Complexation de l'ADN par des composés organoruthénés et étude de l'adhésion cellulaire sur des substrats mous. Thèse de doctorat. Université de Strasbourg. P15-23.
- Do, Q. D., Angkawijaya, A. E., Tran-Nguyen, P. L., Huynh, L. H., Soetaredjo, F. E., Ismadji, S., & Ju, Y.-H. (2014). Effect of extraction solvent on total phenol content, total flavonoid content, and antioxidant activity of *Limnophila aromatica*. *Journal of Food and Drug Analysis*, 22(3), 296–302.
- Doan Thi, Tu Uyen, Trung Thoai Nguyen, Y. Dang Thi, Kieu Hanh Ta Thi, Bach Thang Phan, and Kim Ngoc Pham. "Green Synthesis of ZnO Nanoparticles Using Orange Fruit Peel Extract for Antibacterial Activities." *RSC Advances* 10, no. 40 (2020): 23899-907. <http://dx.doi.org/10.1039/d0ra04926c> .
- Dobručka R, Długaszewska J. 2016 Biosynthesis and antibacterial activity of ZnO nanoparticles using *Trifolium pratense* flower extract. *Saudi J. Biol. Sci.* 23, 517–523 .
- Dulta K, Ağçeli GK, Chauhan P, Jasrotia R, Chauhan PK. 2020 A novel approach of synthesis zinc oxide nanoparticles by *Bergenia ciliata* rhizome extract: antibacterial and anticancer potential. *J. Inorg. Org. met. Poly. Mater.* 31,180190.
- Dunne C., Omahony L., Murphy L., Thornton G., Morrissey D., O'halloran S., Feeney M., Flynn S., Fitzgerald G., Daly C., Kiely B., O'sullivan G.C., Shanahan F and Collins

- J.K.(2001).In vitro selection criteria for probiotic bacteria of human origin: correlation with in vivo findings *Am.J.Clin.Nutr.*,73: 386-392
- E. Lanez, L. Bechki, and T. Lanez, “Computational molecular docking, voltammetric and spectroscopic DNA interaction studies of 9N-(Ferrocenylmethyl)adenine,” *Chem. Chem. Technol.*, vol. 13, no. 1, pp. 11–17, 2019, <http://doi:10.23939/chcht13.01.011> .
- E. R. C. Rivero, A. C. Neves, M. G. Silva-Valenzuela, S. O. M. Sousa, and F. D. Nunes, “Simple salting-out method for DNA extraction from formalin-fixed, paraffin-embedded tissues,” *Pathol. Pract.*, vol. 202, no. 7, pp. 523–529, 2006.
- E. Souri, G. Amin, H. Farsam, M.B. Tehrani, Screening of antioxidant activity and phenolic content of 24 medicinal plant extracts, *J. Pharm. Sci.* 16 (2) (2008) 83-87.
- E. Telfer, N. Graham, L. Stanbra, T. Manley, and P. Wilcox, “Extraction of high purity genomic DNA from pine for use in a high-throughput genotyping platform,” *New Zeal. J. For. Sci.*, vol. 43, no. 1, pp. 1–8, 2013, <http://doi:10.1186/1179-5395-43-3>.
- Ebrahimiasl, S., Zakaria, A., Kassim, A., & Basri, S. N. (2015). Novel conductive polypyrrole/zinc oxide/chitosan bionanocomposite: synthesis, characterization, antioxidant, and antibacterial activities. *International journal of nanomedicine*, 217-227.
- Ebrahimzadeh, M.A., Pourmmorad, F. & Hafezi, S. (2008). Antioxidant activities of Iranian Corn Silk. *Turkish journal of biology*, 32, 43-49.
- Eddouks, M., Maghrani, M., Lemhadri, A., Ouahidi, M.L., & Jouad, H. (2002). Ethnopharmacological survey of medicinal plants used for the treatment of diabetes mellitus, hypertension and cardiac diseases in the south-east region of Morocco (Tafilalet). *Journal of Ethnopharmacology*, 82, 97–103. [https://doi.org/10.1016/S0378-8741\(02\)00164-2](https://doi.org/10.1016/S0378-8741(02)00164-2)
- Eddouks, M., Ouahidi, M.L., Farid, A., Moufid, A., Khalidi, A. et Lemhadri, A. (2007). L'utilisation des plantes médicinales dans le traitement du diabète au Maroc. *Phytothérapie*, 5 : 194-203.
- Edeoga, H. O., Okwu, D., & Mbaebie, B. (2005). Phytochemical constituents of some Nigerian medicinal plants. *African Journal of Biotechnology*, 4(7), 685-688.
- Édouard, Boulos Loutfy, & Vela Errol. (2010). Catalogue synonymique commenté de la flore de Tunisie (Djemali M'naouer, Ed.; 2nd ed.). Banque Nationale de Gènes,pp 500.
- Elavarasan N, Kokila K, Inbasekar G, Sujatha V.2016 Evaluation of photocatalytic activity, antibacterial and cytotoxic effects of green synthesized ZnO nanoparticles by *Secchium edule* leaf extract. *Res. Chem. Intermed.* 43, 3361-3376.

- El-Hadri, Y. (2019). Contribution à l'étude ethnobotanique des plantes médicinales utilisées dans la région de Beni Mellal-Khenifra [Thèse de Doctorat]. Université Mohammed V de Rabat, pp 194. <http://ao.um5s.ac.ma/xmlui/handle/123456789/17236>
- El-Shazly, A., & Wink, M. (2003). Tetrahydroisoquinoline and-Carboline Alkaloids from *Haloxylon articulatum* (Cav.) Bunge (Chenopodiaceae). *Verlag der Zeitschrift für Naturforschung*, 58(7), 477–480. <https://doi.org/10.1515/znc-2003-7-805>
- Epstein, J. H. Biological effect of sunlight. In: Lowe, N. J., Shaath, M. & Pathak, M. A. *Sunscreens: development, evaluation and regulatory aspect*. Marcel Dekker, New York. 1990.
- Ernest, D. J. O. K. O., & Yimta, F. O. U. T. S. E. (2019). Activité cicatrisante d'une pommade à base des feuilles de *Kalanchoe crenata* (Andr.) Haw chez le rat. *IJRAR-International Journal of Research and Analytical Reviews (IJRAR)*, 6(4), 158-178.
- Esho, B., Samuel, B., Akinwunmi, K., Oluyemi, W. (2021). Membrane Stabilization and Inhibition of Protein Denaturation as Mechanisms of the Anti-Inflammatory Activity of some Plant Species. *Trends in Pharmaceutical Sciences*, 7(4), 269-278. <https://doi:10.30476/tips.2021.93160.1118>.
- Ezzeddine, B., Raoudha, J.M., Mohamed, D., & Abdelfattah, E.F. (2016). Therapeutic Efficacy of *Hammada scoparia* Extract Against Ethanol Induced Renal Dysfunction in Wistar Rats. *Journal of Food Biochemistry*, 41(2), 1–8.
- F. Alhakmani, S.A. Khan, A. Aftab, Determination of total phenol, in-vitro antioxidant and anti-inflammatory activity of seeds and fruits of *Zizyphus spina-christi* grown in Oman, *Asian Pac. J. Trop. Biomed.* 4 (2) (2014) S656eS660, <https://doi.org/10.12980/APJTB.4.2014APJTB-2014-0273> .
- F. Schöppler et al., “Molar extinction coefficient of single-wall carbon nanotubes,” *J. Phys. Chem. C*, vol. 115, no. 30, pp. 14682–14686, 2011, <http://doi:10.1021/jp205289h> .
- Falleh, H., Ksouri, R., Chaieb, K., Karray-Bourouai, N., Trabelsi, N., Boulaaba, M. & Abdelly C. (2008). Phenolic composition of *Cynara cardunculus* L. organs, and their biological activities. *Comptes Rendus Biologies*, 331, 372-379.
- Fan, F., et al., Facile synthesis and photocatalytic performance of ZnO nanoparticles self-assembled spherical aggregates. *Materials Letters*, 2015. 158: p. 290-294.
- Fatehi N., Allaoui M., Berbaoui H., Cheriti A., Boulenouar N., & Belboukhari N. (2018). *Haloxylon Scoparium*: An Ethnopharmacological Survey, Phytochemical Screening and Antibacterial Activity against Human Pathogens Causing Nosocomial Infection. *PhytoChem & BioSub Journal*, 11(2), 104–109.

- Favaro-Trindade, C., Heinemann, R. and Pedroso, D., "Developments in probiotic encapsulation", CAB Rev, Vol. 6, (2011), 1-8.
- Ferraq, Y. (2007). Développement d'un modèle de cicatrisation épidermique après une désépidermisation laser (Doctoral dissertation, Université de Toulouse, Université Toulouse III-Paul Sabatier).
- Flor, J., Davolos, M. R., & Correa, M. A. (2007). Protetores solares. *Química Nova* 30(1):153–158.
- Francenia Santos-Sánchez, N., Salas-Coronado, R., Villanueva-Cañongo, C., Hernández-Carlos, B. (2019). Antioxidant Compounds and Their Antioxidant Mechanism. *Antioxidants*. <https://doi:10.5772/intechopen.85270> .
- Fultz, B., Howe, J., 2013. *Transmission Electron Microscopy and Diffractometry of Materials, Graduate Texts in Physics*. Springer Berlin Heidelberg, Berlin, Heidelberg. <https://doi.org/10.1007/978-3-642-29761-8>
- Gago, F. (1998). Stacking Interactions and Intercalative DNA Binding. *Academic Press*, (14) 277–292.
- Gao Y., Xu D., Ren D., Zeng K., Wu X.; 2020. Green synthesis of zinc oxide nanoparticles using *Citrus sinensis* peel extract and application to strawberry preservation: A comparison study. *LWT- Food Sci Technol.*, 126: 1-8.
- Gelin, Z., Mosyakin, S.L., & Clemants, S.E. (2003). *Chenopodiaceae*. *Flora of China*, 5(1), 351-414.
- Ghedadba, N., Hambaba, L., Ayachi, A., Aberkane, M. C., Bousselsela, H& ,. Oued-Mokhtar, S. M. (2015). Polyphénols totaux, activités antioxydante et antimicrobienne des extraits des feuilles de *Marrubium deserti* de Noé. *Phytothérapie*, 13(2), 118-129.
- Gibson, G. R., and Roberfroid, M. B. (1995). Dietary modulation of the human colonic microbiota – introducing the concept of prebiotics. *J. Nutr.* 125, 1401–1412.
- Gillery, P.(2014). Assays of HbA1c and Amadori products in human biology. *Annales pharmaceutiques françaises*,72: 330–6.
- Gontijo, D. C., Brandão, G. C., Gontijo, P. C., de Oliveira, A. B., Diaz, M. A. N., Fietto, L. G., & Leite, J. P. V. (2017). Identification of phenolic compounds and biologically related activities from *Ocotea odorifera* aqueous extract leaves. *Food Chemistry*, 230, 618-626.
- Gopalakrishnan S, Saroja K, Elizabeth JD, Wound healing activity of *Acalypha fruticosa* Forssk , *J of Pharm Res*, 2010; 3,2190

- Granger M. M. R., Passet J., & Arbousset G., (1973). L'essence de *Rosmarinus officinalis*, influence du mode de traitement du matériel végétal. *Parf. Cosm. Sav. France* 3(3): 133-137.
- Griendling, K. K., Camargo, L. L., Rios, F. J., Alves-Lopes, R., Montezano, A. C., & Touyz, R. M. (2021). Oxidative stress and hypertension. *Circulation research*, 128(7), 993-1020.
- Gu R X., Yang Z.Q., Li Z.H., Chen S.L and Luo Z. L (2008). Periodic properties of lactic acid bacteria isolated from stool samples of longevons people in regions of mutant; Xirijiang and Bama; Guangxi; Anaerobe. 14: 313-317.
- Guaratini, T., Callejon, D. R., Pires, D. C., Lopes, J. N. C., Lima, L. M., Giannella, N. D., Sustovich, C. & Lopes, N. P. (2009). Fotoprotetores derivados de produtos naturais: perspectivas de mercado e interações entre o setor produtivo e centros de pesquisa. *Química Nova* 32(3):717–721.
- Guarner, F., & Schaafsma, G. J. (1998). Probiotics. *International journal of food microbiology*, 39(3), 237-238.
- Guillouty, A. (2016). *Plantes médicinales et antioxydants*. thèse de doctorat. Université toulouse III paulsabatie. 95p.
- Gulcin, İ. (2020). Antioxidants and antioxidant methods: An updated overview. *Archives of toxicology*, 94(3), 651-715. <https://doi:10.1007/s00204-020-02689-3> .
- H. Mouada, T. Lanez, and E. Lanez, “Investigations of the binding parametres of the interaction of N'-ferrocenylmethyl-N'-phenylaceto-and propionohydrazide with DNA,” *J. Fundam. Appl. Sci.*, vol. 11, no. 2, pp. 875–882, 2019.
- H. Nasiri, M. Forouzandeh, M. J. Rasae, and F. Rahbarizadeh, “Modified salting-out method: High-yield, high-quality genomic DNA extraction from whole blood using laundry detergent,” *J. Clin. Lab. Anal.*, vol. 19, no. 6, pp. 229–232, 2005, <http://doi:10.1002/jcla.20083> .
- H. W. Wang, C. Bringans, A. J. R. Hickey, J. A. Windsor, P. A. Kilmartin, and A. R. J. Phillips, “Cyclic Voltammetry in Biological Samples: A Systematic Review of Methods and Techniques Applicable to Clinical Settings,” *Signals*, vol. 2, no. 1, pp. 138–158, 2021, <http://doi:10.3390/signals2010012> .
- Hafez, A., Nassef, E., Fahmy, M., Elsabagh, M., Bakr, A., & Hegazi, E. (2019). Impact of dietary nano-zinc oxide on immune response and antioxidant defense of broiler chickens. *Environmental Science and Pollution Research*, 27, 19108-19114.

- Hafidha, B., Khéloufi, B., & Abdelkrim, B. (2017). Caracterisation floristique de la steppe a *Hammada scoparia* dans l'Atlas Saharien Oranais (Naama-Algerie). *Revue Agrobiologia*, 7(2), 483–490.
- Hamdan, S., Pastar, I., Drakulich, S., Dikici, E., Tomic-Canic, M., Deo, S., & Daunert, S. (2017). Nanotechnology-driven therapeutic interventions in wound healing: potential uses and applications. *ACS central science*, 3(3), 163-175.
- Hamrayev, H., Shameli, K., & Korpayev, S. (2021). Green synthesis of zinc oxide nanoparticles and its biomedical applications: A review. *Journal of Research in Nanoscience and Nanotechnology*, 1(1), 62-74 .
- Hamza, N., Berke, B., Umar, A., Cheze, C., Gin, H., & Moore, N. (2019). A review of Algerian medicinal plants used in the treatment of diabetes. *Journal of Ethnopharmacology*, 238,1-111. <https://doi.org/10.1016/j.jep.2019.111841>
- Hanahan D., Weinberg RA. (2011). Hallmarks of cancer: the next generation. *Cell*. 2011 Mar 4;144(5):646-74. <http://doi:10.1016/j.cell.2011.02.013> .
- Handore, A. V., & Khandelwal, S. R. (2017). Identification and Determination of Bioactive Polyphenols of *V. Vinefera* for Phyto-therapeutic Applications. *International Journal of Ayurvedic and Herbal Medicine*. 7(3), 2590–2596.
- Hang, J., Wen, C., Zhang, H., & Duan, Y. (2019). Review of isolation, structural properties, chain conformation, and bioactivities of psyllium polysaccharides. *International journal of biological macromolecules*, 139, 409-420. <https://doi.org/10.1016/j.ijbiomac.2019.08.014> .
- Hanigan D, Truong L, Schoepf J, et al. Trade-offs in ecosystem impacts from nanomaterial versus organic chemical ultraviolet filters in sunscreens. *Water Res*. 2018; 139:281-290.
- Harborne, A. (1998). *Phytochemical methods a guide to modern techniques of plant analysis*. springer science & business media.
- Heklau, H., Gasson, P., Schweingruber, F., & Baas, P. (2012). Wood anatomy of *Chenopodiaceae* (*Amaranthaceae* s. L.). *IAWA Journal*, 33(2), 205–232.
- Helena, A. Y., Schoenfeld, A. J., Makhnin, A., Kim, R., Rizvi, H., Tsui, D., ... & Kris, M. G. (2020). Effect of osimertinib and bevacizumab on progression-free survival for patients with metastatic EGFR-mutant lung cancers: a phase 1/2 single-group open-label trial. *JAMA oncology*, 6(7), 1048-1054.
- Hervert-Hernandez D, Goñi I. Dietary polyphenols and human gut microbiota: a review. *Food Rev Int*. (2011) 27:154.

- Horiuchi N, Nakagava K, Sasaki Y, Minato K, Fujiwara Y, Nezu K, et al. In vitro antitumor activity of mitomycin C derivative (RM-49) and a new anticancer antibiotic (FK973) against lung cancer cell lines determined by tetrazolium dye (MTT) assay. *Cancer Chemother Pharmacol* 1988;22:246-50.
- Hortelano, S., González-Cofrade, L., Cuadrado, I., & de Las Heras, B.(2020) . Current status of terpenoids as inflammasome inhibitors. *Biochemical Pharmacology*, 172, 1 – 23.
- Hunyadi, A. (2019). The mechanism(s) of action of antioxidants: From scavenging reactive oxygen/nitrogen species to redox signaling and the generation of bioactive secondary metabolites. *Medicinal Research Reviews*. <https://doi:10.1002/med.21592> .
- Hussain A, Oves M, Alajmi MF, Hussain I, Amir S, Ahmed J, Rehman MT, El-Seedif HR, Ali I. 2019 Biogenesis of ZnO nanoparticles using Pandanus odorifer leaf extract: anticancer and antimicrobial activities. *RSC Adv.* 9, 15 357–15 369
- I. Lynch, T. Cedervall, M. Lundqvist, C. Cabaleiro-lago, S. Linse, K.A. Dawson, The nanoparticle – protein complex as a biological entity; a complex fluids and surface science challenge for the 21st century, *Adv. Colloid Interface Sci.* 135 (2007) 167–174.
- Ifeanyichukwu UL, Fayemi OE, Ateba CN. 2020.Green synthesis of zinc oxide nanoparticles from Pomegranate (*Punica granatum*) extracts and characterization of their antibacterial activity. *Molecules* 25, 1–22.
- Iravani, S, (2011), Green synthesis of metal nanoparticles using plants, *Green Chem.*, 13, 2638–2650.
- Ismail, A. M., Menazea, A. A., Kabary, H. A., El-Sherbiny, A. E., & Samy, A. (2019). The influence of calcination temperature on structural and antimicrobial characteristics of zinc oxide nanoparticles synthesized by Sol–Gel method. *Journal of Molecular Structure*, 1196, 332-337.
- J. N. Gaaib, A. F. Nassief, and A. H. Al-assi, “Simple salting – out method for genomic DNA extraction from whole blood Abstract: Introduction:,” *Nucleic Acids Res.*, vol. 16, no. 2, pp. 15–17, 2011.
- J. Namukobe, P. Sekandi, R. Byamukama, M. Murungi, J. Nambooze, Y. Ekyibetenga, C.B. Nagawa, S. Asiimwe, Antibacterial, antioxidant, and sun protection potential of selected ethnomedicinal plants used for skin infections in Uganda, *Trop. Med. Health* 49 (1) (2021) 1-10. <http://doi:10.1186/s41182-021-00342-y>.
- J. Ning, J. Liebich, M. Kästner, J. Zhou, A. Schäffer, and P. BuraueI, “Different influences of DNA purity indices and quantity on PCR-based DGGE and functional gene microarray

- in soil microbial community study,” *Appl. Microbiol. Biotechnol.*, vol. 82, no. 5, pp. 983–993, 2009, <http://doi:10.1007/s00253-009-1912-0> .
- J. R. Howe, “DNA extraction from paraffin-embedded tissues using a salting-out procedure: A reliable method for PCR amplification of archival material,” *Histol. Histopathol.*, vol. 12, no. 3, pp. 595–601, 1997.
- Jallad, K. N. (2016). Chemical characterization of sunscreens composition and its related potential adverse health effects. *Journal of Cosmetic Dermatology* 16(3):353–357. <http://doi:10.1111/jocd.12282> .
- Janaki AC, Sailatha E, Gunasekaran S. 2015. Synthesis, characteristics and antimicrobial activity of ZnO nanoparticles. *Spectro. Acta Part A*144, 17–22 .
- Jarraya R., Ben Salah H. and Damak M. 2005. Chemical and radical scavenging activity of constituents from *Hammada scoparia* (Pomel) Iljin. *Journal de la Société Chimique de Tunisie*, 7, pp. 261-266.
- Joel C, Badhusha MSM. 2016 Green synthesis of ZnO Nanoparticles using *Phyllanthus embilica* stem extract and their antibacterial activity. *Der. Pharmacia Lettre* 8, 218–223.
- Johncock, W. (2000). Interação de formulações com filtro solar. *Cosmetics. & Toiletries*. 12:40-50.
- Joudeh, N., Linke, D., 2022. Nanoparticle classification, physicochemical properties, characterization, and applications: a comprehensive review for biologists. *Journal of Nanobiotechnology* 20, 262. <https://doi.org/10.1186/s12951-022-01477-8>
- Juzeniene, A. & Moan, J. (2012). Beneficial effects of UV radiation other than via vitamin D production. *Dermato endocrinology* 4:109–117.
- K. P. Rakesh, K. Shiva Prasad, and K. Shridhara Prasad, “Synthesis and characterization of chromium (III) complexes of 4 (3H) -quinazolinone derived schiff base: antimicrobial and DNA interaction studies,” *Int. J. Res. Chem. Env.*, vol. 2, pp. 221–225, 2012.
- Kalyani RL, Pammi SVN, Kumar PPNV, Swamy PV, Murthy KVR. 2019 Antibiotic potentiation and anti-cancer competence through biomediated ZnO nanoparticles. *Mater. Sci. Eng. C Mater. Biol. Appl.* 103, 109756 .
- Kamatou, G.P.P., Makunga, N.P., Ramogola, W.P.N., & Viljoen, A.M. (2008). South African *Salvia* species: A review of biological activities and phytochemistry. *Journal of Ethnopharmacology*, 119(3), 664–672. <https://doi.org/10.1016/j.jep.2008.06.030>
- Kanter, M., Meral, I., Yener, Z., Ozbec, H. et Demir, H. (2003). Partial regeneration /Proliferation of the β cells in the islets of Langerhans by *Nigella sativa* L.

- instreptozotocin- induced diabetic rats. *Tohoko Journal of Experimental Medecine*, 201(4): 213-219.
- Karous, O. L. F. A., Aichi, H. Y., Jilani, I. B. H., & Ghrabi-Gammar, Z. E. I. N. E. B. (2020). Volatiles profiling, phytotoxic activity, and antioxidant potentiality of *Hammada scoparia* (Pomel) Iljin extracts from southern Tunisia.
- Karous, O., Yousfi Aichi, H., ben Haj Jilani, I., & Ghrabi-gammar, Z. (2020). Volatiles profiling, phytotoxic activity, and antioxidant potentiality of *Hammada scoparia* (Pomel) Iljin extracts from southern Tunisia. *Journal of New Sciences, Agriculture and Biotechnology*, 70(3), 4290–4298.
- Khalafi, T., Buazar, F., & Ghanemi, K. (2019). Phycosynthesis and enhanced photocatalytic activity of zinc oxide nanoparticles toward organosulfur pollutants. *Scientific Reports*, 9(1), 6866. <https://doi.org/10.1038/s41598-019-43368-3>.
- Khan, Ibrahim, Saeed, K., Khan, Idrees, 2019. Nanoparticles: Properties, applications and toxicities. *Arabian Journal of Chemistry* 12, 908–931. <http://doi.org/10.1016/j.arabjc.2017.05.011>
- Khan, M A., Khan, H., Tarqie, S A., Pervez, S. (2015). In Vitro Attenuation of Thermal-Induced Protein Denaturation by Aerial Parts of *Artemisia scoparia*. *Journal of Evidence-Based Complementary & Alternative Medicine*, 20(1), 9-12. <https://doi.org/10.1177/2156587214548458> .
- Khedir SB, Bardaa S, Chabchoub N, Moalla D, Sahnoun Z, Rebai T.l'effet curatif de l'huile de fruit *Pistacia lentiscus* sur la brûlure au laser. *Pharm Biol* . 2017; 55 (1): 1407-1414.
- Kiani, A., Nami, Y., Hedayati, S., Jaymand, M., Samadian, H., & Haghshenas, B. (2021a). Tarkhineh as a new microencapsulation matrix improves the quality and sensory characteristics of probiotic *Lactococcus lactis* KUMS-T18 enriched potato chips. *Scientific Reports*, 11(1), 1–13 .
- Kiani, A., Nami, Y., Hedayati, S., Komi, D. E. A., Goudarzi, F., & Haghshenas, B. (2021b). Application of Tarkhineh fermented product to produce potato chips with strong probiotic properties, high shelf-life, and desirable sensory characteristics. *Frontiers in Microbiology*, 12.
- Kiendrebeogo, M., Coulibaly, K., Sanogo, R., & Kone-Bamba, D. (2016). Mineral salt composition and secondary metabolites of *Ocimum gratissimum* L., an antihyperglycemic plant. *Journal of Pharmacognosy and Phytochemistry*, 5(5), 425.

- Kitture, R., Chordiya, K., Gaware, S., Ghosh, S., More, P. A., Kulkarni, P., ... & Kale, S. N. (2015). ZnO nanoparticles-red sandalwood conjugate: a promising anti-diabetic agent. *Journal of nanoscience and nanotechnology*, 15(6), 4046-4051.
- Kneifel, W. (2000). In vitro growth behaviour of probiotic bacteria in culture media with carbohydrates of prebiotic importance. *Microb. Ecol. Health Dis.* 12, 27–34.
- Korkina, L., Kostyuk, V., Potapovich, A., Mayer, W. & Talib, N., De Luca, C. (2018). Secondary Plant Metabolites for Sun Protective Cosmetics: From Pre-Selection to Product Formulation. *Cosmetics* 5(2):32.
- Krasowska A, Sigler K. How microorganisms use hydrophobicity and what does this mean for human needs? *Front Cell Infect Microbiol.* 2014;4:1–7.
- Kumar B, Vijayakumar M, Govindarajan R, Pushpangadan P, Ethnopharmacological approaches to wound healing--exploring medicinal plants of India, *J Ethnopharmacol*, 2007; 114,103- 113.
- Kumar PT, Lakshmanan VK, Anilkumar TV, Ramya C, Reshmi P, et al. (2012)Flexible and microporous chitosan hydrogel/nano ZnO composite bandages for wound dressing: in vitro and in vivo evaluation. *ACS Appl Mater Interfaces* 4: 2618-2629.
- L. Griffiths and D. Chacon-Cortes, "Methods for extracting genomic DNA from whole blood samples: current perspectives," *J. Biorepository Sci. Appl. Med.*, vol. 2014, no. 2, p. 1, 2014, <http://doi:10.2147/bsam.s46573> .
- L. Truffault, "Synthèse et caractérisation de nanoparticules à base d'oxydes de cérium et de fer pour la filtration des UV dans les produits solaires," 2010
- Lachkar, N., Lamchouri, F., Bouabid, K., Boulfia, M., Senhaji, S., Stitou, M., & Toufik, H.(2021) Mineral Composition, Phenolic Content, and in Vitro Antidiabetic and Antioxidant Properties of Aqueous and Organic Extracts of Haloxylon scoparium Aerial Parts. *Evidence-Based Complementary and Alternative Medicine.* <https://doi.org/10.1155/2021/9011168>
- Lakshmipriya, T., Gopinath, S.C.B., 2021. Introduction to nanoparticles and analytical devices, in: Gopinath, S.C.B., Gang, F. (Eds.), *Nanoparticles in Analytical and Medical Devices*. Elsevier, pp. 1–29. <https://doi.org/10.1016/B978-0-12-821163-2.00001-7>
- Lamchouri, F., Benali, T., Bannani, B., Toufik, H., Ibn, L., Hassani, M., Bouachrine, M., Lyoussi, B., Ben, M., & Maroc, A. (2012). Preliminary phytochemical and antimicrobial investigations of extracts of Haloxylon scoparium. *Journal of Materials and Environmental Science*, 3(4), 754–759.

- Lamoureux L (2000). Exploitation de l'activité β -galactosidase de culture de bifidobactéries en vue d'enrichir des produits laitiers en galacto-oligosaccharides. National Library canada.23-47.
- Le Bronec, M. (2005). Influence des pansements Urgotul® dans la cicatrisation des plaies par seconde intention chez le chien et le chat : étude clinique (Doctoral dissertation).
- Lebonvallet, N., Laverdet, B., Misery, L., Desmoulière, A., & Girard, D. (2018). New insights into the roles of myofibroblasts and innervation during skin healing and innovative therapies to improve scar innervation. *Experimental Dermatology*, 27(9), 950-958.
- Li, Y., Lai, P., Chen, J., Shen, H., Tang, B., Wu, L., & Weng, M. (2016). Extraction optimization of polyphenols, antioxidant and xanthine oxidase inhibitory activities from *Prunus salicina* Lindl. *Food Science and Technology*, 36(3), 520-525.
- Licá, I.C.L., Soares, A.M. dos S., de Mesquita, L.S.S., & Malik, S. (2018). Biological properties and pharmacological potential of plant exudates. *Food Research International*, 105, 1039–1053. <https://doi.org/10.1016/j.foodres.2017.11.051>
- Lívia, P. G. M., Nathália, O. S. G., Mariana, C. M., Andressa, L. S. D., Nayara, L. O. & Edemilson, C. C. (2018). Extract from byproduct *Psidium guajava* standardized in ellagic acid: additivation of the in vitro photoprotective efficacy of a cosmetic formulation. *Revista Brasileira de Farmacognosia* 28(6):692– 696. <https://doi.org/10.1016/j.bjp.2018.08.005>.
- Lodhi, S., Singh Pauer, R., Pal Jain, A., Singhai, A.K., 2006. Wound healing potential of *Tephrosiapurpurea* (Linn.) Pers. In rats. *Journal of Ethnopharmacology* 108, 204 -210.
- Lourens-Hattingh, A. and Viljoen, B.C., "Yogurt as probiotic carrier food", *International Dairy Journal*, Vol. 11, No. 1, (2001), 1-17.
- Lu P.J., Huang S.C., Chen Y.P., Chiueh L.C., Shih D.Y.C.; (2015). Analysis of titanium dioxide and zinc oxide nanoparticles in cosmetics. *J Food Drug Anal.*, 23(3):587-594.
- Lü, J.-M., Lin, P. H., Yao, Q., Chen, C. (2009). Chemical and molecular mechanisms of antioxidants: experimental approaches and model systems. *Journal of Cellular and Molecular Medicine*, 14(4), 840–860. <https://doi:10.1111/j.1582-4934.2009.00897.x> .
- Luca, S. V., Macovei, I., Bujor, A., Miron, A., Skalicka-Woźniak, K., Aprotosoai, A. C., & Trifan, A. (2019). Bioactivity of dietary polyphenols: The role of metabolites. *Critical Reviews in Food Science and Nutrition*, 60(4), 626-659.
- M. Sekar and N. S. A. Jalil, "Formulation and evaluation of novel antibacterial and anti-inflammatory cream containing *Muntingia calabura* leaves extract," *Asian J. Pharm. Clin. Res.*, vol. 10, no. 12, pp. 376–379, 2017.

- M.S. Geier, R.N. Butler, P.M. Giffard, G.S. Howarth, Prebiotic and symbiotic fructooligosaccharide administration fails to reduce the severity of experimental colitis in rats, *Dis. Colon Rectum* 50 (7) (2007) 1061–1069.
- Madonna, S. (2010). Innovation moléculaire à visée thérapeutique : conception, synthèse et évaluation des propriétés anticancéreuses des nouveaux dérivés du : (N-(5-méthyl)-quinolién-8-ol)amine N-substitués. thèse doctora. université de la méditerranée . P19-52.
- Malaikozhundan B, Vaseeharan B, Vijayakumar S, Pandiselvi K, Kalanjiam R, Murugan K, Benelli G. 2017 Biological therapeutics of *Pongamia pinnata* coated zinc oxide nanoparticles against clinically important pathogenic bacteria, fungi and MCF-7 breast cancer cells. *Microb. Pathog.* 104, 68–277.
- Mallikarjunaswamy, C., Lakshmi Ranganatha, V., Ramu, R., Udayabhanu, & Nagaraju, G. (2020). Facile microwave-assisted green synthesis of ZnO nanoparticles: application to photodegradation, antibacterial and antioxidant. *Journal of Materials Science: Materials in Electronics*, 31(2), 1004-1021.
- Manikandan, R., Anand, A. V., & Kumar, S. (2016). Phytochemical and in vitro Antidiabetic activity of *Psidium Guajava* leaves. *Pharmacognosy Journal*, 8.(4)
- Maran, J. P., Manikandan, S., Nivetha, C. V., & Dinesh, R. (2017). Ultrasound assisted extraction of bioactive compounds from *Nephelium lappaceum* L. fruit peel using central composite face centered response surface design. *Arabian Journal of Chemistry*, 10, 1-13.
- Mena P, Domínguez-Perles R, Gironés-Vilaplana A, Baenas N, García-Viguera C, Villaño D. Flavan-3-ols, anthocyanins, and inflammation. *IUBMB Life* 2014 ;66 :745-58.
- Merkantia, A. (2017). Contribution à l'évaluation de l'activité cicatrisante du sous-produit de l'hydro-distillation d'*Artemisia herba alba* (Doctoral dissertation, École Nationale Supérieure Vétérinaire).
- Mezghani-Jarraya R., Hammami H., Ayadi A. and Damak M. 2009. Molluscicidal activity of *Hammada scoparia* (Pomel) Iljin leaf extracts and the principal alkaloids isolated from them against *Galba truncatula*. *Memórias do Instituto Oswaldo Cruz*, 104, pp. 1035-38.
- Michel Wautelet et coll, (2006), « Les Nanotechnologies » 3 ème édition, Dunod, Paris, p 7.
- Mihailovic V, Matic S, Mišić D, Solujic S, Stanic S, Katanic J, et al. Chemical composition, antioxidant and antigenotoxic activities of different fractions of *Gentiana asclepiadea* L. roots extract. *Excli J.* (2013) 12:807–23.

- Miri, A., Mahdinejad, N., Ebrahimi, O., Khatami, M., & Sarani, M. (2019). Zinc oxide nanoparticles: Biosynthesis, characterization, antifungal and cytotoxic activity. *Materials Science and Engineering: C*, 104, 109981.
- Mirza A.U., Kareem A., Nami S.A.A., Bhat S.A., Mohammad A., Nishat N.; 2019. *Malus pumila* and *Juglen regia* plant species mediated zinc oxide nanoparticles: Synthesis, spectral characterization, antioxidant and antibacterial studies. *Microb. Pathog.*, 129:233-241.
- Mishra, P. K., H. Mishra, A. Ekielski, S. Talegaonkar, and B. Vaidya. "Zinc Oxide Nanoparticles: A Promising Nanomaterial for Biomedical Applications." *Drug Discov Today* 22, 12 (2017): 1825-34. <http://dx.doi.org/10.1016/j.drudis.2017.08.006> .
- Mohanpuria, P., N.K. Rana, and S.K. Yadav, Biosynthesis of nanoparticles: technological concepts and future applications. *Journal of nanoparticle research*, 2008. 10(3): p. 507-517.
- Monneret, C. (2010). Impact actuel des produits naturels sur la découverte de nouveaux médicaments anticancéreux. In *Annales pharmaceutiques françaises*. 68(4), pp. 218-232.
- Morel N., Eustache F., Lange M., Joly F., Giffard B. ; (2010). L'impact du cancer et de ses traitements sur les fonctions cognitives : l'exemple du cancer du sein. *Revue de neuropsychologie*, 2: 250-254.
- Morere JF., Mornex F., Piccart M., Nabholz JM. (2001). *Thérapeutique du cancer*. edition spinger, pp 5-18.
- Mota, M. D., Morte, A. N., Silva, L. C & Chinalia, F. (2020). Sunscreen protection factor enhancement through supplementation with Rambutan (*Nephelium lappaceum* L) ethanolic extract. *Journal of Photochemistry and Photobiology B Biology* 205:111837.
- Moulin, Y. V. E. T. T. E. (2001). Comprendre le processus de cicatrisation. *L'infirmière du Québec*, 9(1), 37-40.
- Mourdikoudis, S., Pallares, R.M., Thanh, N.T.K., 2018. Characterization techniques for nanoparticles: comparison and complementarity upon studying nanoparticle properties. *Nanoscale* 10, 12871–12934. <https://doi.org/10.1039/C8NR02278J>
- Moussi, A., Abba, A., Harrat, A., & Petit, D. (2011). Desert acridian fauna (Orthoptera, Acridomorpha): comparison between steppic and oasian habitats in Algeria. *Comptes rendus. Biologies*, 334(2), 158-167.
- Movsesyan H, Barsova N (2020) Nanoparticules ZnO et CuO : une menace pour les organismes du sol, les plantes et la santé humaine. *Géochimie environnementale et santé* 42 :147-158.

- Muniyandi, K., George, E., Sathyanarayanan, S., George, B. P., Abrahamse, H., Thamburaj, S., & Thangaraj, P. (2019). Phenolics, tannins, flavonoids and anthocyanins contents influenced antioxidant and anticancer activities of Rubus fruits from Western Ghats, India. *Food Science and Human Wellness*, 8(1), 73-81.
- N. Shahabadi, S. Kashanian, M. Mahdavi, and N. Sourinejad, "DNA interaction and DNA cleavage studies of a new platinum (II) complex containing aliphatic and aromatic dinitrogen ligands," *Bioinorg. Chem. Appl.*, vol. 2011, 2011.
- Naghizadeh A., Mohammadi-Aghdam S., Mortazavi-Derazkola S.; 2020. Novel CoFe₂O₄@ZnO-CeO₂ ternary nanocomposite: Sonochemical green synthesis using *Crataegus microphylla* extract, characterization and their application in catalytic and antibacterial activities. *Bioorg. Chem.*, 103: 1-11.
- Nejjari, R., Benabbes, M., Amrani, M., Meddah, B., Bouatia, M., & Taoufik, J. (2019). Phytochemical screening and wound healing activity of *Telephium imperati* (L.) In rats. *South African Journal of Botany*, 123, 147-151.
- Noor, H.M., 2018. Potential of carrageenans in foods and medical applications. *Global Health Management Journal*, 2(2), pp.32-36 .
- Nounah, I., Hajib, A., Harhar, H., Gharby, S., Kartah, B., Charrouf, Z., & Bougrin, K. (2019). Moroccan Journal of Chemistry Phytochemical Screening and Biological Activity of Leaves and stems extract of *Hammada Scoparia*. *Moroccan Journal of Chemistry*, 7, 1–009.
- Nounah, I., Hajib, A., Oubihi, A., Hicham, H. A. R. H. A. R., gharby, S., Kartah, B. E., ... & Bougrin, K. (2019). Phytochemical screening and biological activity of leaves and stems extract of *hammada scoparia*. *Moroccan Journal of Chemistry*, 7(1), J-Chem.
- O. Yamamoto, "Influence of particle size on the antibacterial activity of zinc oxide," *International Journal of Inorganic Materials*, vol. 3, pp. 643-646, 2001.
- Olbert, M., J. Gdula-Argasinska, G. Nowak, and T. Librowski. "Beneficial Effect of Nanoparticles over Standard Form of Zinc Oxide in Enhancing the Anti-Inflammatory Activity of Ketoprofen in Rats." *Pharmacol Rep* 69, 4 (2017): 679-82. <http://dx.doi.org/10.1016/j.pharep.2017.02.004>.
- Ooi, L.L., Zhou, H., Kalak, R., Zheng, Y., Conigrave, A.D., Seibel, M.J., Dunstan, C.R., 2010 . Vitamin D deficiency promotes human breast cancer growth in a murine model of bone metastasis. *Cancer Res.* 70, 1835–1844.
- Osman, N I., Sidik, N J., Awal, A., Adam, N A., Rezali, N I. (2016). In vitro xanthine oxidase and albumin denaturation inhibition assay of *Barringtonia racemosa* L. and total

- phenolic content analysis for potential anti-inflammatory use in gouty arthritis. *Journal of Intercultural Ethnopharmacology*, 5(4), 343-349. <https://doi:10.5455/jice.20160731025522> .
- Osmond MJ, McCall MJ. Zinc oxide nanoparticles in modern sunscreens: an analysis of potential exposure and hazard. *Nanotoxicology*. 2010;4(1):15-41.
- Oubré, A.Y., Carlson, T.J., King, S.R. et Reaven, G.M. (1997). From plant to patient: an ethnomedical approach to the identification of new drugs for the treatment of NIDDM. *Diabetologia*, 40: 614-617.
- Ouibrahim, A, (2015). Evaluation de l'effet antimicrobien et antioxydant de trois plantes aromatiques (*Laurus nobilis* L., *Ocimum basilicum* L. et *Rosmarinus officinalis* L.) de l'Est Algérien. UNIVERSITE BADJI MOKHTAR–ANNABA. P, 15.
- Ozdal T, Sela DA, Xiao J, Boyacioglu D, Chen F, Capanoglu E. The reciprocal interactions between polyphenols and gut microbiota and effects on bioaccessibility. *Nutrients*. (2016) 8:78.
- Özdemir D, Kahyaoğlu Dt. Identification of microbiological, physical, and chemical quality of milk from milk collection centers in Kastamonu Province. *Turkish Journal of Veterinary & Animal Sciences*. 2020;44(1):118-30.
- Ozenda P. (2004). *Flore et végétation du Sahara* (3^{ème} édition). BARNÉOUD, pp 662.
- Özgür, Ü., et al., A comprehensive review of ZnO materials and devices. *Journal of Applied Physics*, 2005. 98(4): p. 11.
- P. Schofield, D. Mbugua, A.N. Pell, D.M. Mbugua, A.N. Pell, Analysis of condensed tannins: a review, *Anim. Feed. Sci. Technol.* 91 (1-2) (2001) 21-40. [http://doi:10.1016/S0377-8401\(01\)00228-0](http://doi:10.1016/S0377-8401(01)00228-0) .
- Padmavathy N, Vijayaraghavan R (2008) Enhanced bioactivity of ZnO nanoparticles - an antimicrobial study. *Sci Technol Adv Mater* 9: 1-7.
- Palomares I. C., Prérez-Morales R et Acedo-félise E (2007). Evaluation of probiotic properties in *Lactobacillus* isolated from small intestine of piglets. *Rev. Latinoan. Microbiol.* 49 (3-4):46-54.
- Parashar, U.K., P.S. Saxena, and A. Srivastava, Bioinspired synthesis of silver nanoparticles. *Digest Journal of Nanomaterials & Biostructures (DJNB)*, 2009. 4.(1)
- Park, H. J. & Cha, H. C. (2003). Flavonoids from leaves and exocarps of the grape Kyoho. *Korean journal of biological society*, 7, 327-330.
- Perera, W. P. T. D., Ranga K. Dissanayake, U. I. Ranatunga, N. M. Hettiarachchi, K. D. C. Perera, Janitha M. Unagolla, R. T. De Silva, and L. R. Pahalagedara. "Curcumin Loaded

- Zinc Oxide Nanoparticles for Activity- Enhanced Antibacterial and Anticancer Applications." RSC Advances 10, no. 51 (2020): 30785-95. <http://dx.doi.org/10.1039/d0ra05755j> .
- Perugini, P., Simeoni, S., Scalia, S., Genta, I., Modena, T., Conti, B. & Pavanetto, F. (2002). Effect of nanoparticle encapsulation on the photostability of the sunscreen agent, 2-ethylhexyl-p- methoxycinnamate. *International Journal of Pharmaceutics* 246(1-2):37–45.
- Petera, B., (2016), Extraction et caractérisations (structurale et physico-chimique) de polysaccharides hydrosolubles issus de cladodes de *Cereus triangularis*, thèse de doctorat Université Blaise Pascal-Clermont-Ferrand II ,142p. <https://theses.hal.science/tel-01548829/> .
- Piccart M., Dochy E., Cardoso F., (2003). News in the medical treatment et breast cancer. *bull cancer*, 90(1): 46-52.
- Pillai, S.C., et al., The effect of processing conditions on varistors prepared from nanocrystalline ZnO. *Journal of Materials Chemistry*, 2003. 13(10): p. 2586-2590.
- Polonini, H., Brandao, H., Raposo, N., Mouton, L., Yepremian, C., Couté, A. & Brayner, R. (2014). Ecotoxicological studies of micro- and nanosized barium titanate on aquatic photosynthetic microorganisms. *Aquatic toxicology (Amsterdam, Netherlands)*. 154C:58–70. [10.1016/j.aquatox.2014.05.005](https://doi.org/10.1016/j.aquatox.2014.05.005).
- Pottier, A. (2003). Conception, synthèse et évaluation pharmacologique de Pyrrolo[3,4-b]Quinoleines condensées, ligands potentiels de l'ADN. Thèse de doctorat. Université de LILLE I. P19.
- Prasad KS et al. 2021 Antitumor potential of green synthesized ZnONPs using root extract of *Withania somnifera* against human breast cancer cell line. *Separations* 8, 1–9 .
- Procopiou, M. (2006). HbA1c: review and recent developments. *Revue Médicale Suisse*; 2: 1473, 1479.
- Pushpalatha, C., Suresh, J., Gayathri, V., Sowmya, S., Augustine, D., Alamoudi, A., Zidane, B., Mohammad Albar, N.H., Patil, S., 2022. Zinc Oxide Nanoparticles: A Review on Its Applications in Dentistry. *Frontiers in Bioengineering and Biotechnology* 10.
- R. Esmailzadeh Kenari, R. Razavi, Phenolic profile and antioxidant activity of free/bound phenolic compounds of sesame and properties of encapsulated nanoparticles in different wall materials, *Food Sci. Nutr.* 10 (2) (2022) 525-535, <https://doi.org/10.1002/fsn3.2712>.

- R. Heckel, I. Shomorony, K. Ramchandran, and D. N. C. Tse, "Fundamental limits of DNA storage systems," in IEEE International Symposium on Information Theory - Proceedings, 2017, pp. 3130–3134. <http://doi:10.1109/ISIT.2017.8007106> .
- R. Re, N. Pellegrini, A. Proteggente, A. Pannala, M. Yang, C. Rice-Evans, Antioxidant activity applying an improved ABTS radical cation decolorization assay, *Free Radic. Biol. Med.* 26 (9-10) (1999) 1231e1237. [http://doi:10.1016/S0891-5849\(98\)00315-3](http://doi:10.1016/S0891-5849(98)00315-3).
- R. Whitlock, H. Hipperson, M. Mannarelli, and T. Burke, "A high-throughput protocol for extracting high-purity genomic DNA from plants and animals," *Mol. Ecol. Resour.*, vol. 8, no. 4, pp. 736–741, 2008, <http://doi:10.1111/j.1755-0998.2007.02074.x> .
- R.M. Alwan, Q.A. Kadhim, K.M. Sahan, R.A. Ali, R.J. Mahdi, N.A. Kassim, A.N. Jassim, Synthesis of zinc oxide nanoparticles via sol-gel route and their characterization, *Nanosci. Nanotechnol.* 5 (2015) 1-6.
- Rafique, Muhammad, Rabbia Tahir, S. S. A. Gillani, M. Bilal Tahir, M. Shakil, T. Iqbal, and M. O. Abdellahi. "Plant-Mediated Green Synthesis of Zinc Oxide Nanoparticles from *Syzygium Cumini* for Seed Germination and Wastewater Purification." *International Journal of Environmental Analytical Chemistry.* (2020): 1-16. <http://dx.doi.org/10.1080/03067319.2020.1715379> .
- Raha, S., & Ahmaruzzaman, M. (2022). ZnO nanostructured materials and their potential applications: progress, challenges and perspectives. *Nanoscale Advances*, 4(8), 1868-1925.
- Rahimi Kalateh Shah Mohammad, Ghasem, Masoud Homayouni Tabrizi, Touran Ardalani, Soheyla Yadamani, and Elham Safavi. "Green Synthesis of Zinc Oxide Nanoparticles and Evaluation of Anti-Angiogenesis, Anti-Inflammatory and Cytotoxicity Properties." *Journal of Biosciences* 44, no. 2 (2019). <http://dx.doi.org/10.1007/s12038-019-9845-y>.
- Rahman, F., Majed Patwary, M. A., Bakar Siddique, M. A., Bashar, M. S., Haque, M. A., Akter, B., ... & Royhan Uddin, A. K. M. (2022). Green synthesis of zinc oxide nanoparticles using *Cocos nucifera* leaf extract: characterization, antimicrobial, antioxidant and photocatalytic activity. *Royal Society Open Science*, 9(11), 220858.
- Rajakumar, G., M. Thiruvengadam, G. Mydhili, T. Gomathi, and I. M. Chung. "Green Approach for Synthesis of Zinc Oxide Nanoparticles from *Andrographis Paniculata* Leaf Extract and Evaluation of Their Antioxidant, Anti-Diabetic, and Anti-Inflammatory Activities." *Bioprocess Biosyst Eng* 41, no. 1 (Jan 2018): 21-30. <http://dx.doi.org/10.1007/s00449-017-1840-9> .

- Rajapriya M., Sharmili S.A., Baskar R., Balaji R., Alharbi N.S., Kadaikunnan S., Vaseeharan B.; 2019. Synthesis and characterization of Zinc Oxide nanoparticles using *Cynara scolymus* leaves: enhanced hemolytic, antimicrobial, antiproliferative, and photocatalytic activity. *J. Clust. Sci.*, 31:791-801.
- Rajashri SK, Amruta B, Vrinda PB, Koyar SR (2011) Bactericidal action of N doped ZnO in sunlight. *Biointerface. Res Appl Chem* 1: 57.
- Rajendran NK, George BP, Houreld NN, Abrahamse H. 2021, Synthesis of zinc oxide nanoparticles using *Rubus fairholmianus* root extract and their activity against pathogenic bacteria. *Molecules* 26, 1–11 .
- Rajeshkumar S, Kumar SV, Ramaiah A, Agarwal H, Lakshmi T, Roopan SM. 2018 Biosynthesis of zinc oxide nanoparticles using *Mangifera indica* leaves and evaluation of their antioxidant and cytotoxic properties in lung cancer (A549) cells. *Enzyme Microb. Technol.* 117, 91–95 .
- Rajeshkumar, S., S. Venkat Kumar, Arunachalam Ramaiah, Happy Agarwal, T. Lakshmi, and Selvaraj Mohana Roopan. "Biosynthesis of Zinc Oxide Nanoparticles Using *Mangifera Indica* Leaves and Evaluation of Their Antioxidant and Cytotoxic Properties in Lung Cancer (A549) Cells." *Enzyme and Microbial Technology* 117 (2018): 91-95. <http://dx.doi.org/10.1016/j.enzmictec.2018.06.009> .
- Rajput V, Minkina T, Sushkova S, Behal A, Maksimov A, Blicharska E, Ghazaryan K, Rambabu K., Bharath G., Banat F., Show P.L.; 2020. Green synthesis of zinc oxide nanoparticles using *Phoenix dactylifera* waste as bioreductant for effective dye degradation and antibacterial performance in wastewater treatment. *J. Hazard. Mater.*, 402 (15):1-36.
- Randa Fawzi Elsupikhe, Mansor B. Ahmad, Kamyar Shameli, Nor Azowa Ibrahim, Norhazlin Zainuddin. "Photochemical Reduction as a Green Method for the Synthesis and Size Control of Silver Nanoparticles in K-Carrageenan." *Nanoscale Research Letters*.(2015)
- Rangeela, M, S Rajeshkumar, T Lakshmi, and Anitha Roy. "Anti-Inflammatory Activity of Zinc Oxide Nanoparticles Prepared Using Amla Fruits." *Drug Invention Today* 11, 10 .(2019)
- Rasouli, H., Farzaei, M. H., & Khodarahmi, R. (2017). Polyphenols and their benefits: A review. *International Journal of Food Properties*, 20(2), 1700-1741.
- Reddy J.S., Rao P.R., Reddy M.S., Wound healing effects of *Heliotropium indicum*, *Plumbago zeylanicum* and *Acalypha indica* in rats, *J of Ethnopharm*, 2002; 79,249-251.

- Rehana, D., Mahendiran, D., Kumar, R. S., & Rahiman, A. K. (2017). In vitro antioxidant and antidiabetic activities of zinc oxide nanoparticles synthesized using different plant extracts. *Bioprocess and biosystems engineering*, 40(6), 943-957.
- Reid, G., Sanders, M., Gaskins, H.R., Gibson, G.R., Mercenier, A., Rastall, R., Roberfroid, M., Rowland, I., Cherbut, C. and Klaenhammer, T.R., "New scientific paradigms for probiotics and prebiotics", *Journal of Clinical Gastroenterology*, Vol. 37, No. 2, (2003), 105-118.
- Reyes-Gavilan C.G., Suarez A., Fernandez –Garcia M., Margolles A., Gueimonde Met Ruas-Madiedo P (2011). Adh sion of bile –adapted Bifidobacterium strains to the HT296MTX cell line is modified after sequential gastro-intestinal challenge simulated in vitro using human gastric and duodenal juices. *Res. Microbiol.*162: 514-519.
- Ribeiro, C. (2006). *Cosmetologia aplicada a dermoest tica*. Pharmabooks.
- Richard, C.L., Farach-Carson, M.C., Rohe, B., Nemere, I., Meckling, K.A., 2010. Involvement of 1, 25D3-MARRS (membrane associated, rapid response steroid- binding), a novel vitamin D receptor, in growth inhibition of breast cancer cells. *Exp. Cell Res.* 316, 695–703.
- Rodr guez-S anchez, S., Fern andez-Pacheco, P., Sese na, S., Pintado, C., & Palop, M. L.(2021). Selection of probiotic Lactobacillus strains with antimicrobial activity to be used as biocontrol agents in food industry. *Lebensmittel-Wissenschaft und -Technologie*, 143, Article 111142.
- Rosales, P. F., Bordin, G. S., Gower, A. E., & Moura, S. (2020). Indole alkaloids: 2012 until now, highlighting the new chemical structures and biological activities. *Fitoterapia*, 1-26.
- Ruangtong J, T-Thienprasert J, T-Thienprasert NP. 2020 Green synthesized ZnO nanosheets from banana peel extract possess anti-bacterial activity and anti-cancer activity. *Materials Today Commun.* 24, 101224.
- S. A. Miller, D. D. Dykes, and H. F. Polesky, "A simple salting out procedure for extracting DNA from human nucleated cells," *Nucleic Acids Res.*, vol. 16, no. 3, p. 1215, 1988, <http://doi:10.1093/nar/16.3.1215> .
- S. Lousinian, D. Missopolinou, C. Panayiotou, Fibrinogen adsorption on zinc oxide nanoparticles: A Micro-Differential Scanning Calorimetry analysis, *J. Colloid Interface Sci.* 395 (2013) 294–299.

- S. Schalka, V. Manoel, S. Dos Reis, Sun protection factor: meaning and controversies, An. Bras. Dermatol. 86 (3) (2011) 507-522, <https://doi.org/10.1590/S0365-05962011000300013> .
- S. Yarrappagaari, R. Gutha, L. Narayanaswamy, L. Thopireddy, L. Benne, S.S. Mohiyuddin, V. Vijayakumar, R.R. Saddala, Eco-friendly synthesis of silver nanoparticles from the whole plant of *Cleome viscosa* and evaluation of their characterization, antibacterial, antioxidant and antidiabetic properties, Saudi J. Biol. Sci. 27 (12) (2020) 3601-3614. <http://doi:10.1016/j.sjbs.2020.07.034> .
- S.T. Fardood, A. Ramazani, S. Moradi, P.A. Asiabi, Green synthesis of zinc oxide nanoparticles using Arabic gum and photocatalytic degradation of direct blue 129 dye under visible light, J. Mater. Sci. Mater. Electron. 28(2017) 13596-13601.
- Sá, R D C S., Andrade, L N., Sousa, D P D. (2013). A Review on Anti-Inflammatory Activity of Monoterpenes. Molecules, 18(1), 1227-1254. <https://doi.org/10.3390/molecules18011227> .
- Sabir S, Arshad M, Chaudhari SK (2014) Nanoparticules d'oxyde de zinc pour révolutionner l'agriculture : synthèse et applications. Le Journal du monde scientifique 2014.
- Sachin, Jaishree, N. Singh, R. Singh, K. Shah, and B. K. Pramanik, "Green synthesis of zinc oxide nanoparticles using lychee peel and its application in antibacterial properties and CR dye removal from wastewater," Chemosphere, vol. 327, pp. 1–10, Jun. 2023. <https://doi:10.1016/J.CHEMOSPHERE.2023.138497>
- Sachin, Jaishree, N. Singh, R. Singh, K. Shah, and B. K. Pramanik, "Green synthesis of zinc oxide nanoparticles using lychee peel and its application in antibacterial properties and CR dye removal from wastewater," Chemosphere, vol. 327, pp. 1–10, Jun. 2023. <https://doi:10.1016/J.CHEMOSPHERE.2023.138497> .
- Sadhasivam, Sahana, Megala Shanmugam, Pillai Divya Umamaheswaran, Anbazhagan Venkattappan, and Anusuya Shanmugam. "Zinc Oxide Nanoparticles: Green Synthesis and Biomedical Applications." Journal of Cluster Science (2020). <http://dx.doi.org/10.1007/s10876-020-01918-0>.
- Saidi, S.A., Bourogâa, E., Bouaziz, A., Mongi, S., Chaaben, R., Jamoussi, K., Mezghani-Jarraya, R., van Pelt, J., & El-Feki, A. (2015). Protective effects of *Hammada scoparia* flavonoid-enriched fraction on liver injury induced by warm ischemia/reperfusion. Pharmaceutical Biology, 53(12), 1810-1817. <https://doi.org/10.3109/13880209.2015.1010737>

- Salah, H. ben, Jarraya, R., Martin, M.-T., Veitch, N.C., Grayer, R.J., Simmonds, M.S.J., & Damak, M. (2002). Flavonol Triglycosides from the Leaves of *Hammada scoparia* (POMEL) ILJIN. *Chemical and Pharmaceutical Bulletin*, 50(9), 1268–1270.
- Saleh AA (2014) Effect of dietary mixture of Aspergillus probiotic and selenium nanoparticles on growth, nutrient digestibilities, selected blood parameters and muscle fatty acid profile in broiler chickens. *Anim Sci Pap Rep* 32:65–79.
- Salman, A. Ali. "Application of nanomaterials in environmental improvement." *Nanotechnology and the Environment* (2020): 17-36.. <https://doi.org/10.5772/intechopen.91438>
- Sampaio, S. A. P. & Rivitti, E. A. *Dermatologia*. (2a ed.), Artes Médicas, 629–42, 839–846, 878–886.
- Sangeetha, A., Jaya Seeli, S., Bhuvana, K. P., Kader, M. A., & Nayak, S. K. (2019). Correlation between calcination temperature and optical parameter of zinc oxide (ZnO) nanoparticles. *Journal of Sol-Gel Science and Technology*. 91:261–272.
- Sankhalkar, S., & Vernekar, V. (2016). Quantitative and Qualitative analysis of Phenolic and Flavonoid content in *Moringa oleifera* Lam and *Ocimum tenuiflorum* L. *Pharmacognosy research*, 8(1), 16.
- Sayed Ahmed. B, (2018), Etude de l'agroraffinage de graines d'Apiaceae, Lamiaceae et Chenopodiaceae pour la production de molécules biosourcées en vue d'application en industrie cosmétique, thèse de doctorat université de Toulouse, 177p. <https://oatao.univ-toulouse.fr/19767> .
- Scheen, N., Paquot, B. et Jandrain, P.J. (2002). Physiopathologie, conséquences cliniques et approches diététiques. *Revue Médicale du Liège*, 57 (3): 138-141.
- Sefidkon F., Abbasi K., Jamzad Z. and Ahmadi S., (2007). The effect of distillation methods and stage of plant growth on the essential oil content and composition of *Satureja Rechingeri jamzad*. *Food chemistry*. 100, 1054-1058.
- Seok, S. U., Kang, S. Y., Seo, J. W., Kim, S. H., Hwang, K. M. & Park, E. S. (2016). Formulation of Nanoparticle Containing Everolimus Using Microfluidization and Freeze-Drying. *Chemical & Pharmaceutical Bulletin* 64(10):1445–1449. 10.1248/cpb.c16-00049.
- Shafqat, A., Ghulam, Y., Zareen, Z., Zhanpeng, W., Ian, S. B., Badshah, A., Imtiaz, U. D. (2015). Ferrocene-Based Bioactive Bimetallic Thiourea Complexes Synthesis and Spectroscopic Studies. *Bioinorganic Chemistry and Applications*, <http://doi.org/10.1155/2015/386587> .

- Shahid S, Fatima U, Sajjad R, Khan SA. 2019. Bioinspired nanotheranostic agent: zinc oxide; green synthesis and biomedical potential. *Dig. J. Nanomat. and Biostruc.* 14, 1023–1031.
- Shahnaza M, Danish M, Hisyamuddin M, Ismail B, Ansari MT, Ibrahim MNM. 2019. Anticancer and apoptotic activity of biologically synthesized zinc oxide nanoparticles against human colon cancer HCT-116 cell line- in vitro study. *Sust. Chem. Pharm.* 14, 1–7.
- Shaikhaldein, H.O., Al-Qurainy, F., Khan, S., Nadeem, M., Tarroum, M., Salih, A.M., Gaafar, A.-R.Z., Alshameri, A., Alansi, S., Alenezi, N.A., Alfarraj, N.S., 2021. Biosynthesis and Characterization of ZnO Nanoparticles Using *Ochradenus arabicus* and Their Effect on Growth and Antioxidant Systems of *Maerua oblongifolia*. *Plants (Basel)* 10, 1808. <https://doi.org/10.3390/plants10091808>
- Shamasi, Z., Es-haghi, A., Taghavizadeh Yazdi, M. E., Amiri, M. S., & Homayouni-Tabrizi, M. (2021). Role of *Rubia tinctorum* in the synthesis of zinc oxide nanoparticles and apoptosis induction in breast cancer cell line. *Nanomedicine Journal*, 8(1), 65-72.
- Sharma, T., Pandey, B., Shrestha, B. K., Koju, G. M., Thusa, R., & Karki, N. (2020). Phytochemical screening of medicinal plants and study of the effect of phytoconstituents in seed germination. *Tribhuvan University Journal*, 35(2), 1-11.
- Simis, T. & Simis, D. (2006). Doenças da pele relacionadas à radiação solar. *Revista Faculdade de Ciências Médicas de Sorocaba* 8(1):234–242.
- Singh, T. A., Sharma, A., Tejwan, N., Ghosh, N., Das, J., & Sil, P. C. (2021). A state of the art review on the synthesis, antibacterial, antioxidant, antidiabetic and tissue regeneration activities of zinc oxide nanoparticles. *Advances in Colloid and Interface Science*, 295, 102495.
- Singh, A., Jain, D., Upadhyay, M.K., Khandelwal, N., Verma, H.N., (2010), Green synthesis of silver nanoparticles using *Argemone mexicana* leaf extract and evaluation of their antimicrobial activities, *Digest Journal of Nanomaterials and Biostructures* 5, 483–489.
- Sirajuddin, M. Ali, S. Amin Badshah, A. (2013). Drug–DNA interactions and their study by UV–Visible, fluorescence spectroscopies and cyclic voltametry. *Journal of Photochemistry and Photobiology B: Biology*, (124) 1–19.
- Sirelkhatim, A., Mahmud, S., Seeni, A., Kaus, N. H. M., Ann, L. C., Bakhori, S. K. M., ... & Mohamad, D. (2015). Review on zinc oxide nanoparticles: antibacterial activity and toxicity mechanism. *Nano-micro letters*, 7, 219-242.

- Skarupova, D., Vostalova, J. & Rajnochova Svobodova, A. (2020). Ultraviolet A protective potential of plant extracts and phytochemicals. *Biomedical papers of the Medical Faculty of the University Palacký , Olomouc, Czechoslovakia* 164(1):1–22.
- Smijs TG, Pavel S. Titanium dioxide and zinc oxide nanoparticles in sunscreens: focus on their safety and effectiveness. *Nanotechnol Sci Appl.* 2011; 4:95-112.
- Southon, S., Gee, J. M., & Johnson, I. T. (1984). Hexose transport and mucosal morphology in the small intestine of the zinc-deficient rat. *British Journal of Nutrition*, 52(2), 371.
- Srivastava, G. K., Martinez-Rodriguez, S., Md Fadilah, N. I., Looi Qi Hao, D., Markey, G., Shukla, P., ... & Panetsos, F. (2024). Progress in Wound-Healing Products Based on Natural Compounds, Stem Cells, and MicroRNA-Based Biopolymers in the European, USA, and Asian Markets: Opportunities, Barriers, and Regulatory Issues. *Polymers*, 16(9), 1280.
- Sudheer Kumar K.H., Dhananjaya N., Yadav L.S.R.; 2018. E. tirucalli plant latex mediated green combustion synthesis of ZnO nanoparticles: Structural, photoluminescence and photocatalytic activities. *J Sci Adv Mater Devices.*, 3(3): 303-309.
- Sukara, E.; Salamah, A.; Dinoto, A.; Mangunwardoyo, W. Identification of lactic acid bacteria in sayur asin from Central Java (Indonesia) based on 16S rDNA sequence. *Intern. Food Res. J.* 2014, 21, 527–532.
- Sukri SNAM, Shameli K, Wong MMT, Teow SY, Chew J, Ismail NA. 2019 Cytotoxicity and antibacterial activities of plant-mediated synthesized zinc oxide (ZnO) nanoparticles using Punica granatum (pomegranate) fruit peels extract. *J. Mol. Struc.* 1189, 57–65 .
- Sun, Y., G.M. Fuge, and M.N. Ashfold, Growth of aligned ZnO nanorod arrays by catalyst-free pulsed laser deposition methods. *Chemical Physics Letters*, 2004. 396(1-3): p. 21-26.
- Suresh PG, Dharmalingam RGM., Baskar S, Senthil kumar P, Evaluation of Wound Healing Activity of “Abutilon Indicum” Linn In Wister Albino Rats, *Int J Biol Med Res.*,2011; 2,908-911
- Suresh, D., Nethravathi, P. C., Rajanaika, H., Nagabhushana, H., & Sharma, S. C. (2015). Green synthesis of multifunctional zinc oxide (ZnO) nanoparticles using Cassia fistula plant extract and their photodegradative, antioxidant and antibacterial activities. *Materials Science in Semiconductor Processing*, 31, 446-454.
- T. Lanez, H. Benaicha, E. Lanez, and M. Saidi, “Electrochemical, spectroscopic and molecular docking studies of 4-methyl-5-((phenylimino)methyl)-3H- and 5-(4-fluorophenyl)-3H-

- 1,2-dithiole-3-thione interacting with DNA,” J. Sulfur Chem., vol. 39, no. 1, pp. 76–88, 2018, <http://doi:10.1080/17415993.2017.1391811> .
- Taïbi, K., Abderrahim, L.A., Ferhat, K., Betta, S., Taïbi, F., Bouraada, F., & Boussaid, M. (2020). Ethnopharmacological study of natural products used for traditional cancer therapy in Algeria. Saudi Pharmaceutical Journal, 28(11), 1451-1465. <https://doi.org/10.1016/j.jsps.2020.09.011>
- Taïr K., Kharoubi O., Taïr O.A., Hellal N., Benyettou I. and Aoues A. 2016. Aluminium-induced acute neurotoxicity in rats: Treatment with aqueous extract of *Arthrophytum (Hammada scoparia)*. Journal of acute disease, 5, pp. 470-482.
- Taïr, K., Kharoubi, O., Taïr, O.A., Hellal, N., Benyettou, I., & Aoues, A. (2016). Aluminium-induced acute neurotoxicity in rats: Treatment with aqueous extract of *Arthrophytum (Hammada scoparia)*. Journal of Acute Disease, 5(6), 470-482. <https://doi.org/10.1016/J.JOAD.2016.08.028>
- Temmerman R., Pot B., Huys G and Swings J (2003). Identification and antibiotic susceptibility of bacterial isolates from probiotic products. Int. J. Food Microbiol.81 :1-10.
- Thangapazham, R.L., Singh, A.K., Sharma, A., Warren, J., Gaddipati, J.P., Maheshwari, R.K., 2007. Green tea polyphenols and its constituent epigallocatechin gallate inhibits proliferation of human breast cancer cells in vitro and in vivo. Cancer Lett. 245, 232–241.
- Thirumorthy, G. S., Balasubramaniam, O., Kumaresan, P., Muthusamy, P., & Subramani, K. (2021). Tetraselmis indica mediated green synthesis of zinc oxide (ZnO) nanoparticles and evaluating its antibacterial, antioxidant, and hemolytic activity. BioNanoScience, 11(1), 172-181.
- Thornton, G. M. (1996). Probiotic bacteria: selection of *Lactobacillus* and *Bifidobacterium* strains from the healthy human gastrointestinal tract; characterisation of a novel *Lactobacillus*-derived antibacterial protein (Doctoral dissertation, NUI).
- Toffetti, M. H. F. C. & De Oliveira, V. R. (2006). A importância do uso do filtro solar na prevenção do fotoenvelhecimento e do câncer de pele. Investigaçao 6.(1)
- Toyoshima, M., Hosoda, K., Hanamura, M., Okamoto, K., Kobayashi, H. & Negishi, T. (2004). Alternative methods to evaluate the protective ability of sunscreen against photogenotoxicity. Journal of Photochemistry and Photobiology B: Biology 73(1-2):59–66.

- Trease, G., & Evans, W. (1989). *Pharmacognosy*. 13th. ELBS/Bailliere Tindall, London, 345-346.
- Turkmen, N., Sari, F., & Velioglu, Y. S. (2006). Effects of extraction solvents on concentration and antioxidant activity of black and black mate tea polyphenols determined by ferrous tartrate and Folin–Ciocalteu methods. *Food chemistry*, 99,(4) 835-841.
- U.P. Nyayiru Kannaian, J.B. Edwin, V. Rajagopal, S. Nannu Shankar, B. Srinivasan, Phytochemical composition and antioxidant activity of coconut cotyledon, *Heliyon* 6 (2) (2020) e03411, 1-7, <http://doi:10.1016/j.heliyon.2020.e03411> .
- Umar H, Kavaz D, Rizaner N. 2019 Biosynthesis of zinc oxide nanoparticles using *Albizia lebeck* stem bark, and evaluation of its antimicrobial, antioxidant, and cytotoxic activities on human breast cancer cell lines. *Int. J. Nanomed.* 14, 87–100 .
- Umar, H., Kavaz, D., & Rizaner, N. (2019). Biosynthesis of zinc oxide nanoparticles using *Albizia lebeck* stem bark, and evaluation of its antimicrobial, antioxidant, and cytotoxic activities on human breast cancer cell lines. *International journal of nanomedicine*, 87-100.
- V.L. Singleton, R. Orthofer, R.M. Lamuela-Ravent's, Analysis of total phenols and other oxidation substrates and antioxidants by means of folin-ciocalteu reagent, *Meth. Enzymol.* 299 (1999) 152e178, [https://doi.org/10.1016/S0076-6879\(99\)99017-1](https://doi.org/10.1016/S0076-6879(99)99017-1) .
- Vijayakumar S, Vaseeharan B, Malaikozhundan B, Shobiya M, Pharmacother B. 2016 *Laurus nobilis* leaf extract mediated green synthesis of ZnO nanoparticles: characterization and biomedical application. *Biomed. Pharmacother.* 84, 1213–1222 .
- Vimalaa K, Sundarraja S, Paulpandia M, Vengatesanc S, Kannan S. 2014 Green synthesized doxorubicin loaded zinc oxide nanoparticles regulates the Bax and Bcl-2 expression in breast and colon carcinoma. *J. Proc. Biochem.* 49, 160–172.
- Violante, I. M. P., Souza, I. M., Venturini, C. L., Ramalho, A. F. S., Santos, R. A. N. & Ferrari, M. (2009). Avaliação in vitro da atividade fotoprotetora de extratos vegetais do cerrado de Mato Grosso. *Revista Brasileira de Farmacognosia.* 19(2):452–457.
- Vladi'c J, Cebovi'c T, Vidovi'c S, Joki'c S. Evaluation of anticancer activity of *Satureja montana* supercritical and spray-dried extracts on ehrlich's ascites carcinoma bearing mice. *Plants.* (2020) 9:1532.
- Wang, J & Mazza, G. (2002). Effects of anthocyanins and other phenolic compounds on the production of tumor necrosis factor α in LPS/IFN- γ -activated RAW 264.7 macrophages. *Journal of Agricultural and Food Chemistry*, 50,(4) 850–857.

- Wang, L., Ling, Y., Chen, Y., Li, C.L., Feng, F., You, Q.D., Lu, N., Guo, Q.L., 2010. Flavonoid baicalein suppresses adhesion, migration and invasion of MDA-MB- 231 human breast cancer cells. *Cancer Lett.* 297, 42–48.
- Widjonarko, N., 2016. Introduction to Advanced X-ray Diffraction Techniques for Polymeric Thin Films. *Coatings* 6, 54. <https://doi.org/10.3390/coatings6040054>
- Wolf, R., Wolf, D., Morganti, P. & Ruocco, V. (2001). Sunscreens. *Clinics in Dermatology.* 19(4):452–459.
- X. Tzounis, A. Rodriguez-Mateos, J. Vulevic, G.R. Gibson, C. Kwik-Urbe, J.P. Spencer, Prebiotic evaluation of cocoa-derived flavanols in healthy humans by using a randomized, controlled, double-blind, crossover intervention study, *Am. J. Clin. Nutr.* 93 (1) (2011) 62–72,
- Xiong W. T., GU L., Wang C., Sun H. X. and Liun X. (2013). Anti-hyperglycemic and hypolipidemic effects of *Cistanche tubulosa* in type 2 diabetic db/db mice. *Journal of Ethnopharmacology*, (150) 935-945.
- Y. B. Saab, W. Kabbara, C. Chbib, and P. R. Gard, “Buccal cell DNA extraction: Yield, purity, and cost: A comparison of two methods,” *Genet. Test.*, vol. 11, no. 4, pp. 413–416, 2007, <http://doi:10.1089/gte.2007.0044> .
- Yam, M. F., Ang, L. F., Ameer, O. Z., Salman, I. M., Aziz, H. A., & Asmawi, M. Z. (2009). Anti-inflammatory and analgesic effects of *Elephantopus tomentosus* ethanolic extract. *Journal of Acupuncture and Meridian Studies*, 2(4), 280-287.
- Yetisgin A.A., Cetinel S., Zuvin M., Kosar A., Kutlu O.; (2020). Therapeutic nanoparticles and their targeted delivery applications. *Molecules (Basel, Switzerland)*., 25(9):1-31.
- Yung MMN, Mouneyrac C, Leung KMY. 2014. Ecotoxicity of zinc oxide nanoparticles in the marine environment. *Encyclo. Nanotech.* 1–17.
- Z.J. Deng, G. Mortimer, T. Schiller, A. Musumeci, D. Martin, R.F. Minchin, Differential plasma protein binding to metal oxide nanoparticles, *Nanotechnology.* 20 (2009) 1–9.
- Z.J. Deng, M. Liang, I. Toth, M. Monteiro, R.F. Minchin, Plasma protein binding of positively and negatively charged polymer-coated gold nanoparticles elicits different biological responses, *Nanotoxicology.* 7 (2013) 314–322.
- Zare E, Pourseyedi S, Khatami M, Darezereshki E. 2017 Simple biosynthesis of zinc oxide nanoparticles using nature’s source, and it’s in vitro bio-activity. *J. Mol. Struct.* 1146, 96–103.
- Zeghoud S, Hemmami H, Seghir BB, Amor IB, Kouadri I, Rebiai A, Messaoudi M, Ahme d S, Pohl P, Simal-Gandara J (2022) Une revue sur la synthèse verte biogénique de





- nanoparticules de ZnO par la biomasse végétale et leurs applications. Matériaux aujourd'hui Communications : 104747.
- Zerriouh, M., Zerriouh, M., Merghache, S., Djazin, R., Selles, C., & Sekkal, F.Z. (2014). Investigation of *Hammada scoparia* antidiabetic activity and toxicity in rat. International Journal of Phytomedicine, 6(3), 327–334.
- Zheng Y., Huang Y., Shi H., Fu L.; 2019. Green biosynthesis of ZnO nanoparticles by plectranthus amboinicus leaf extract and their application for electrochemical determination of norfloxacin. Inorg. Nano-Met. Chem., 49(9): 277-282.
- Zhen-Yuan, Z. H. U., Zhang, J. Y., Li-Jing, C. H. E. N., Xiao-Cui, L. I. U., Yang, L. I. U., Wan-Xiao, W. A. N. G., & Zhang, Y. M. (2014). Comparative evaluation of polysaccharides isolated from Astragalus, oyster mushroom, and yacon as inhibitors of α -glucosidase. Chinese Journal of Natural Medicines, 12(4), 290-293.
- Zhong, K., & Wang, Q. (2010). Optimization of ultrasonic extraction of polysaccharides from dried longan pulp using response surface methodology. Carbohydrate polymers, 80(1), 19-25.
- Zouhair Sofiani, (2007), Contributions à l'étude des propriétés optiques non linéaires de nanoparticules en couches minces `à base de ZnO, these de doctorat, Université d'Angers - Université d'Ibn Tofail, France, pp141.

Annexes

Annexe 01: Rapport of Biochemical identification of LAB isolated strain using API 10S strip

OPERATOR: not logged!
 DATABASE VERSION: Bacillus 4.7.9-032024
 STRAIN CODE: unknown

BIOCHEMICAL IDENTIFICATION - RESULTS

- 1. Paenibacillus contaminans**

 No opposing tests Similarity: 99% Probability: 55.7% Matrix integrity: 100%
- 2. Bacillus pumilus (possibility of B. safensis)**

 No opposing tests Similarity: 94.1% Probability: 28.1% Matrix integrity: 100%
- 3. Bacillus megaterium**

 No opposing tests Similarity: 89.2% Probability: 14.2% Matrix integrity: 100%
- 4. Bacillus cibi**

 Opposing tests: Arabinose⁺ Similarity: 89.2% Probability: 0.6% Matrix integrity: 100%
- INPUT TESTS: ONPG⁺, Oxidase⁺, Urease⁻, LDC⁻, ODC⁻, Indole⁻, Citrate⁺, Nitrates⁻, Arabinose⁺ and Glucose⁺

Legend: ■ 90-99% ■ 75-89% ■ 25-74% ■ 11-24% ■ 01-10%

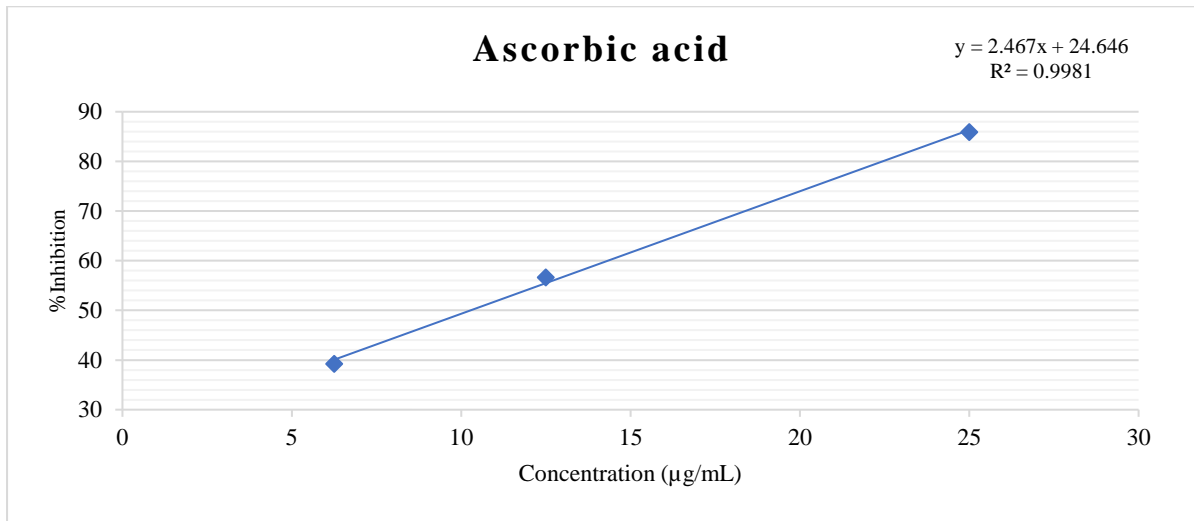
Annex 02: Calibration curve for determination of capacity antioxidant of samples

Figure: Calibration curve Ascorbic Acid for determination of ABTS radical scavenging

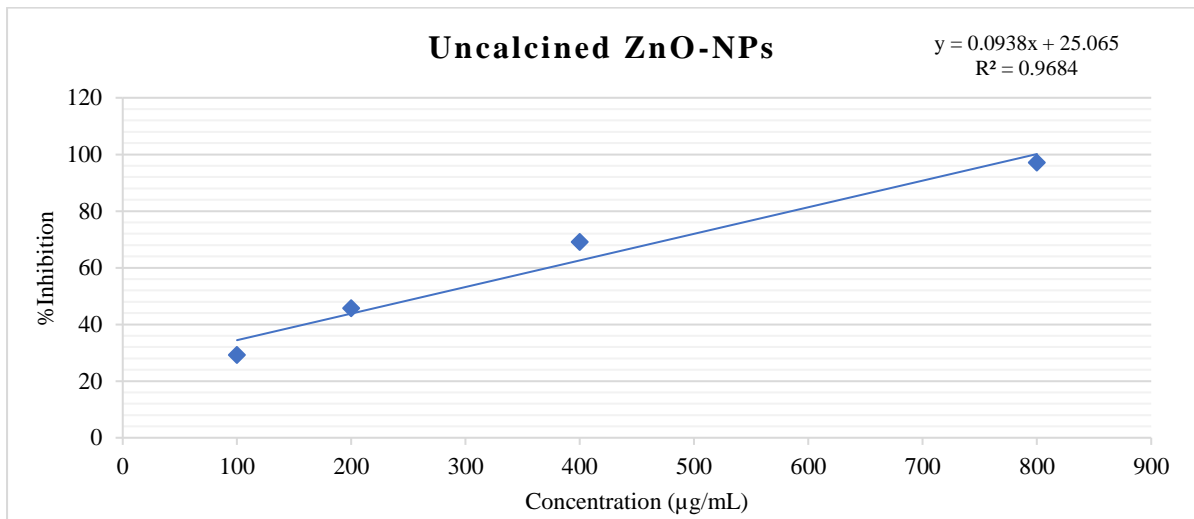
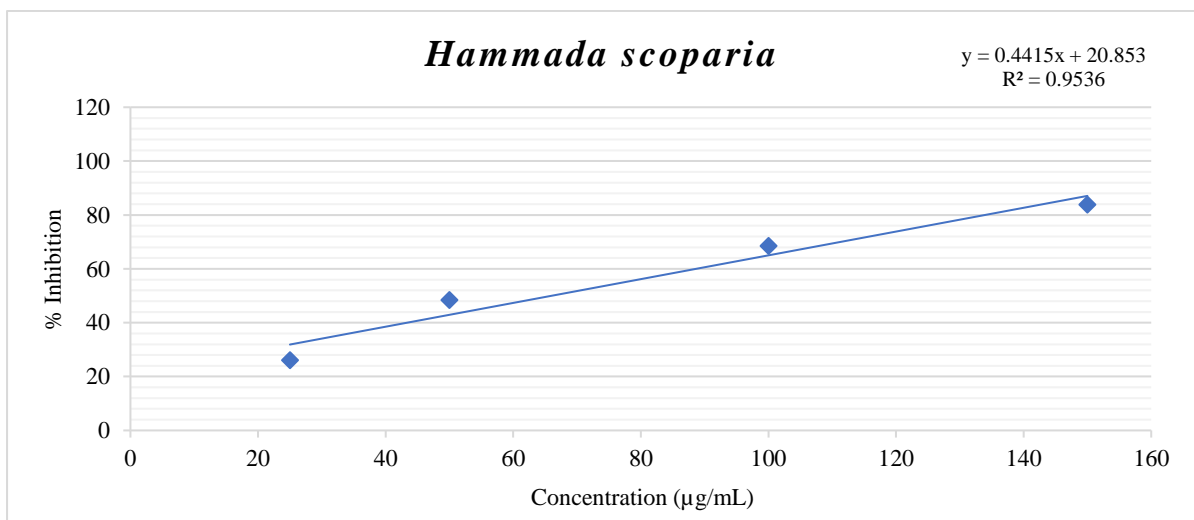


Figure: Uncalcined ZnO-NPs calibration curve for determination of ABTS radical scavenging

Figure: *Hammada scoparia* calibration curve for determination of ABTS radical scavenging

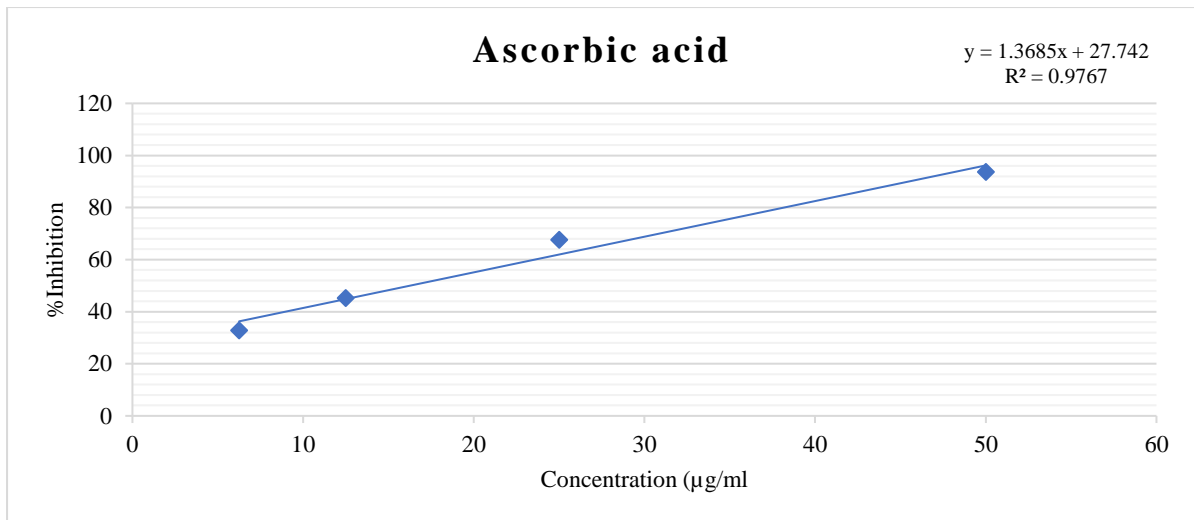


Figure: Calibration curve Ascorbic Acid for determination of DPPH radical scavenging

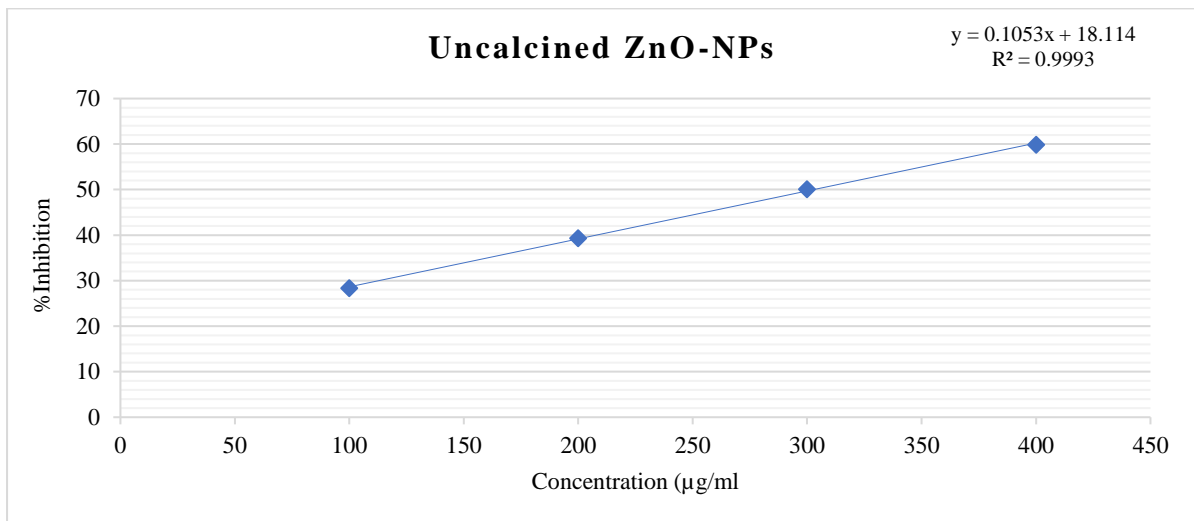


Figure: Uncalcined ZnO-NPs calibration curve for determination of DPPH radical scavenging

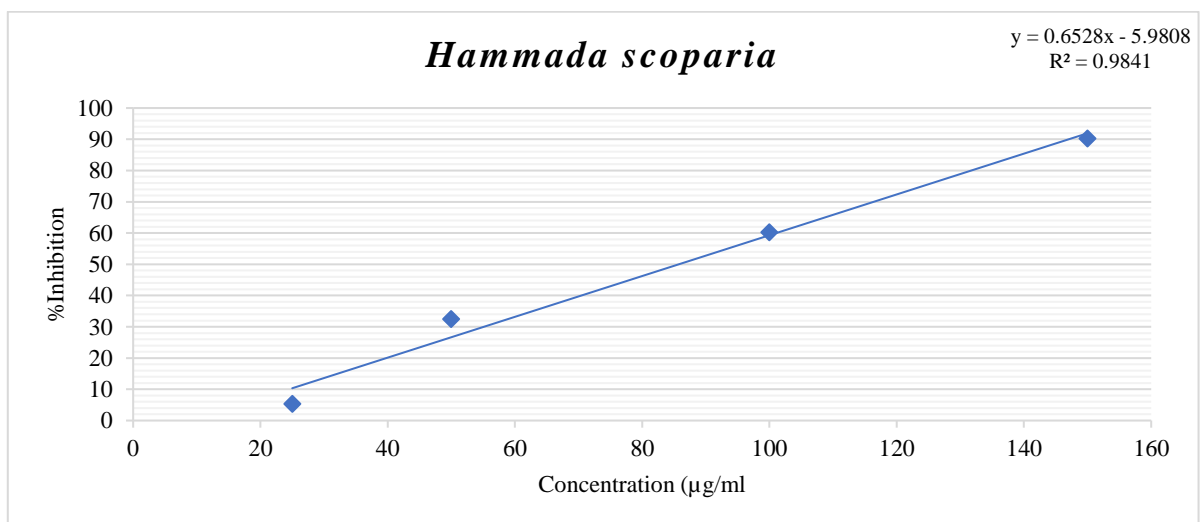


Figure: *Hammada scoparia* calibration curve for determination of DPPH radical scavenging

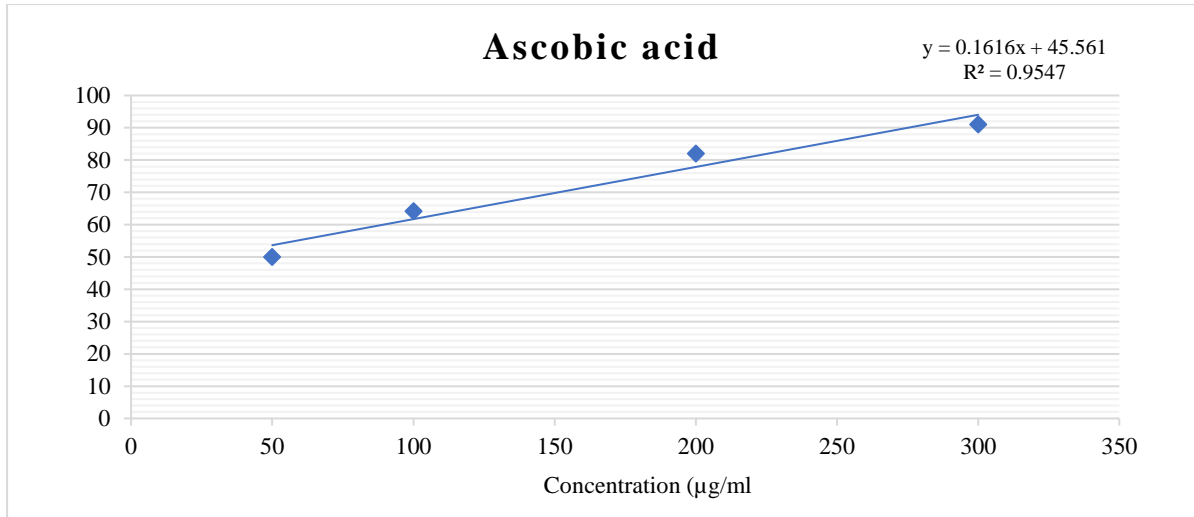


Figure: Calibration curve Ascorbic Acid for determination of reducing power capacity

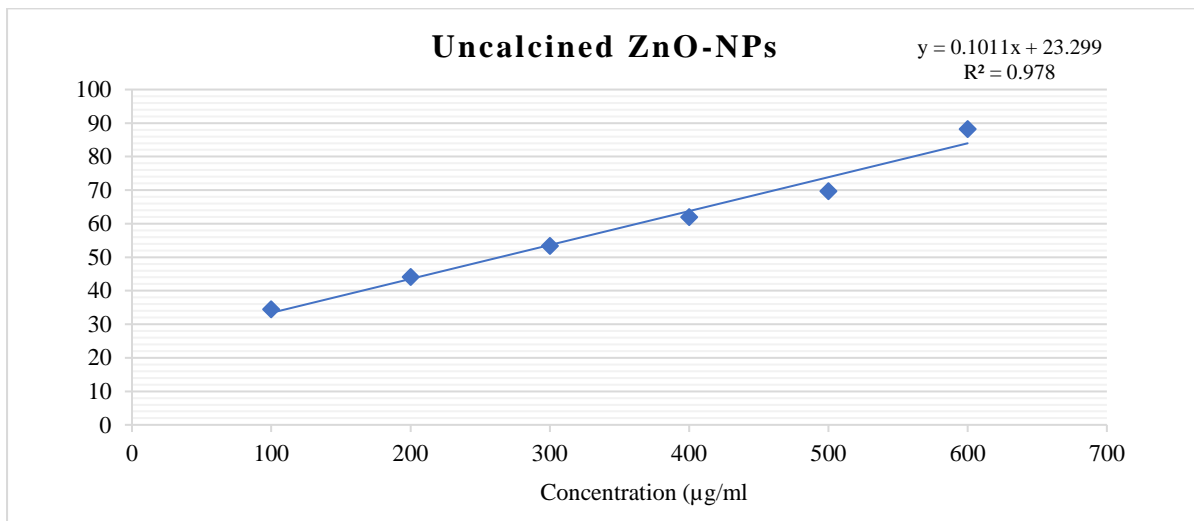


Figure: Uncalcined ZnO-NPs calibration curve for determination of reducing power capacity

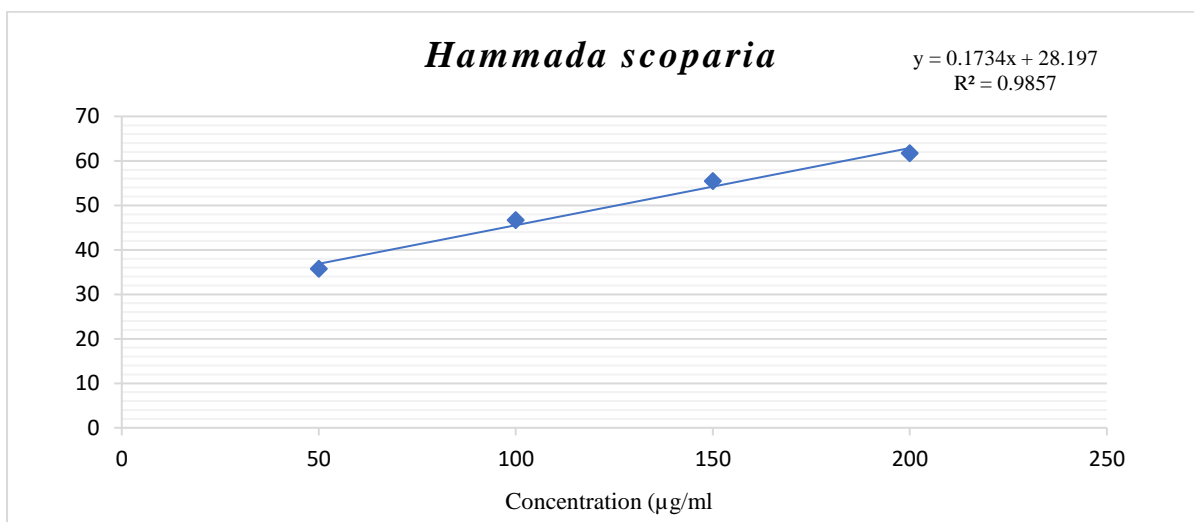


Figure: *Hammada scoparia* calibration curve for determination of reducing power capacity

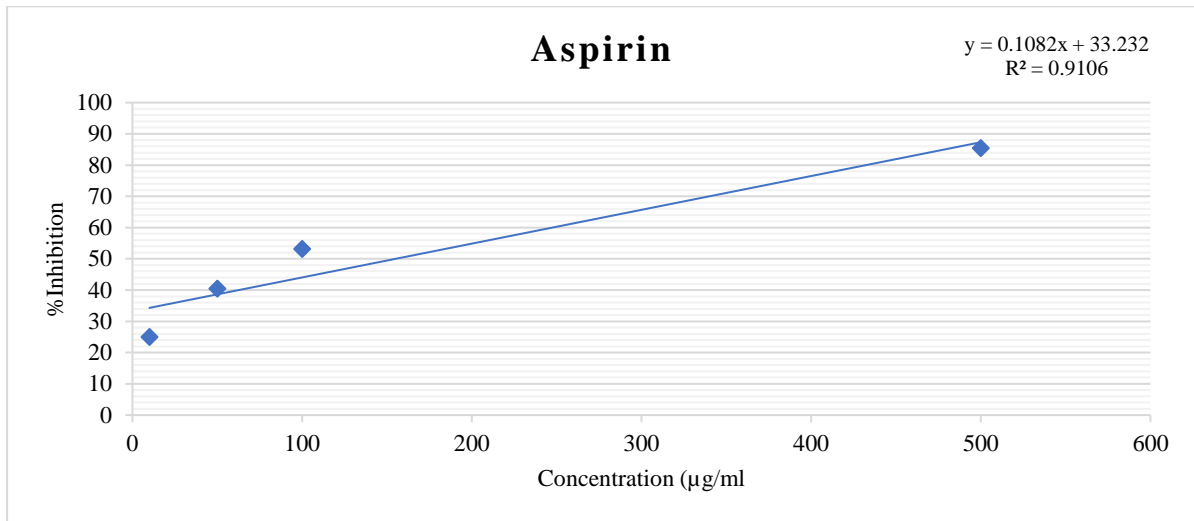
Annex 03: Calibration curve for determination of capacity anti-inflammatory of samples

Figure: Aspirin calibration curve for determination of anti-inflammatory capacity

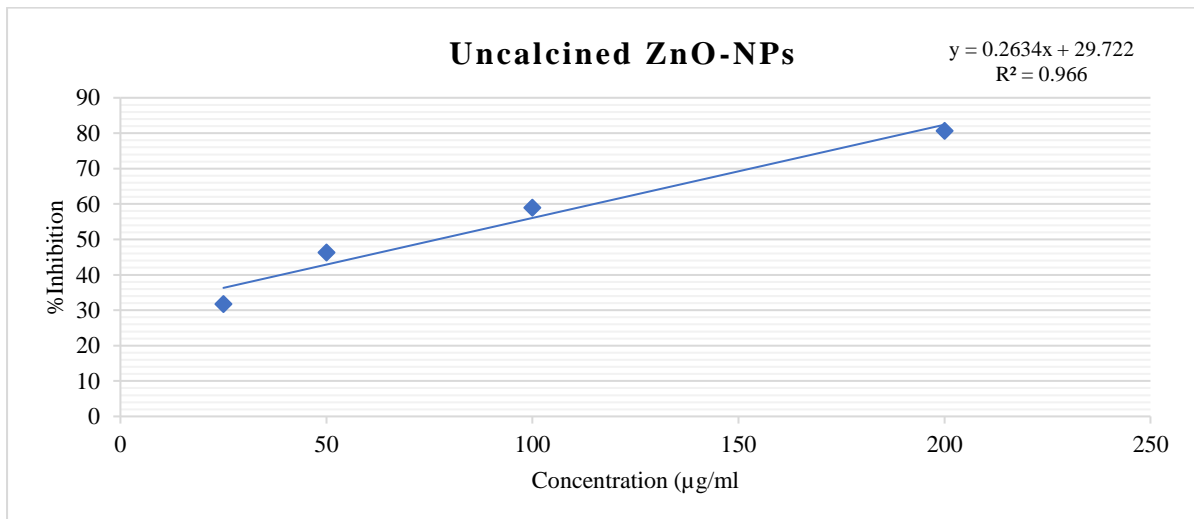


Figure: Uncalcined ZnO-NPs calibration curve for determination of anti-inflammatory capacity

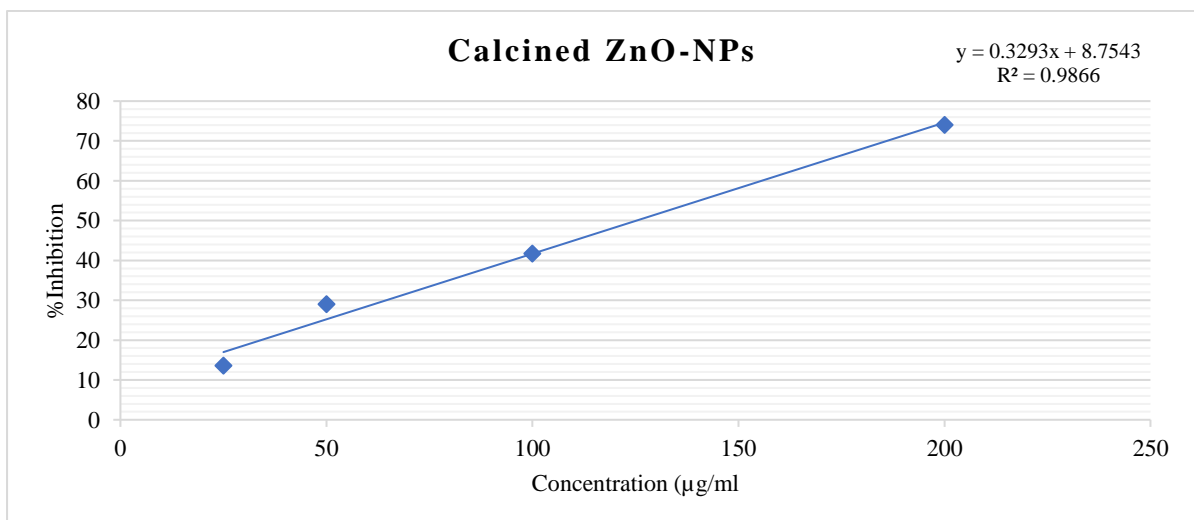


Figure: Calcined ZnO-NPs calibration curve for determination of anti-inflammatory capacity

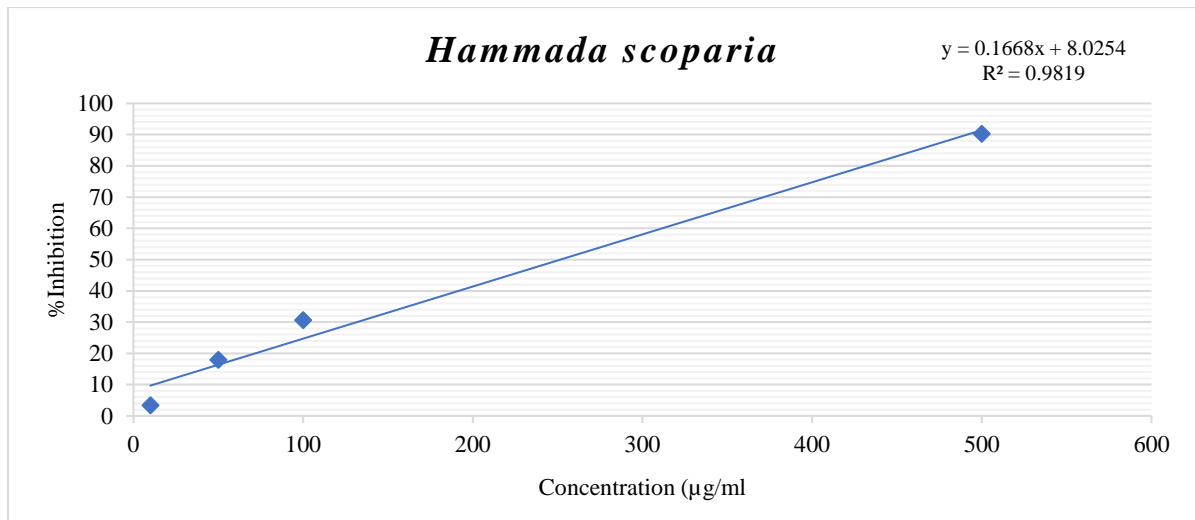


Figure: *Hammada scoparia* calibration curve for determination of anti-inflammatory capacity

Annex 04: Calibration curve for determination of capacity antidebitic by Hemoglobin glycosylation of samples

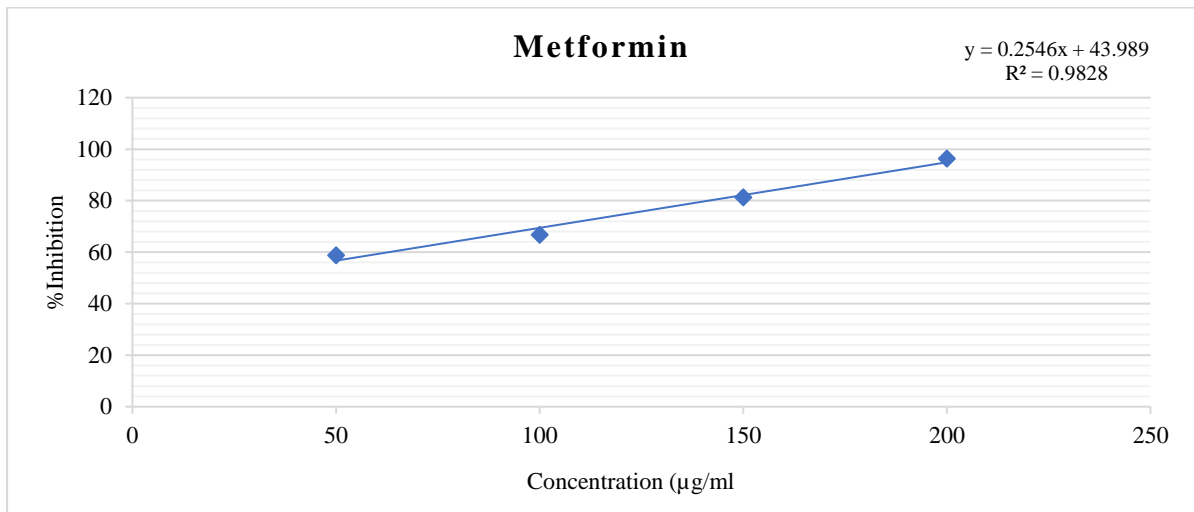


Figure: Metformin calibration curve for determination of antidebitic capacity

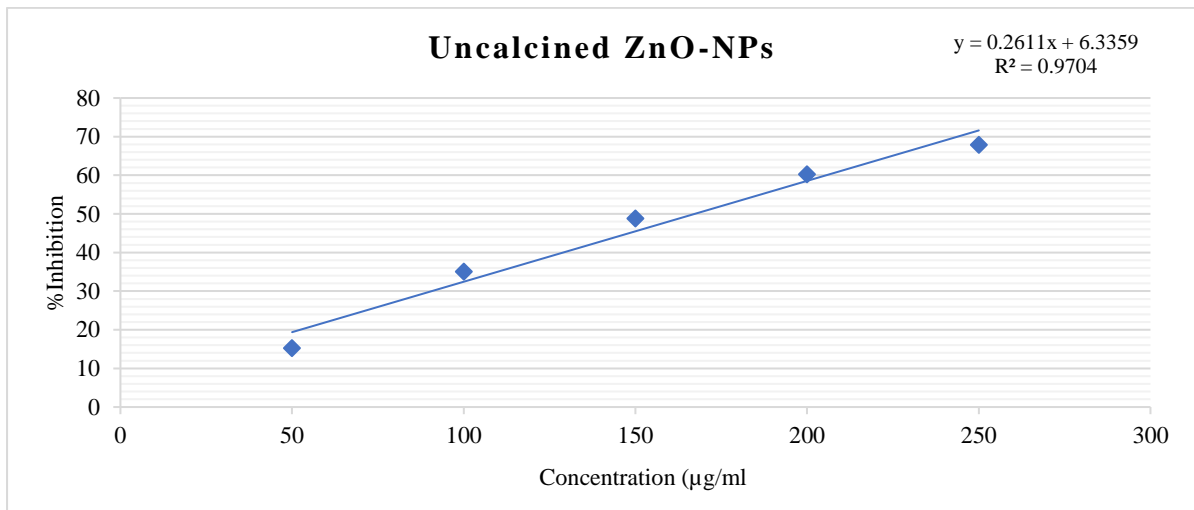


Figure: Uncalcined ZnO-NPs calibration curve for determination of antidebitic capacity

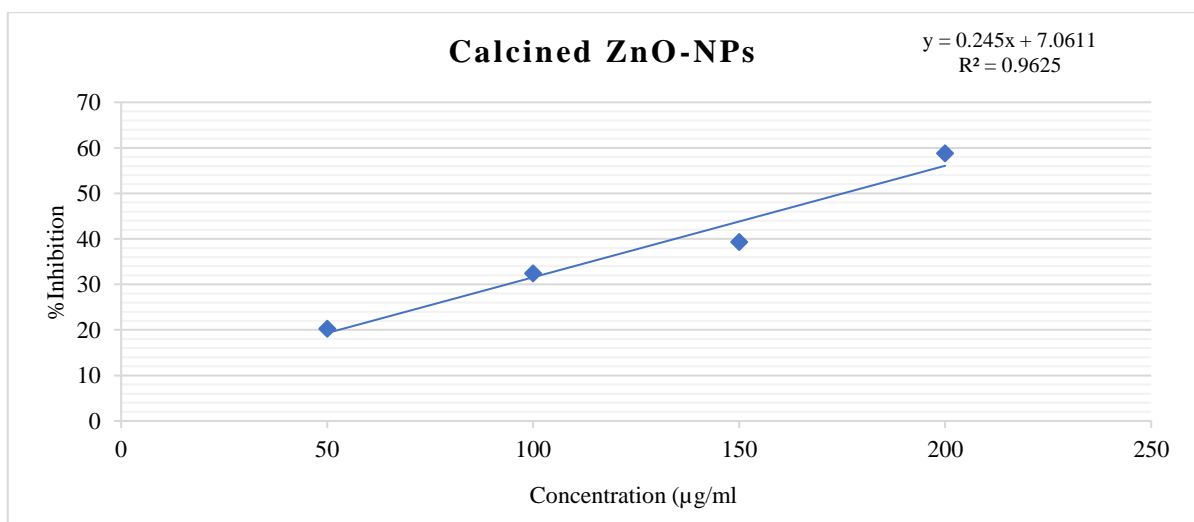


Figure: Calcined ZnO-NPs calibration curve for determination of antidebitic capacity

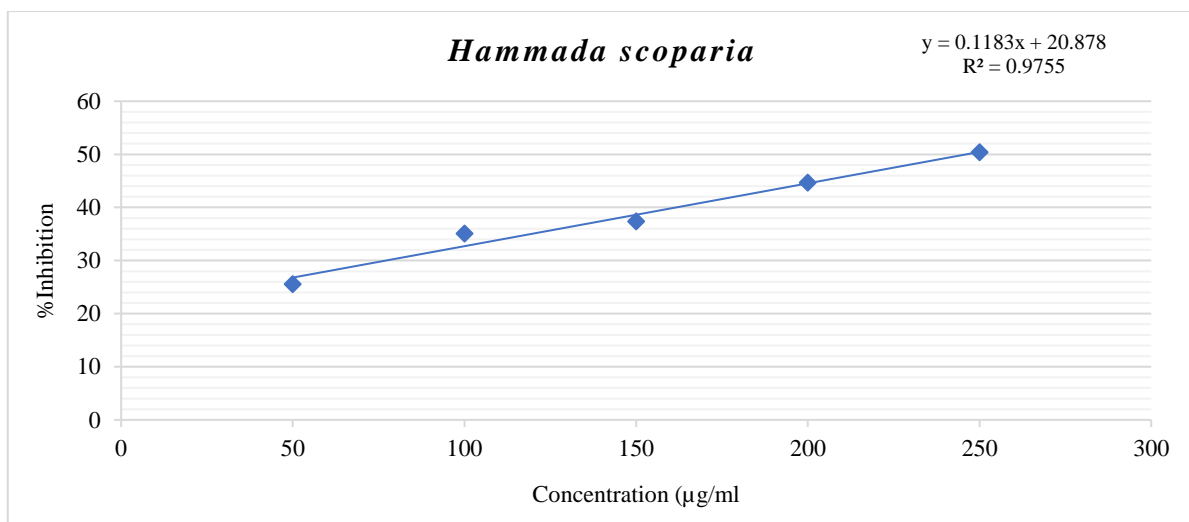


Figure: Calcined ZnO-NPs calibration curve for determination of antidebitic capacity